

Examining the role of *Zfrp8* with respect to iron/heme homeostasis and ecdysone production

by

Dipanjan Dey

A thesis submitted in partial fulfillment of the requirements for the degree of

Master of Science

in

Molecular Biology and Genetics

Department of Biological Sciences

University of Alberta

© Dipanjan Dey, 2020

Abstract

Ecdysone, the primary steroid hormone in insects produced primarily in the prothoracic gland during larval development, is responsible for coordinating developmental transitions such as larval molts and metamorphosis during the *Drosophila* life-cycle. The ecdysone biosynthesis pathway, which involves the conversion of dietary cholesterol to the biologically active form of ecdysone, requires cytochrome P450 enzymes to synthesize its steps. The cytochrome P450 enzymes require heme as a co-factor in order to function properly, which results in high demand for heme during the massive increase in cytochrome P450 enzyme production throughout the larval development and especially during the late larval ecdysone peak. Since free heme is highly toxic, it is produced when required through the heme biosynthesis pathway. Whenever the heme biosynthesis pathway is disrupted as a result of mutations in the latter stages of the pathway, it results in the accumulation of heme precursors in the prothoracic gland, which displays visible red autofluorescence on exposure to UV light. Since only two other tissues that are known to highly express cytochrome P450 enzymes also display red autofluorescence signifying the accumulation of heme precursors, this establishes the relationship between cytochrome P450 enzymes and heme by proving the importance of heme for the cytochrome P450 enzymes. Genetic screens conducted by King-Jones lab in collaboration with two other labs by knocking down genes of the entire *Drosophila* genome specifically in the prothoracic gland investigated for ecdysone-deficient phenotypes such as the arrest of larval molts, delay in metamorphosis which resulted in ~1,906 genes that were screened further in the King-Jones lab to classify ring glands based on their size and ability to display red autofluorescence under UV exposure. This resulted in 34 genes, which also included *Zfrp8*, the gene that I have investigated in my thesis. I hypothesized that *Zfrp8* plays a role in iron/heme homeostasis and ecdysone production, for which I needed to observe the developmental effects

when *Zfrp8* is knocked down specifically in the prothoracic gland. This resulted in significant third instar larval arrest and big red ring gland under UV exposure, which resulted from the accumulated heme precursors. In order to determine the exact mechanism as to how *Zfrp8* is regulating iron/heme homeostasis as well as ecdysone production, I decided to rescue the developmental defects by supplementing the diet of the *PG>Zfrp8*-RNAi animals with components of the ecdysone biosynthetic pathway as well as iron and heme. Interestingly, sterol supplements, namely 7-dC, 20E, and cholesterol, were able to rescue the developmental defects of the *PG>Zfrp8*-RNAi animals by a significant degree, but not completely. At the same time, dietary iron and exogenous heme failed to rescue the developmental defects of the animals mentioned above. Knocking down *Zfrp8*, specifically in the prothoracic gland, also resulted in the downregulation of the ecdysteroidogenic genes as determined by qPCR. Based on the results, I propose that *Zfrp8* participates in the process of heme production not by the conventional heme biosynthesis pathway but by a yet-to-be-identified pathway or mechanism which allows the cytochrome P450 enzymes to function properly and produce the biologically active form of ecdysone. The significant rescue demonstrated by 7-dehydrocholesterol supplementation suggests that *Zfrp8* possibly branches off to a separate pathway which is responsible for regulating iron or heme metabolism instead of feeding into the conventional ecdysone biosynthesis pathway.

Acknowledgements

I want to sincerely thank Dr. Kirst King-Jones for accepting me as a graduate student in his lab and allowing me to pursue my graduate studies. I would like to show my appreciation towards Kirst with respect to the important feedback I got during lab meetings, seminar presentations and most importantly on my project. I would like to thank my committee member Dr. Andrew Waskiewicz for being patient with me, providing feedback and suggestions on future experiments during the committee meetings and also during the course I took under his supervision.

I would like to thank all the lab members of the King-Jones lab for answering all my queries and helping me out with my experiments when I started working in the lab by showing certain techniques and sharing their experiences with me.

I would like to thank my parents for their unwavering support towards me. It would not have been possible for me to come all this way without their prayers and the faith they have always showed in me. They have always been understanding, shown patience and supported all the decisions that I have taken till date. Thank you for all the sacrifices that you have made.

Table of Contents

Chapter 1.0 Introduction	1
1.1 Steroid hormones and what we know about them.....	5
1.2 <i>Drosophila</i> as a model organism.....	7
1.3 Introduction to steroid hormones.....	9
1.4 Heme biosynthesis and iron homeostasis in mammals and <i>D. melanogaster</i>	14
1.5 Relation between steroid hormone synthesis and iron homeostasis in <i>D. melanogaster</i>	19
1.6 Genetic screens conducted to identify candidate genes involved in iron/heme homeostasis and ecdysone production.....	21
1.7 CRISPR.....	23
1.8 Role of different supplements implemented to rescue the developmental defects.....	26
1.9 Introduction to <i>Zfp8</i>	28
Chapter 2.0 Material and Methods	33
2.1 <i>Drosophila</i> stocks and their maintenance.....	34
2.2 Preparation of Nutrifly food.....	34
2.3 Preparation of special fly media.....	35
2.3.1 Preparation of Iron supplemented diet.....	35
2.3.2 Preparation of Hemin supplemented diet.....	36
2.3.3 Preparation of Iron chelator supplemented diet.....	36
2.3.4 Preparation of Cholesterol supplemented diet.....	36
2.3.5 Preparation of 20-hydroxyecdysone supplemented diet.....	37
2.3.6 Preparation of 7-dehydrocholesterol supplemented diet.....	37
2.4 Collecting eggs and analyzing vials for rescue experiments.....	37
2.5 Staging.....	38
2.6 Generation of CRISPR constructs.....	39
2.6.1 Identification of candidate target sites for gRNA.....	39
2.6.2 Validation of candidate target sites.....	39
2.6.3 Preparing pCFD5 backbone.....	39
2.6.4 Preparing gRNA fragments (two gRNAs).....	40
2.6.5 Gibson reaction.....	40

2.6.6	Purification of plasmid DNA.....	41
2.6.7	Transformation.....	42
2.6.8	Screening for positive cloning.....	42
2.6.9	Midiprep.....	43
2.7	Embryo injections.....	44
2.8	RNA extraction of Whole-body samples.....	46
2.9	Verification of extracted RNA quality.....	47
2.10	cDNA synthesis.....	48
2.11	Validating qPCR primers.....	48
2.12	Preparation of Grape food plates.....	49
2.13	Extracting DNA from adult flies.....	50
2.14	Purification of PCR products.....	51
2.15	Preparation of Competent cells.....	52
2.16	Preparation of PBS.....	53
2.17	Preparation of Antibiotics.....	53
2.18	Immunofluorescence.....	53
2.19	ImageJ.....	54
Chapter 3.0	Results.....	64
3.1	Loss-of- <i>Zfrp8</i> through RNA interference and mutation results in developmental defects.....	65
3.1.1	Loss-of- <i>Zfrp8</i> results in accumulation of heme precursors in the prothoracic gland.....	68
3.2	Iron supplementation fails to rescue the developmental defects of <i>PG>Zfrp8-RNAi1</i> animals.....	72
3.3	Hemin supplementation fails to rescue the developmental defects of <i>PG>Zfrp8-RNAi1</i> animals.....	77
3.4	Iron chelation fails to rescue the developmental defects of <i>PG>Zfrp8-RNAi1</i> animals.....	82
3.5	7-dehydrocholesterol or 7-dC supplementation results in a significant rescue of <i>PG>Zfrp8-RNAi1</i> animals.....	86
3.6	20-hydroxyecdysone or 20E supplementation rescues the developmental	

defects of <i>PG>Zfrp8</i> -RNAi1 animals, but not as efficiently as 7-dC feeding.....	91
3.7 Cholesterol supplementation rescues the developmental defects of <i>PG>Zfrp8</i> -RNAi1 animals, but less efficiently than 7-dC.....	95
3.8 Loss-of- <i>Zfrp8</i> results in downregulation of ecdysteroidogenic genes in whole-body samples.....	99
3.9 <i>Zfrp8</i> localization in the prothoracic gland.....	102
Chapter 4.0 Discussion	104
4.1 The importance of <i>Zfrp8</i> with respect to the proper development of <i>Drosophila</i>	105
4.2 <i>Zfrp8</i> does not feed into the heme biosynthesis pathway.....	109
4.3 <i>Zfrp8</i> feeds into a yet-to-be ascertained pathway to produce heme required for ecdysone synthesis but may not feed into the conventional ecdysone biosynthesis pathway.....	111
4.4 Establishing parallels between <i>PDCD2</i> and <i>Zfrp8</i>	114
4.5 Future directions.....	117
4.5.1 Determining the upregulation of ecdysteroidogenic titers in the presence of sterol supplements.....	117
4.5.2 Determining the efficiency of the 2xgRNA line.....	118
4.5.3 Elucidating the interaction of <i>Zfrp8</i> with piRNA pathway proteins.....	119
4.5.4 Validating the interaction between <i>Zfrp8</i> and piRNA pathway proteins in S2 cells.....	121
4.6 Conclusions.....	122

List of Figures

Introduction

Figure 1.1. Ecdysone concentration mapped throughout all the developmental stages of <i>Drosophila melanogaster</i>	12
Figure 1.2. Ecdysone biosynthesis takes place in the prothoracic gland of ring gland.....	13
Figure 1.3. Heme biosynthetic pathway.....	17
Figure 1.4. Late biosynthetic enzymes like <i>Ppox</i> when mutated results in red autofluorescence of specific tissues signifying the accumulation of heme precursors.....	18
Figure 1.5. Schematic diagram of the <i>GAL4/UAS</i> system.....	31
Figure 1.6. Proposed model linking <i>Zfrp8</i> to iron/heme homeostasis and ecdysone production	32

Materials and Methods

Figure 2.1. Illustration of <i>Zfrp8</i> transcription unit.....	56
Figure 2.2. Illustration of the transgenic 2xgRNA line constructed.....	57

Results

Figure 3.1. <i>PG>Zfrp8-RNAi1</i> affected development whereas <i>PG>Zfrp8-RNAi2</i> did not....	70
Figure 3.2. Iron supplementation fails to rescue <i>PG>Zfrp8-RNAi1</i> animals.....	75
Figure 3.3. Hemin supplementation fails to rescue <i>PG>Zfrp8-RNAi1</i> animals.....	80
Figure 3.4. Iron chelator supplementation fails to rescue <i>PG>Zfrp8-RNAi1</i> animals.....	84
Figure 3.5. 7-Dehydrocholesterol or 7-dC supplementation results in significant, but not complete rescue of <i>PG>Zfrp8-RNAi1</i> animals.....	89
Figure 3.6. 20-hydroxyecdysone or 20E supplementation results in rescue of <i>PG>Zfrp8-RNAi1</i> animals, but less significant compared to 7-dC.....	93
Figure 3.7. Cholesterol supplementation results in rescue of <i>PG>Zfrp8-RNAi1</i> animals, but to a lesser degree compared to 7dC.....	97
Figure 3.8. <i>Zfrp8-RNAi</i> reduced the expression of ecdysteroidogenic genes.....	101

Figure 3.9. Transgenic GFP-tagged *Zfrp8* did not show any localization in the prothoracic gland..... 103

Discussion

Figure 4. Updated proposed model linking *Zfrp8* to iron/heme homeostasis and ecdysone production..... 125

List of Tables

Materials and Methods

Table 2.1. <i>Drosophila melanogaster</i> lines used for the experiments conducted in this thesis....	58
Table 2.2. Primers used for qPCR, cloning and sequencing.....	59
Table 2.3. Reagents required to set up PCR reactions for double gRNA cloning.....	60
Table 2.4. Thermocycling conditions for PCR.....	60
Table 2.5. Reagents required for Gibson reaction.....	61
Table 2.6. Reagents required to digest plasmid with BbsI restriction enzyme.....	61
Table 2.7. Reagents required to do DpnI digestion.....	61
Table 2.8 Reagents used for cDNA synthesis.....	62
Table 2.9. Thermocycling conditions for cDNA synthesis.....	62
Table 2.10. Reagents used to prepare competent cells.....	63

Abbreviations

PG	Prothoracic gland
RG	Ring gland
PTTH	Prothoracicotropic hormone
gRNA	guideRNA
P450	cytochrome P450
7-dC	7-dehydrocholesterol
20E	20-hydroxyecdysone
BPS	Bathophenanthroline disulfonic acid
FAC	Ferric Ammonium Citrate
CRISPR	Clustered regularly interspaced short palindromic repeats
ALAS	Aminolevulinic acid synthase
<i>Ppox</i>	Protoporphyrinogen Oxidase
CPOX	Coproporphyrinogen Oxidase
FECH	Ferrochelatase
L1	First instar larvae
L2	Second instar larvae
L3	Third instar larvae
hr/hrs	Hour/Hours
min/mins	Minute/Minutes
JH	Juvenile hormone
UV	Ultraviolet
RNAi	Ribonucleic Acid Interference
ALAD	Aminolevulinic acid dehydratase
PBGD	Porphobilinogen Deaminase
URO3S	Uroporphyrinogen III synthase
UROD	Uroporphyrinogen Decarboxylase
L2P	Second instar Prepupa
<i>E. coli</i>	<i>Escherichia coli</i>
DNA	Deoxyribonucleic acid
crRNA	crisprRNA

tracrRNA	trans-activating RNA
PAM	Proto-spacer adjacent motifs
cDNA	complementary DNA
<i>cas</i>	crispr associated genes
PDCD2	Programmed Cell death 2
HSC	Hematopoietic stem cell
piRNA	piwi-interacting RNA
FMRP	Fragile-X Mental retardation protein
Tral	trailer hitch
KD	Knockdown
VDRC	Vienna Drosophila Resource Center
BDSC	Bloomington Drosophila Stock Center
M	Molar
NaOH	Sodium Hydroxide
DRSC	Drosophila RNAi screening center
TRiP	Transgenic RNAi project
PCR	Polymerase Chain Reaction
NEB	New England Biolabs
LB	Luria Bertani
MBSU	Molecular Biology Service Unit
Rpm	Revolution per minute
EMS	Ethyl methanesulphonate
pg	Picogram
mL	milliliter
RT	Room temperature
mg	milligram

Chapter 1

Introduction

1. Introduction:

Summary/Overview

Hormones are known to influence a multitude of biological processes throughout the lifespan, which includes alterations in anatomy and physiology during the transition from one developmental stage to another¹. One such group of hormones, steroid hormones, is responsible for controlling metabolism, immune functions, development of sexual characteristics, and many other functions in humans²⁻⁶. In insects, steroid hormones are responsible for coordinating the developmental transitions such as molting and metamorphosis. The principle steroid hormone in *Drosophila* is called ecdysone, which is produced in the prothoracic gland during larval development.

Since the detailed mechanisms underlying the regulation of ecdysone synthesis are not known, the King-Jones lab, in collaboration with other labs, conducted a genome-wide screen to identify genes that take part in ecdysone biosynthesis. Specific phenotypes such as the failure to undergo the transition from one larval stage to another or the inability to enter metamorphosis were observed as a result of prothoracic gland-specific depletion of candidate genes that came out of this screen. A secondary screen was conducted in the King-Jones lab, whereby the phenotypes of the ring glands were observed and further classified into two categories: large red ring glands and large ring glands. The red autofluorescence observed on exposure to UV light is due to the accumulation of heme precursors as a result of a defective heme biosynthetic pathway. The high expression of cytochrome P450 genes during larval development and the further increase in their expression in the late larval stage correlates with the increase in requirement of iron and heme (there is a heme-iron center at the active site of cytochrome P450 enzymes) to keep the cytochrome P450 functional. This particular observation established the relationship between heme and ecdysone. One such

gene that came out of the screen and is the focus of my thesis is *Zfrp8* or Zinc-finger protein RP8, categorized as having large red ring glands as a result of PG-specific depletion.

Since *Zfrp8* came out of the screen, I hypothesized that *Zfrp8* must have a role concerning iron or heme homeostasis as well as ecdysone biosynthesis. However, it needs to be investigated whether *Zfrp8* is acting through the heme biosynthesis pathway or the ecdysone biosynthesis pathway. Knocking down *Zfrp8* specifically in the prothoracic gland using RNAi technique results in the major arrest of third instar larvae and also delays the transition of L2 to L3 by an entire day. *Zfrp8* mutant was not able to survive beyond the first instar stage, further strengthening my hypothesis. In order to determine which pathway *Zfrp8* is acting through, I decided to rescue the developmental defects when *Zfrp8* was knocked down in the prothoracic gland by supplementing the diet of the affected animals with different steroid intermediates of the ecdysone biosynthesis pathway as well as heme and dietary iron to overcome the deficiencies of the disrupted heme biosynthesis pathway. In work embodied in this thesis, I have been able to conclude that *Zfrp8* acts through the ecdysone biosynthesis pathway since the developmental defects were rescued by the components of the pathway mentioned above, namely, 7-dehydrocholesterol, 20-hydroxyecdysone, and cholesterol but failed to be rescued by heme and related components. The rescue demonstrated by the ecdysone-related supplements were not complete but significant based on statistical analysis. I have also demonstrated that knocking down *Zfrp8* results in the downregulation of the ecdysteroidogenic genes, which is consistent with the developmental defects reported earlier in this section. I also generated *Zfrp8* CRISPR KO construct to validate the phenotypes displayed by *Zfrp8*-RNAi since RNAi presents the concern of potential off-targets. Finally, I would like to conclude that *Zfrp8* does play a role in iron or heme homeostasis as well as ecdysone biosynthesis but does not act through the conventional heme biosynthesis pathway and quite possibly may not

act through the conventional ecdysone biosynthesis pathway too. However, the detailed mechanism responsible for this interaction is yet to be elucidated.

1.1 Steroid hormones and what we know about them

Steroid hormones are a group of hormones acting as signaling molecules. They are responsible for the regulation of multiple physiological processes occurring within the body ranging from influencing cell growth and development through controlling the synthesis of particular proteins to the regulation of female and male reproductive processes^{7,8,9}. Steroid hormones are essential for controlling stress in humans, and prolonged stress leads to the impairment of reproductive functions¹⁰ and also leads to endocrine disorders¹¹. The mammalian system has six different types of steroid hormones, and the differentiation is strictly based on a structural and biological basis. The six different types of steroid hormones are as follows: 1) Mineralocorticoids which are responsible for instructing the renal tubule to retain sodium. 2) Glucocorticoids are responsible for exerting multiple effects on carbohydrate metabolism, which includes regulating glucose (produced when carbohydrates undergo digestion or are metabolized by the body) metabolism along with imparting anti-inflammatory effects to the immune system. 3) Progestins are essential for reproduction. 4) Estrogens that are responsible for inducing secondary female sexual characteristics which include the growth of pubic hair, development of breasts, and the beginning of the menstrual cycle. 5) Androgens are responsible for inducing secondary sexual characteristics in men, which includes the growth of body and facial hair, enlarged muscles involving an increase in both muscle mass and strength, enlargement of the larynx, and a few other characteristics. 6) Vitamin D, also known as 1,25- dihydroxy vitamin D₃, which is responsible for bone growth and development as well as regulation of calcium and phosphorus homeostasis¹². The mineralocorticoids and glucocorticoids are produced in the adrenal cortex, while progestins, androgens, and estrogens, which are sex steroid hormones are primarily produced in the gonads¹³.

Steroid hormones are produced as timed pulses to aid in the developmental transitions from childhood to adolescence and eventually leading to the formation of a fully-grown adult and are primarily produced in the mitochondria and smooth endoplasmic reticulum¹⁴. Misregulation concerning the timed release of steroid hormones may lead to tissue-specific alterations in human physiology, specifically during critical developmental periods. Beginning from the late 1940s and the early 1950s, there was a dramatic increase related to the experimentation with synthetic steroid hormones, more specifically testosterone, to enhance athletic performance^{15,16}. However, starting from the 21st century onwards, the widespread misuse of the so-called “anabolic steroids” coupled with the long-term adverse effects of steroid hormones has led to anabolic steroids being banned. Although it is recommended to use steroids under professional medical supervision, not all steroid use is taken under medical supervision.

1.2 *Drosophila* as a model organism

Drosophila melanogaster has been chosen as a model organism because flies are easy to manipulate, have a short life-cycle, can be easily reared in a laboratory setting and can grow from embryo to adult within ten days. The entire fly genome has also been sequenced, and along with the availability of RNAi lines and multiple mutants from different stock centers has made *Drosophila* an attractive model organism to study the various human diseases and find potential cures by studying them. It has been reported that a plethora of basic biological, neurological as well as physiological properties are conserved between mammals and *D. melanogaster* as well as nearly 75% of human disease-causing genes have been reported to have a homolog in the fruit fly¹⁷.

At a temperature of 25°C, the journey from freshly hatched embryos to fully grown adults takes place within ten days. Embryogenesis takes approximately 24 hours, after which, the first instar larvae start feeding on the medium to assimilate the nutrients essential for growth and surviving metamorphosis. The second instar larvae make their way into the medium where they undergo the transition to third instar larvae after another 24 hours. The newly transitioned larvae keep on feeding on the medium until the late third instar larvae stage, where they then make their way out of the nutrient medium and climb up the walls of the vials and bottles in which they are growing and enter the wandering stage. The wandering stage involves complete withdrawal from feeding and finding a suitable pupariation site. The wandering stage is followed by puparium formation for the next 24 to 48 hours. The adults finally eclose from the pupae ten days after egg laying. The flies usually grow at different rates at different temperatures, which is evident from the fact that the journey from a freshly-hatched embryo to a full-grown fruit fly takes different duration at different temperatures.

The reason for choosing *Drosophila* to study steroid hormones is because *Drosophila* is the only model organism where the steroid hormone titer changes have been measured throughout all the stages of the fruit fly development (Figure 1.1). *Drosophila* is also a holometabolous insect, which means its life-cycle can be divided into multiple life-stages, namely egg, larva, pupa, and adults, which makes it easier to observe and examine the changes at each developmental stage^{18,19}. Majority of the experiments conducted in the King-Jones lab require dissection of the 3rd instar larvae, which is also the last larval stage and is chosen for the following reasons: 1) The ring gland in the third instar larvae is much bigger compared to the ring gland in the first instar and the second instar larvae which makes the dissection much more comfortable to carry out. 2) The developmental stage involving the third instar larvae constitutes three minor ecdysone pulses which are not present in the first instar and the second instar larvae thereby making it possible to correlate the expression profile of the genes with these pulses. 3) It is easy to synchronize the third instar larvae at the L2/L3 molt since the third instar larvae are morphologically distinct from the second instar larvae²⁰.

1.3 Introduction to steroid hormones

Steroid hormones are well-known chemical messengers that are responsible for regulating different biological functions such as regulation of developmental timings, effecting cellular metabolism, and maintaining physiology. More importantly, steroid hormones play a role in regulating the growth and development of higher organisms (both in the animal and plant kingdom). Steroid hormones are lipophilic molecules and are known to act on a wide variety of tissues as well as biological functions^{21,22}.

Ecdysone is the primary or principal steroid hormone in insects, which is specifically produced in the prothoracic gland during the larval developmental stages. The prothoracic gland itself is part of the endocrine ring gland, which is also composed of the corpus allatum and the corpora cardiaca, which are responsible for secreting Juvenile hormone and adipokinetic hormone respectively (Figure 1.2). The conversion of dietary cholesterol to the prohormone α -ecdysone takes place in the prothoracic gland itself and is mediated by the Halloween enzymes^{23,24,25}. The Halloween genes are responsible for encoding seven cytochrome P450 monooxygenases which includes *phantom*, *disembodied*, *spook*, *spookier*, *shadow*, *shade*, *Cyp6t3*, a short-chain dehydrogenase/reductase called *Shroud* and a Rieske-electron oxygenase called *Neverland*. The steroid hormone biosynthesis pathway starts with the conversion of dietary cholesterol to 7-dehydrocholesterol. The reaction is carried out by the enzyme *Neverland*. The next step involves the conversion of 7-dehydrocholesterol to 5 β -ketodiol, which involves multiple steps and have been termed by the researchers as the "Black box" because these steps are yet to be characterized. Interestingly, none of the intermediates believed to be a part of the black box have been identified because the intermediates are unstable in the prothoracic gland, which makes it difficult to isolate those intermediates and characterize them^{26,27}. However, some of the enzymes have been identified

that function within the black box. The genes that are responsible for encoding the enzymes in the black box are *shroud (sro)*, *spook (spo)* or *spookier (spok)*, and *Cyp6t3*^{28,29,30,31}. *Shroud* belongs to a family of short-chain dehydrogenases/ reductases and does not require iron to function. *Spook*, *Spookier* and *Cyp6t3* have been identified to be cytochrome P450 monooxygenases. *Spook* and *Spookier* are duplicated genes in the *Drosophilidae* genome, where both of them are involved in ecdysone biosynthesis, particularly during the embryonic and postembryonic development respectively. The three Halloween enzymes, namely *phantom*, *disembodied*, and *shadow*, which encode cytochrome P450 hydroxylases, are responsible for carrying out the conversion from the 5 β -ketodiol to the prohormone α -ecdysone of the ecdysone biosynthesis pathway in the prothoracic gland itself. After release into the hemolymph, the prohormone α -ecdysone is converted to its biologically active form 20-hydroxyecdysone in the target tissues, namely midgut, and fat body, and is mediated by the cytochrome P450 enzyme *shade*³².

For many years, insects have been used as model organism to study the molecular mechanisms that are responsible for driving the developmental transitions. Insects are preferred because they go through a series of molts and eventually metamorphoses, which helps researchers to understand the driving influence behind the timely transition from one stage of the multicellular organisms to the next stage during their development. Till now, three different circulating factors have been found to be responsible for the insect developmental transitions, namely: PTTH or Prothoracicotrophic hormone³³, JH or juvenile hormone^{34,35,36}, and ecdysone. PTTH is secreted by two pairs of the lateral neurosecretory cells of the insect brain and is a major but not the only factor responsible for the initiation of ecdysteroidogenesis in insects. It has been established that removing the functions of PTTH in the prothoracic gland neurons of *Drosophila* results in a major developmental delay, which leads to a longer feeding period for the larvae, thereby delaying the metamorphosis. The more extended feeding period means the flies have a larger body size when

compared to the flies having normal PTH activity. This led to the conclusion that PTH is in charge of coordinating the different developmental transitions and the final body size of *Drosophila* but does not affect the molting and the metamorphosis of the model organism.

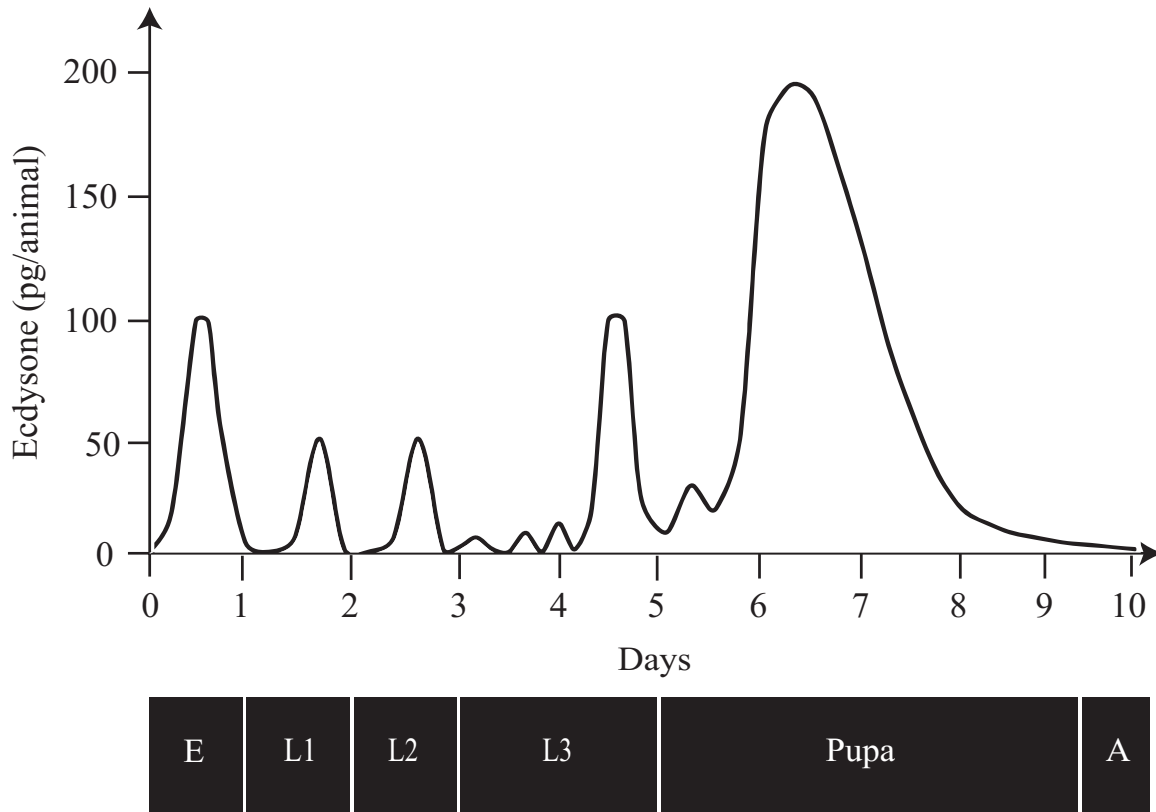


Figure 1.1: Ecdysone concentration mapped throughout all the developmental stages of *Drosophila melanogaster*: *Drosophila* is the only model organism where steroid hormone pulses have been measured throughout all of its developmental stages. The embryo makes its way through the first instar larval stage or L1 followed by second instar larval stage or L2 and third instar larval stage or L3. L3 undergoes metamorphosis to form pupae which then ecloses 10 days after egg-laying to form a fully-grown adult. Ecdysone pulses accompany the transition from first instar larvae to second instar and then to third instar. A major ecdysone pulse that is released 44 hrs after the transition from second instar to third instar results in puparium formation. E=embryo, L1=first instar larvae, L2=second instar larvae, L3=third instar larvae, A=adult.

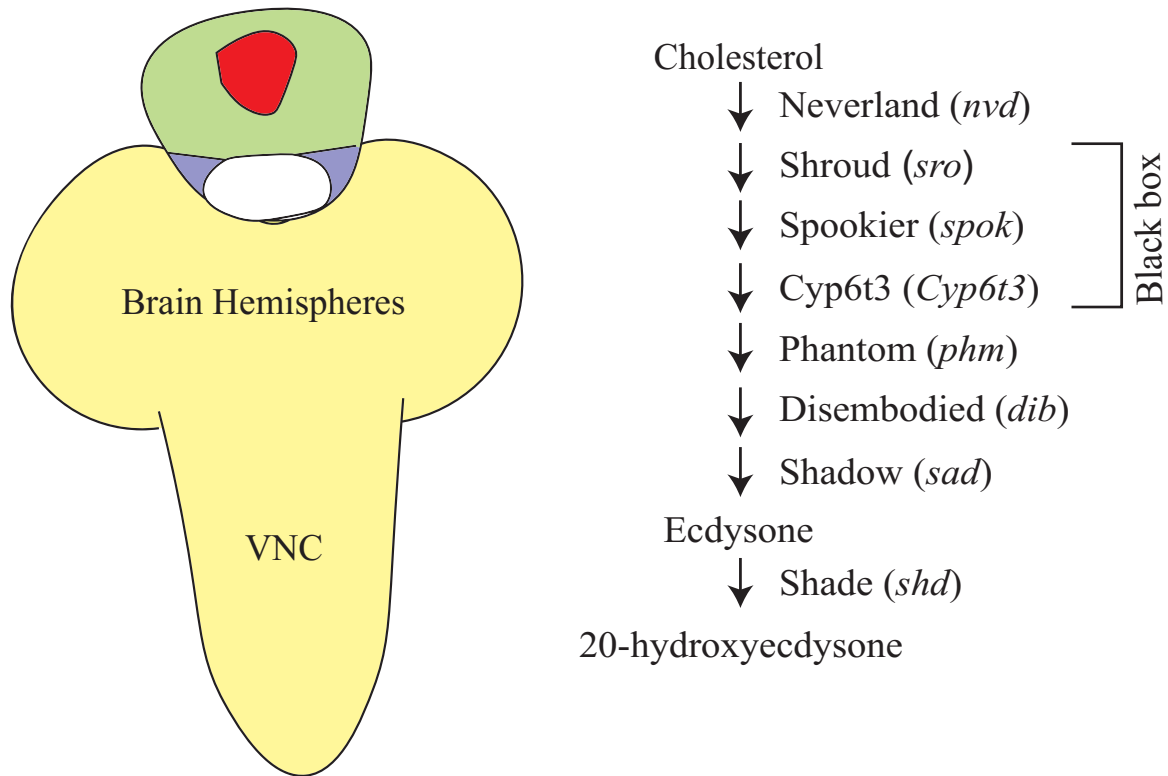


Figure 1.2: Ecdysone biosynthesis takes place in the prothoracic gland of ring gland: The ring gland is a tripartite structure composed of prothoracic gland (shown in green), corpus allatum (shown in red) and corpora cardiaca (shown in light purple). Ecdysone is the principle steroid hormone in insects which is produced primarily in the prothoracic gland during the larval stages. VNC=Ventral Nerve Cord. The major steroid hormone, ecdysone is synthesized from dietary cholesterol by a series of enzymatic steps that are carried out by enzymes mentioned on the right (*gene name*) of the ecdysone biosynthesis pathway. The black box, given such a name because the intermediates constituting the box are yet to be characterized as a result of their high instability and short life-cycle. The black box also contains the rate-limiting enzyme of the ecdysone biosynthesis pathway. Prohormone α -ecdysone is released into the hemolymph, where it is taken up by the target tissues and converted to its biologically active form, 20-hydroxyecdysone.

1.4 Heme biosynthesis and iron homeostasis in mammals and *D. melanogaster*

Heme is an essential compound for living aerobic organisms (Sawicki et al., 2015). Heme is a tetrapyrrole ring with iron at the center³⁷. Heme has been known to be involved in several important biological functions ranging from the storage and transport of oxygen in hemoglobin and myoglobin to the generation of energy, electron transport, and chemical transformation in cytochromes by acting as a prosthetic group³⁸. Previous studies have shown heme to be responsible for controlling gene expression by means of regulating transcription, the stability of messenger RNA, splicing, synthesis of protein, and finally, post-translational modification^{39,40}.

Glycine and Succinyl-CoA are the precursors of the heme biosynthesis pathway. A total of eight enzymes are responsible for carrying out the reactions of the heme biosynthesis pathway⁴¹. All of the enzymes are encoded in the nucleus and the mRNA of the genes encoding for the enzymes undergo translation in the cytoplasm. In the first step of the heme biosynthesis pathway, which is also the rate-limiting step, the reaction takes place in the mitochondria where Glycine and Succinyl-CoA are converted to ALA or Aminolevulinic acid^{42,43} and carried out by the enzyme *Alas* or Aminolevulinic acid synthase. Interestingly, mammals have two forms of *ALAS*- *ALAS1* and *ALAS2*⁴⁴, but *Drosophila* has only one form of *Alas*. *ALAS1* is expressed by the non-erythroid precursors, whereas *ALAS2* is expressed by the erythroid precursors. The reaction now shifts to the cytoplasm where ALA is converted to porphobilinogen, and the reaction is carried out by the cytoplasm-based *Pbgs* or Aminolevulinic acid Dehydratase. Porphobilinogen is converted to Hydroxymethylbilane by the enzyme *l(3)02640* or Porphobilinogen Deaminase⁴⁵ in the next step. Hydroxymethylbilane is converted to Uroporphyrinogen III by the enzyme *CG1885* or Uroporphyrinogen III Synthase^{46,47}. As evident from the name of Uroporphyrinogen III Synthase, the enzyme is a porphyrinogen, which is basically porphyrin precursors and are

linked together by methyl (CH₂) bridges. Interestingly, the porphyrinogens on being exposed to light and oxygen spontaneously convert to porphyrins, thereby gaining the ability to fluoresce. The next reaction involves the conversion of Uroporphyrinogen III to Coproporphyrinogen III and is carried out by the enzyme *Updo* or Uroporphyrinogen Decarboxylase. The heme biosynthesis pathway shifts back to the mitochondria, where the last three steps of the pathway take place. The Coproporphyrinogen III that was synthesized in the cytoplasm is converted to Protoporphyrinogen IX in the mitochondria and is carried out by the mitochondria-based enzyme *Coprox* or Coproporphyrinogen Oxidase. *Ppox* or Protoporphyrinogen Oxidase now converts Protoporphyrinogen IX to Protoporphyrin IX which leads to the last step of the heme biosynthesis pathway involving the incorporation of ferrous ion (Fe⁺² ion) into the tetrapyrrole ring structure leading to the conversion of Protoporphyrin IX to Heme and is carried out by the enzyme Ferrochelatase^{48,49} (Figure 1.3).

Loss-of-*Ppox*, the gene which is responsible for encoding the penultimate enzyme Protoporphyrinogen Oxidase in the heme biosynthesis pathway leads to a reduction in cellular heme levels. The *Ppox* mutation also leads to a major third larval arrest, which means that the third instar larvae are never transformed to pupae and hence never undergo metamorphosis to transform to adults. The third instar larvae remain in the same stage for the next several weeks. In order to further examine the effects of the *Ppox* mutation, the third instar larvae were dissected and were found to be bigger than the control. The prothoracic gland also showed red autofluorescence under UV light (Figure 1.4). The red autofluorescence is due to the accumulation of heme precursors caused due to a blockage in the heme biosynthesis pathway. The accumulation of heme precursors is known to cause a certain group of human diseases known as porphyria. This paves the way for *Drosophila* to be utilized as a model to study the different types of porphyria and find a potential solution to cure the disease completely.

Porphyrias are defined as a group of rare metabolic disorders that could be either inherited or could be acquired based on disruptions along the heme biosynthesis pathway⁵⁰. Porphyrias are subdivided into their hepatic and erythropoietic forms based on the expression site of the enzyme that is dysfunctional. However, it is more convenient to classify porphyrias based on their clinical manifestations namely acute or neurovisceral porphyria and non-acute or cutaneous porphyria⁵¹. The initial symptoms of acute porphyria are usually abdominal pain, inability to concentrate, and severe fatigue. If not treated in time or neglected, the symptoms become more severe, leading to full body paralysis, seizures, and eventually resulting in death. Porphyrias are also called “Vampire disease” because of the fact that in its most severe form, which is Gunther's disease⁵², the gums retreat, and the teeth become longer. The affected patients also suffer from skin disease on exposure to sun and hence have no option but to go out at night. The possibility that drinking blood may have stopped an acute attack, something that heme injections are capable of doing further strengthened the bias for calling porphyria as “Vampire disease”. The neurovisceral attacks are due to the neurotoxic nature of the accumulated precursors, and the sensitivity of the skin to light is due to the fluorescent nature of the porphyrins. The treatments suggested based on the research progress made on porphyria alleviation include hemin and glucose transfusions which have proved quite effective with respect to decreasing the generation of protoporphyrins as well as their buildup in the body^{53,54}.

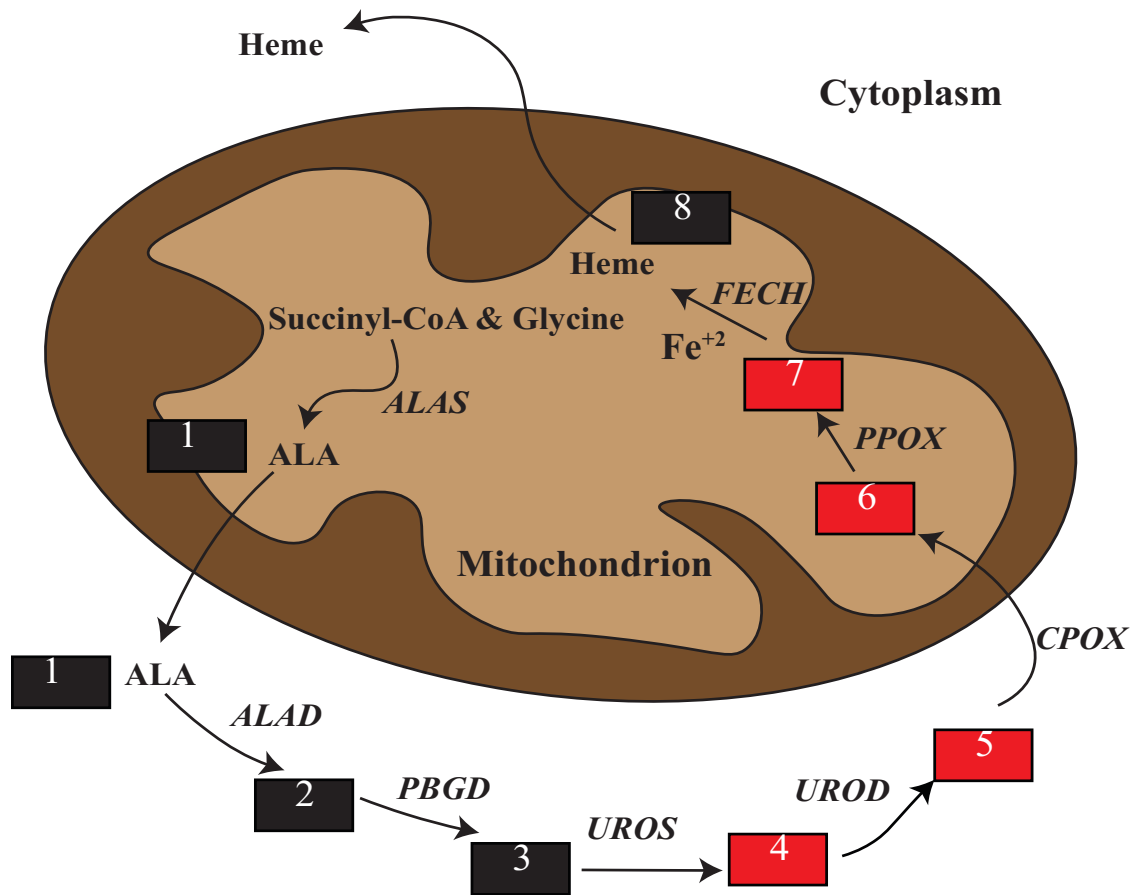


Figure 1.3: Heme biosynthesis pathway: Glycine and Succinyl-CoA which are the precursors of the heme biosynthesis pathway results in the formation of heme after going through a series of steps that are carried out by eight conserved enzymes. The enzymes are encoded in the nucleus and undergo translation in the cytoplasm. Heme precursors are numbered starting from 1 to 8. After the formation of a porphyrin ring, the heme precursors display red autofluorescence on exposure to UV light and are depicted in the form of red square. The incorporation of Fe^{+2} in the porphyrin ring which is also the last step of the heme biosynthesis pathway leads to the loss of red autofluorescence. ALAS= Aminolevulinate synthase, ALAD= Aminolevulinic acid dehydratase, PBGS= Porphobilinogen synthase, UROS= Uroporphyrinogen III synthase, UROD= Uroporphyrinogen decarboxylase, CPOX= Coproporphyrinogen oxidase, PPOX= Protoporphyrinogen oxidase, FECH= Ferrochelatase.

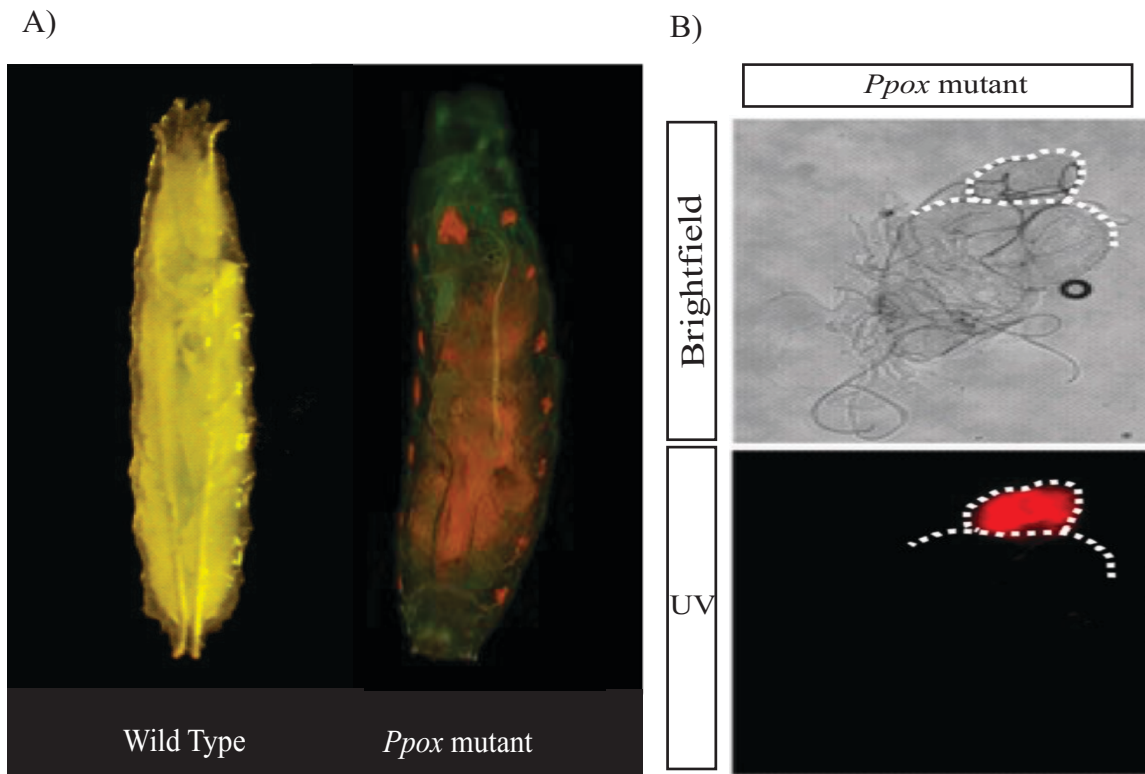


Figure 1.4: Late heme biosynthetic enzymes like *Ppox* when mutated results in red autofluorescence of specific tissues signifying the accumulation of heme precursors:

A) Wild type and *Ppox* mutant L3 larvae viewed under UV light. Disrupted heme biosynthetic pathway in the *Ppox* mutant results in the accumulation of heme precursors which can be observed as red autofluorescence in prothoracic gland, gut and oenocytes under UV exposure while no such accumulation takes place in wild type. Wild type photo credit: Dr. Qiuxiang Ou, *Ppox* mutant photo credit: Dr. Arash Bashirullah B) Brain ring gland from a *Ppox* mutant L3 larvae. The top panel shows the brightfield image and the bottom panel shows the same ring gland under UV exposure. The ring gland and the top part of the brain hemisphere is outlined in white in both the top and bottom panel. The red autofluorescence is attributed to the accumulation of heme precursors signifying the disruption in the heme biosynthesis pathway. Image credit: Dr. Brian Phelps.

1.5 Relation between steroid hormone synthesis and iron homeostasis in *D. melanogaster*

The Halloween enzymes that are responsible for the conversion of dietary cholesterol to the biologically active hormone, 20-hydroxyecdysone, require iron to function except *shroud*. *Neverland* requires an Fe-S cluster in its catalytic center while most of the cytochrome P450 enzymes bind to heme in a non-covalent manner. Most of the cytochrome P450 enzymes that play a role in ecdysteroidogenesis have an extremely high expression throughout the larval developmental stages (Ou et al., 2016). The expression of the cytochrome P450 genes such as *phantom* increases as the larvae transition from the early phases of third instar larvae to the late phases of third instar larvae, which incidentally corresponds to the major late larval ecdysone peak as mentioned earlier. *Phantom* is nearly 200-fold induced during the developmental stage of the third instar, although it has been observed that the expression levels of *phantom* are already high at the beginning of the third instar larvae, specifically the 4-hour time point after the L2/L3 molt.

Since the cytochrome P450 enzymes require iron to function, the massive increase in the production of the cytochrome P450 enzymes during the larval developmental stages and before metamorphosis also requires a massive increase in the amount of iron and heme needed. Heme that is not bound to proteins are usually considered as the labile heme pool which is generated from two possible sources: the first one being the newly synthesized heme which is yet to be incorporated into the hemoproteins and the second one being the heme that is released from the hemoproteins as a result of oxidative stress or under oxidative conditions. We know that free heme is highly toxic since an abundant source of free heme or iron can participate in the Fenton reaction^{55,56} which involves the breakdown of free active iron resulting in the creation of hydroxyl radical and hydroperoxyl radical- two oxygen-radical species along with water ($H^+ + OH^-$) as a byproduct. The free oxygen-radical species are highly toxic to the cell and damage the

lipid membranes, proteins, and nucleic acids along with altering protein expression and also perturbing membrane channels. Because of the high toxicity of free heme and its subsequent detection at low cellular concentrations, the prothoracic gland cells cannot store heme and produce heme only when there is a high demand for it. This makes it important that the amount of free heme should be tightly controlled in order to maintain cellular homeostasis and avoid potential pathological conditions.

1.6 Genetic screens conducted to identify candidate genes involved in iron/heme homeostasis and ecdysone production

Steroid hormones regulate the developmental transitions of the fruit fly, *Drosophila melanogaster* during the different stages of postembryonic development starting from first instar formation followed by second instar, third instar, prepupa and pupa which eventually leads to the formation of a fully-grown adult fruit fly by a process called metamorphosis. Steroid hormones are produced by endocrine cells, more specifically the prothoracic gland cells of the ring gland during larval development.

In order to identify the genes and pathways that are responsible for regulating steroid production, a genome-wide genetic screen targeting a total of 12,500 RNAi lines was conducted by the King-Jones lab in collaboration with Dr. Michael B. O'Connor and Dr. Kim F. Rewitz's labs⁵⁷. The *Drosophila* genome-wide *in-vivo* RNAi screen resulted in the identification of 1,906 genes that were potentially responsible for steroid hormone production or steroidogenesis as well as timing the developmental transitions from one stage to another. The screening was conducted by triggering RNAi in the prothoracic gland since the objective was to identify the genes required for the endocrine steroidogenic cell function. The candidate genes were identified based on different developmental defects that were observed, namely, arrest in the first instar larvae (L1), arrest in the second instar larvae (L2), and third instar larvae (L3). Developmental delays observed concerning the eclosion of the adult flies ranged from a delay of approximately one day termed as minor delay, a delay of approximately two days termed as delay, and finally a developmental delay of approximately two days which was termed as a major delay. Apart from screening for the aforementioned developmental delays and defects, the researchers also screened for the premature entry of the second instar larvae into metamorphosis, also called L2prepupa or L2P and observing

lethality in the pupal stage termed as P lethal. A secondary screen was then conducted in the King-Jones lab, whereby approximately 800 genes that survived to L3 and were a subset of the 1,906 genes that came out of the primary screen were targeted again, but this time their effects were observed on the ring glands. A total of 34 genes came out of the secondary screen, of which 21 genes showed large red ring glands, and 13 genes showed large ring glands. The large red ring glands resulted from the accumulation of porphyrins, while the large ring glands resulted from the accumulation of protoporphyrinogens which don't have the ability to fluoresce. The ability of the ring glands to display visible red autofluorescence under UV exposure is attributed to the accumulation of heme precursors, clearly suggesting that all these genes have a possible link to iron/heme homeostasis as well as ecdysone production.

1.7 CRISPR

CRISPR or Clustered Regularly Interspaced Short Palindromic Repeats is a unique family of repeated DNA sequences that consist of 24 to 40 recurrent nucleotide motifs and are separated by regularly-spaced sequences that have a similar size compared to the recurrent units⁵⁸. They were first discovered in the prokaryotic genome, more specifically in *E. coli* back in 1987⁵⁹. The regularly-spaced sequences are called spacer DNA and are not identical. Both *in silico* and biological analysis have established that the spacer DNA has sequence homology with foreign elements, especially bacteriophages, as well as plasmid sequences^{60,61}. The prokaryotes use this fact to their advantage since the CRISPR system allows integration of short pieces of these viral DNA molecules, also called spacer DNA into the CRISPR locus^{62,63}. The CRISPR sequences are transcribed in the cell into pieces of RNA called crRNA or crisprRNA that are subsequently used together with proteins that are encoded by the *cas* genes or crispr associated genes to form interference complexes. More importantly, the tracrRNA or the trans-activating CRISPR RNA, which is derived from the host bacterial cell, is responsible for recruiting the crRNA obtained from the invading virus and, in turn, recruit them to the *cas* genes or proteins^{64,65,66}. This information is then basically used to base-pair with matching sequences from the viral DNA and is responsible for targeting the foreign viral DNA and inhibiting them functionally. The CRISPR-Cas system is an adaptive immune system that has been adopted by the bacteria and archaea to fight against the invading viruses and plasmids⁶⁷⁻⁷². The *cas* proteins contain domains that are characteristic of helicases (responsible for unwinding DNA), nucleases (responsible for cutting DNA), polymerases (responsible for synthesizing DNA from deoxyribonucleotides) and a number of RNA-binding proteins⁷³. PAMs or Proto-spacer adjacent motifs are responsible for determining the spacer precursors or proto-spacers from the invading viral DNA. The PAMs are important since they are

responsible for guiding or directing the *Cas* nuclease to the cut site and are generally found three to eight nucleotides downstream from the cut site^{74,75}. The *Cas9* protein (CRISPR associated protein 9) belongs to the type II CRISPR-Cas system. For the CRISPR constructs that are being generated in the lab these days, it requires the synthetic guide RNA or gRNA, which is essentially a combination of the crRNA and the tracrRNA fused depending on their RNA constructs. The gRNA then combines with the *Cas9* endonuclease to give rise to the highly efficient CRISPR/Cas9 system, which has been proved to work for a variety of animal models such as *Drosophila*, mice, zebrafish as well as human stem cells⁷⁶⁻⁸³.

To generate CRISPR constructs, I followed by the protocol described in Huynh et al., 2018⁸⁴. Since the prothoracic gland is a polytene tissue, it leads to increased nuclear gene content whereby the C value reaches 64 by the end of the third instar larvae⁸⁵. It has become really important to validate the phenotype shown by the target gene of interest using CRISPR/Cas9 since the RNAi has potential off-target sites, multiple RNAi lines need to be present for a particular gene, and all of them need to show similar phenotypic effects for full-proof validation, partial blockage of the expression of the target mRNA is another issue that makes it difficult to trust the RNAi system completely. It is also very challenging to combine two or more RNAi lines since there is a high risk that non-specific targets would be generated. When it comes to overexpressing a particular gene, it is required to clone the full-length of a cDNA for cDNA overexpression, which is quite cumbersome. It is important to choose the right isoform for transgenic cDNA line since it has possible implications concerning the conclusions that are to be drawn from the experiment. Even the GAL4-UAS system shown in Figure 1.5 is not foolproof and has potential loopholes: Gal4 has a strong activation domain, which results in signal amplification and eventually affects how strongly the cDNA is going to be expressed. Also, the UAS-related transgenes show a certain degree of leakiness, which is based on the tissue under inspection as well as the developmental

time. Using more than one UAS-related transgenes results in them competing for the Gal4 binding spot, which leads to the quenching of expression of either transgene. Since Gal4 has been reported to bind non-specifically to endogenous loci, it results in the up and downregulation of hundreds of other genes that are not under consideration and eventually ends up complicating the interpretation of gene expression studies conducted on a genome-wide scale. All the factors as mentioned above highlight the importance of using CRISPR/Cas9 in order to manipulate the gene expression in specific tissues, more specifically in the prothoracic gland.

1.8 Role of different supplements implemented to rescue the developmental defects

We know based on the results from the primary screen conducted in King-Jones lab, Michael O'Connor's lab and Kim F. Rewitz's lab and the secondary screen conducted solely in King-Jones lab that the 34 genes that eventually came out of the screens show certain developmental defects such as delay in pupariation, major third instar larval arrest, major second instar arrest and a few other phenotypes (Danielsen et al., 2016). When the genes were knocked down, the prothoracic gland also displayed red autofluorescence under UV exposure, which corresponds to the accumulation of heme precursors. The phenotypes mentioned above are similar to the phenotypes displayed by the prothoracic gland-specific depletion of heme biosynthetic enzymes such as PPOX, UROD, and FECH. This led me to believe that the developmental defects or delays and the accumulation of heme precursors could be caused by the reduction in cellular iron or heme levels. The objective of trying to rescue the developmental defects displayed because of reduction in cellular heme or iron levels would involve supplementing the fly food with heme, iron, and related supplements and then observe the response of the animals reared on these particular supplements. In order for these experiments to work, Ferric Ammonium Citrate or FAC was employed as a direct substitute for iron⁸⁶. Since iron is required to be incorporated into protoporphyrin IX in order to produce heme in the final step of the heme biosynthesis pathway, observing any degree of rescue by supplementing iron would indicate that the defect was in the final step of the heme biosynthesis pathway and offer further solutions to tackle this problem. If we observe the heme biosynthesis pathway, the normal end product is heme. When heme is produced in excess of what is needed for the production of heme proteins or hemoproteins, the excess heme is oxidized to hematin, which is composed of a hydroxyl group attached to a ferric (Fe^{+3}) atom. When the hydroxyl group is replaced by a chloride ion, it results in the production of

hemin. We know that when heme is not produced as required because of defects in any part of the heme biosynthesis pathway, Aminolevulinic acid synthase (*Alas*) is transcriptionally upregulated in order to compensate for the low levels of cellular heme. Both hemin and heme are known to inhibit ALA synthase allosterically and thereby contribute to the alleviation of the developmental defects that I have already mentioned in the previous sections^{87,88,89}. Hemin was therefore employed as a supplement and observed if hemin feeding was enough to rescue the developmental defects/delays and the accumulation of heme precursors in the prothoracic gland. BPS or Bathophenanthroline sulfonic acid is a known iron chelator that we use to reduce the iron levels in the fly food when added as a supplement. The iron chelator would tackle the problem of iron overload resulting from the accumulation of excess iron in the mitochondria, which leads to oxidative stress-induced cell damage, eventually resulting in developmental defects^{90,91}.

Ecdysone is the principal steroid hormone in insects and responsible for regulating the transition from one developmental stage to another. Halloween enzymes which are responsible for synthesizing the various intermediates of the ecdysone biosynthesis pathway on being depleted, results in the reduction of ecdysteroids, which ends up arresting or delaying the development of affected animals. Neverland⁹², which requires an iron-sulfur center in its catalytic center, displays weak red autofluorescence when knocked down specifically in the prothoracic gland suggesting that feeding the affected animals with components/intermediates of the ecdysone biosynthesis pathway could result in rescuing the developmental defects of the concerned animals. For this purpose, the affected animals were reared on diets that were supplemented with 7-dehydrocholesterol or 7-dC, 20-hydroxyecdysone, or 20E and cholesterol respectively. If the sterol supplements are successful in rescuing the developmental defects of the affected animals, it would suggest the *Zfyp8* does indeed feed into the ecdysone biosynthetic pathway.

1.9 Introduction to *Zfrp8*

Zfrp8 or Zinc-finger protein RP8 is a zinc finger transcription factor gene and is the *Drosophila* ortholog of human *PDCD2* or Programmed Cell Death 2. According to DIOPT⁹³, *Zfrp8* and *PDCD2* share an identity of 40% and a similarity of 53%. PG-specific depletion of *Zfrp8* resulted in the major arrest of third instar larvae. Generating a mutation in *Zfrp8* by mobilizing a P-element located at the 5' end of the *Zfrp8* protein-coding region, *Df(2R)SM206* resulted in severe growth and developmental delays in the concerned animals and were not able to survive beyond the larval stages, although it is not clear which larval stages the authors referred to^{94,95}. Few of the larvae that were able to make it up to the pupal stage have been found to be smaller in size compared to their heterozygous siblings. Approximately 2% of the embryos became adults and were termed escapers, but these animals had poor viability, and the females displayed fertility defects. Another deficiency, *Zfrp8*^{M-1-1}, which was generated by means of an EMS screen and had the conserved glutamic acid 296 changed to a lysine displayed approximately 5% adult survival. *Zfrp8* is important for fly hematopoietic stem cells or HSCs, but their expression decreased as the stem cells differentiated into more mature cells. The human ortholog *PDCD2* has also been found to be highly expressed in human hematopoietic stem cells as well as precursor cells^{96,97,98}. After identifying the requirement of *Zfrp8* in *Drosophila* hematopoiesis, researchers wanted to investigate the molecular function of the gene and on studying the *Zfrp8* phenotype in ovaries were able to find out that loss of *Zfrp8* results in abnormal development of both germline as well as somatic stem cell-derived cells. The *Drosophila* ovary was chosen since it contains two distinct populations of stem cells: Germline stem cells as well as somatic or follicle stem cells located in the germarium⁹⁹⁻¹⁰⁵. *Zfrp8* was also found to be critical for the functioning and survival of stem cells as loss-of-*Zfrp8* resulted in both germline and somatic stem cells to stop dividing and leading

to them being ultimately lost. Interestingly, the loss of germline and somatic stem cells because of loss-of-*Zfrp8* were rescued by the expression of human *PDCD2*, which demonstrated that the molecular function of *Zfrp8/PDCD2* is conserved. Knocking down *Zfrp8* in the ovaries using the *nos-GAL4* germline-specific driver resulted in disorganization of the germarium as well as egg chambers, and this phenotype was rescued by expressing GFP-tagged human *PDCD2* under the same driver which further proved the strong functional conservation between fly *Zfrp8* and human *PDCD2* proteins. *Zfrp8* was reported to interact with the piRNA pathway, which is conserved throughout all metazoans and is also essential for the maintenance of germline stem cells. Further investigation of the piRNA pathway components led the investigators to Fragile-X mental retardation protein or FMRP, which functions as a translational repressor and is also involved in RNA silencing^{106,107}. In *Drosophila*, FMRP is required to maintain germline stem cells and the loss of *Fmr1*, the gene that is responsible for encoding FMRP results in infertility as well as developmental defects in oogenesis and neural development¹⁰⁸⁻¹¹¹. *Fmr1* play a critical role in not only vertebrates but *Drosophila* as well for the maintenance of neural stem cells^{112,113}. In the cytoplasm, FMRP was found to co-localize and associate with Trailer Hitch or *tral* resulting in the formation of a translational repressor complex¹¹⁴. Loss of *tral* in *Drosophila* resulted in phenotypes in the ovary that have similarities with the phenotypes displayed by the piRNA pathway mutants¹¹⁵⁻¹¹⁷. Both FMRP and *tral* are part of the *Zfrp8* complex, whereby it was proved that *Zfrp8* interacts antagonistically with both *Fmr1* and *tral* and suppresses their oogenesis defects. *Zfrp8* is required within the nucleus and is responsible for controlling FMRP localization within the cytoplasm. *Zfrp8* protein is present in both the nucleus and cytoplasm of the *Drosophila* ovary. Based on the interaction between Rps2, which is a component of the small ribosomal subunit¹¹⁸ and *Zfrp8*, it has been proposed that *Zfrp8/PDCD2* interacts with the small ribosomal subunit but not free Rps2 since knocking down *Zfrp8* has been shown to affect the cytoplasmic

levels of several other 40S components namely RpS11(u17) and RpS13(uS15). Although *Zfrp8* KD cells resulted in the reduction of RpS2 levels, the expression of multiple other proteins was not affected and was maintained at normal levels, which led the investigators to suggest that lack of *Zfrp8* affects translation but in a transcript specific manner. Since no clear relation between *Zfrp8* and heme or iron homeostasis and ecdysone biosynthesis has been established to date, my thesis aims to investigate the relationship between *Zfrp8* and iron or heme homeostasis as well as ecdysone biosynthesis based on my proposed model outlined in Figure 1.6.

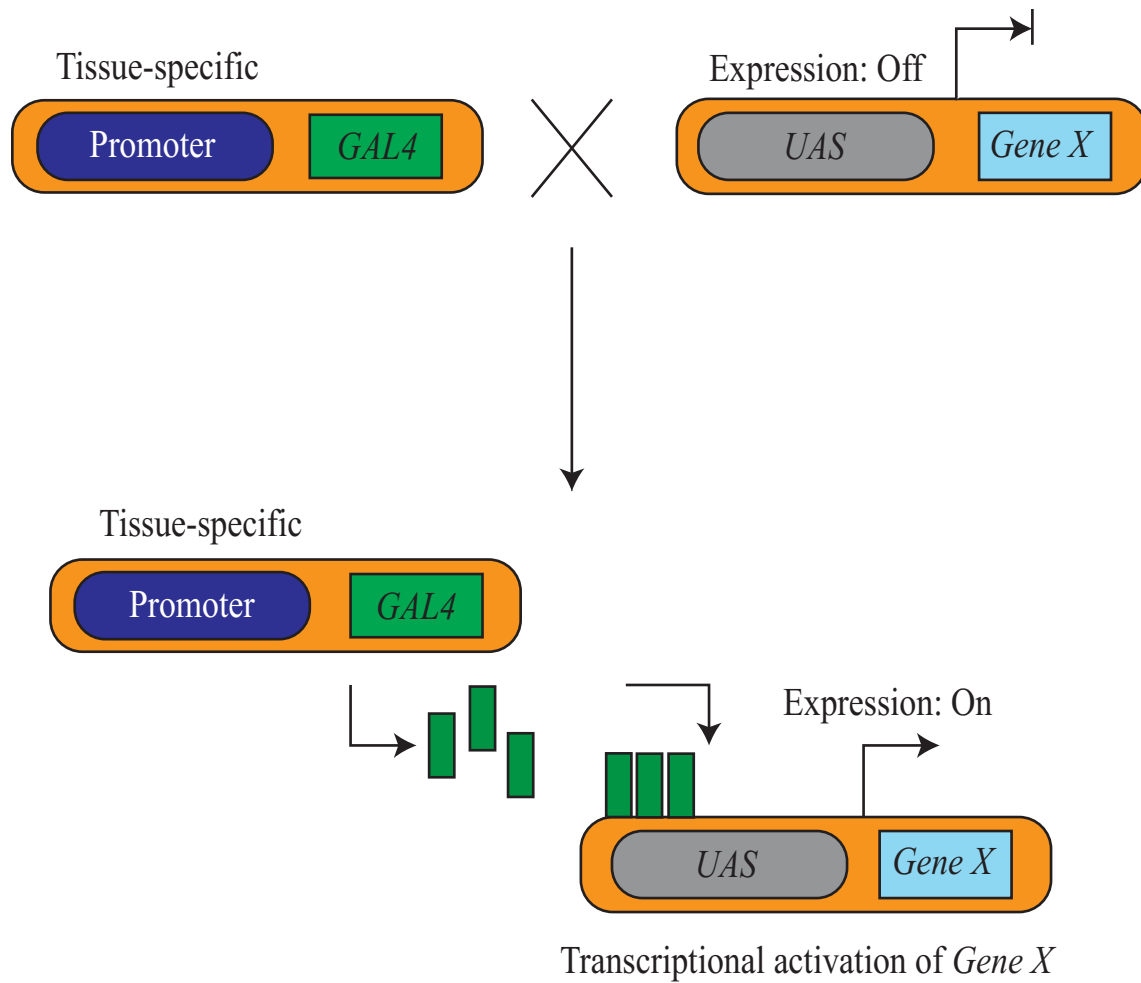


Figure 1.5: Schematic diagram of the *GAL4/UAS* system: The insertion of *GAL4* randomly into the genome drives the *GAL4* expression from different genomic enhancers. The targeted gene is silent in the absence of *GAL4* and its expression is off. In order to activate the gene in a tissue-specific manner, flies expressing *GAL4* are crossed with flies which carry the target gene (*UAS-Gene X*). This activates the gene and the expression of the targeted gene is turned on. Adapted from Brand and Perrimon, 1993.

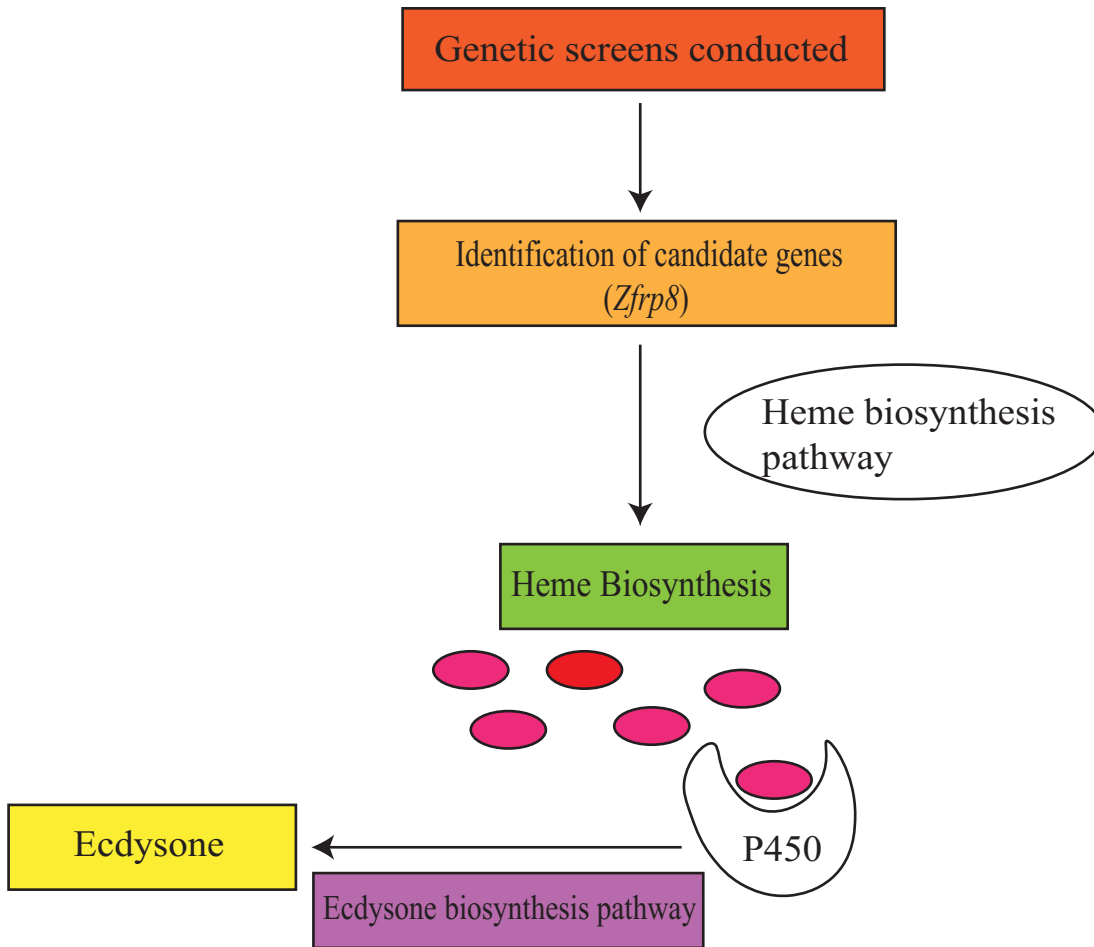


Figure 1.6: Proposed model linking *Zfrp8* to iron/heme homeostasis and ecdysone production: In this model, *Zfrp8* which is one of the candidate genes that came out of the genetic screens conducted when knocked down specifically in the prothoracic gland displayed developmental defects namely major third instar larval arrest and visible red autofluorescence in the prothoracic gland under UV exposure caused due to the accumulation of heme precursors as a result of disruptive heme biosynthesis pathway. The developmental arrest and the delay of the L2/L3 transition by an entire day is caused due to the reduced ecdysone production as a result of disruptions in the ecdysone biosynthesis pathway. Because of the phenotypes associated with the developmental defects, I proposed that *Zfrp8* acts through the heme biosynthesis pathway thereby participating in heme production which results in functional cytochrome P450 enzymes. The P450s synthesize the steps of the ecdysone biosynthesis pathway eventually resulting in ecdysone production.

Chapter 2

Materials and Methods

2. Materials and Methods:

2.1 *Drosophila* stocks and their maintenance

Drosophila melanogaster was maintained on a standard cornmeal medium and Nutrifly Bloomington formulation at a temperature of 25°C to expand the desired stocks. The standard cornmeal medium was made in the fly facility, G-411, Bioscience building at the University of Alberta. The Nutrifly food was made in the lab, and Propionic acid was added as a preservative in order to provide protection against fungal growth and to eliminate isolated instances of mold problems. The fly stocks were kept at a temperature of 18°C for two different purposes: i) The fly stocks were kept overnight to collect virgins in order to set up experimental crosses. ii) The fly stocks were kept in the 5th floor Centre Wing incubator of Bioscience building, University of Alberta, for long-term maintenance. The stocks used in this thesis work has been ordered from the Vienna Drosophila Resource Center (VDRC), Bloomington Drosophila Stock Center (BDSC), donated by Dr. Ruth Steward's lab and are outlined in table 2.1. The *Zfp8*-RNAi1 line has been obtained from VDRC, the *Zfp8*-RNAi2 line from BDSC and *Df(2R)SM206* from Dr. Ruth Steward's lab.

2.2 Preparation of Nutrifly food

The standard composition for preparing 100 ml of Nutrifly food in the lab is as follows: 100 ml of Milli Q water, 17.6 grams of Nutrifly powder (Genesee Scientific, catalog number: 66-113), and 450 µL of propionic acid. The single-source ingredients of the Nutri-fly Bloomington formulation include Yellow cornmeal, Corn syrup solids, Inactive nutritional yeast, Nutri-fly

Drosophila agar, Gelidium, and Soy Flour. First of all, 50 mL of Milli Q was measured in a graduated cylinder and added to an autoclaved flask containing a magnetic bar followed by the addition of 17.6 grams of Nutrifly powder. The entire setup was placed on a magnetic stirrer and heater, and the magnetic bar ensured the homogenous mixing of the already added components in the conical flask. The remaining 50 mL of Milli Q water was then added along the sides of the conical flask to collect the Nutrifly food that adhered while adding it to the flask. The entire mixture was then brought to a boil, the heat was reduced immediately afterward, and the mixture was covered to simmer for 10 mins. The mixture was occasionally stirred during this period of 10 mins. After the mixture cooled down, 450 μ L of propionic acid was added to the mixture. The final mixture was then mixed thoroughly by vigorous shaking and added to vials, bottles, and caps for experimental purposes. In order to prepare higher volumes of food, all of the components, as mentioned earlier, required to make Nutrifly food were multiplied by the same factor to maintain consistency throughout the experiments.

2.3 Preparation of special fly media

2.3.1 Preparation of Iron supplemented diet

To prepare Nutrifly food supplemented with iron, Ferric Ammonium Citrate, or FAC (Sigma Aldrich, CAS number: 1185-57-5, MW: 261.98 g/mol) stock solution at a concentration of 1M was prepared in Milli Q water. 200 μ L of the stock solution was then added to 200 mL of Nutrifly food to achieve a final concentration of 1 mM.

2.3.2 Preparation of Hemin supplemented diet

To prepare Nutrifly food supplemented with Hemin, Hemin (Sigma Aldrich, catalog number: H9039-1G) stock solution was prepared by dissolving 0.25-gram Hemin powder in 10 mL 1.4 M NaOH. The resulting stock solution had a concentration of 38.3 mM. To achieve a final working concentration of 1 mM, 2.61 mL of the Hemin stock solution was added to 100 mL of Nutrifly food. To prepare the control food, 2.61 mL of 1.4 M NaOH was added to 100 mL of Nutrifly food.

2.3.3 Preparation of Iron chelator supplemented diet

To chelate the available iron in the Nutrifly food, Bathophenanthrolinedisulfonic acid, or BPS (Sigma Aldrich, catalog number: 146617-1G), the stock solution was prepared at a concentration of 0.5 M by mixing with Milli Q water and stored at -20°C. To achieve a final working concentration of 100 µM, 40 µL of the stock solution was added to 200 mL of Nutrifly food.

2.3.4 Preparation of Cholesterol supplemented diet

To prepare Nutrifly food supplemented with Cholesterol, 4 mg of Cholesterol (Sigma Life Science, catalog number: C8667-25G) was added to 1 mL of 100% ethanol and mixed thoroughly by placing on a shaker to prepare the stock solution. To achieve a final working concentration of 0.02 mg/mL, 1 mL of the stock solution was added to 200 mL of Nutrifly food. To prepare control food, 1 mL of 100% ethanol was added to 200 mL of Nutrifly food and mixed properly.

2.3.5 Preparation of 20-Hydroxyecdysone supplemented diet

To prepare Nutrifly food supplemented with 20-Hydroxyecdysone or 20E, 66 mg of 20E (Steraloids, inc. catalog number: C7980-000) was added to 1 mL of 100% ethanol and mixed thoroughly by placing on a shaker to prepare the stock solution. To achieve a final working concentration of 0.33 mg/mL, 1 mL of the stock solution was added to 200 mL of Nutrifly food. To prepare control food, 1 mL of 100% ethanol was added to 200 mL of Nutrifly food and mixed properly.

2.3.6 Preparation of 7-dehydrocholesterol supplemented diet

To prepare Nutrifly food supplemented with 7-dehydrocholesterol or 7-dC, 20 mg of 7dC (Steraloids, inc. catalog number: C3000-000) was added to 1 mL of 100% ethanol and mixed thoroughly by placing on a shaker to prepare the stock solution. To achieve a final working concentration of 0.1 mg/ mL, 1 mL of the stock solution was added to 200 mL of Nutrifly food. To prepare control food, 1 mL of 100% ethanol was added to 200 mL of Nutrifly food and mixed properly.

2.4 Collecting eggs and analyzing vials for rescue experiments

Crosses were set up in cages and kept in a 25°C incubator for the following two days. After two days, the caps on the cages containing Nutrifly food were replaced with grape fruit caps for the next two hours. From the 3rd hour onwards, eggs were collected for each replicate. Fifty eggs were collected for each replicate and transferred to the caps containing fresh Nutrifly food or

Nutrifly food containing the desired supplement. The eggs were collected from 3rd hour onwards to increase the possibility of collecting new eggs. Grape fruit caps were used for better visibility of the eggs during their collection. The food containing the eggs were staged 48 hours or 72 hours after the collection of eggs, depending on the crosses set up. The larvae undergoing the L2/L3 molt were identified and transferred to the vials and kept in the 25°C incubator. For the next few days, the vials were observed at regular intervals, and the number of pupae and the number of adults that eclosed from the vials were noted down until no more adults eclosed from the vials.

2.5 Staging

The staging is done during the transition from second instar larvae (L2) to third instar larvae (L3). Staging involves going through the food containing the larvae to select the larvae that have freshly transitioned from late second instar larvae to new third instar larvae. When the food is staged for the first time, the larvae that have already transitioned to the third instar are discarded since we do not know the exact time the third instar larvae underwent the transition. The food is then staged after one hour from that time point onwards until the required number of larvae has been collected. The ring glands are then dissected 42 hours after the L2/L3 molt corresponding to the major ecdysone pulse.

2.6 Generation of CRISPR constructs

2.6.1 Identification of candidate target sites for gRNA

The sequence location for the target gene was obtained from Flybase and entered into the “Enter Gene ID, Symbol or chromosome location” section of the “Find CRISPR” sub-section of the DRSC/TRiP Functional genomics resources website (<https://www.flyrnai.org/crispr/>)¹¹⁹. The options chosen made sure that there were no predicted off-target sites, and the selection was the most stringent concerning mismatches. A map was generated on the submission of the query highlighting the sites with no off-target sites.

2.6.2 Validation of candidate target sites

DNA was extracted from flies on which the embryo injection was performed along with the G0 cross and the balancer lines to make sure that the target sites also exist in those lines. PCR primers listed in table 2.2 were designed to cover the region of interest. PCR followed by sequencing was conducted to verify the accuracy of the target sites. The map of the desired plasmid was then generated using SnapGene Viewer.

2.6.3 Preparing pCFD5 backbone

The gRNA plasmid was digested with BbsI restriction enzyme by mixing the following reagents: 2 μ L of 10X CutSmart Buffer (NEB B7204S), 9.2 μ L of gRNA plasmid, 1 μ L of BbsI HF (NEB R3539S) and 7.8 μ L of Nuclease-free water. The reaction was then incubated overnight

at 37°C. Following the incubation overnight, 1 µL of CIP (NEB M0290S) was added to the reaction and incubated at 37°C for 1 hour. This step reduced the self-ligation of the two phosphorylated ends of the backbone after digestion. The digested backbone was then purified using ethanol precipitation mentioned in section 3.14. The backbone was eluted with nuclease-free water to bring the final concentration to approximately 50-100 ng/µL. The final product was used for several other cloning reactions later.

2.6.4 Preparing gRNA fragments (two gRNAs)

The gRNAs were cloned by setting up a PCR reaction using High Fidelity Polymerase (NEB M0491S). The reagents used in the reaction are outlined in table 2.3. The reagents were then mixed by centrifuging them in a mini-centrifuge for 30 seconds, followed by vigorously shaking them for another 20 seconds. The reaction was then run in a thermocycler following the conditions outlined in table 2.4. Following the completion of the PCR, the PCR product was run on a gel to check the accuracy of the result. The PCR product was then digested with DpnI (NEB R0176S) overnight at 37°C to eliminate the original template. The PCR fragment was then purified following the instructions mentioned in section 3.14.

2.6.5 Gibson reaction

In order to set up a Gibson assembly reaction, the amount of each fragment to be used in the reaction was calculated from the website <https://nebiocalculator.neb.com/#!/ligation>. Based on the calculations, insert DNA length of 233 bp, vector DNA length of 6443 bp, and vector DNA mass of 105.51 ng was used. The recommended ratio for PCR fragment: backbone was 5:1

corresponding to which the insert DNA mass was 19.08 ng. Following the calculations, the reagents were mixed in the following amounts: 1 μL of the PCR fragment, 1 μL of the backbone, and 6 μL of the Gibson master mix (NEB E2611S). The reaction was then incubated in a thermocycler at 50°C for 4 hours. The reagents are outlined in table 2.5.

2.6.6 Purification of plasmid DNA

DH5 α bacterial culture was harvested by centrifugation at 4000 rpm in an Eppendorf centrifuge 5810R (15 amp version) for 10 minutes at room temperature. 250 μL of resuspension culture was added to the pelleted cells, and vortexed to resuspend the pelleted cells. 250 μL of lysis solution was added to the sample, and the tube was inverted for 4 to 6 times to ensure homogenous mixing. The sample was then incubated at room temperature for 5 minutes. Following the incubation, 350 μL of Neutralization reaction was added to the sample, and the tube was inverted for 4 to 6 times. The sample was then centrifuged at 13000 rpm for 5 minutes at RT. The supernatant was then transferred to the Thermo scientific GeneJET spin column, centrifuged at 13000 rpm for 1 minute at RT, and the flow-through was discarded. This resulted in the plasmid DNA binding to the column. 500 μL of wash solution was added to the column and centrifuged at 13000 rpm for 1 minute at RT. The procedure mentioned in the last line was repeated one more time. The flow-through was discarded both the times after the centrifugation. The empty column was then centrifuged at 13000 rpm for 1 minute at RT. The column was then transferred to a new tube. 50 μL of elution buffer was added to the column and incubated for 2 minutes. Following the incubation, the sample was centrifuged for 13000 rpm for 2 minutes at RT. The flow-through was collected, which contains the plasmid DNA. Nanodrop was used to measure the plasmid DNA

concentration. Thermo scientific GeneJET Plasmid Miniprep Kit (#K0503) was used for this experiment.

2.6.7 Transformation

A tube of competent cells was taken out from -80°C , thawed on ice for approximately 10 to 15 minutes. $2\ \mu\text{L}$ of the Gibson mixture containing $1\ \mu\text{g}$ - $100\ \text{ng}$ of plasmid DNA was added to $50\ \mu\text{L}$ of the competent cells. The tube was carefully flicked for 4 to 5 times to mix the cells and DNA properly. The mixture was placed on ice for 30 minutes. The mixture was then given a heat shock at exactly 42°C for 30 seconds, followed by placing the mixture on ice for 5 mins. The heat shock creates a pressure difference between the interior and the exterior of the cell which results in the formation of pores thereby facilitating the entry of plasmid DNA. $950\ \mu\text{L}$ of room temperature LB was then added to the mixture and placed at 37°C for 60 mins and shaken vigorously at 250 rpm. During this period, the selection plates containing Ampicillin were warmed to 37°C . After an hour, $250\ \mu\text{L}$ of the mixture was spread onto a selection plate. This was done for a total of four plates, and the plates were incubated overnight at 37°C .

2.6.8 Screening for positive cloning

The transformation plates were collected after an incubation period of approximately 18 to 20 hrs. Eight individual colonies were then picked up from the transformation plates, and aseptically transferred to 8 individual liquid cultures. The liquid cultures were then incubated overnight at

37°C. The next day, the plasmids were purified following the instructions mentioned in section 3.6.6 and sent for sequencing in MBSU. The primer used was pCFDseq (Table 2.2).

2.6.9 Midiprep

High-efficiency transformation of the samples that gave positive cloning results after sequencing was conducted following the instructions mentioned in section 3.6.7. Following transformation, a bacterial colony was added to 100 mL of LB containing 100 µL of Ampicillin and was incubated at 37°C overnight. The bacterial culture was divided into two 50 mL falcon tubes the following day. The bacterial cells were harvested by centrifuging them at 6000 rpm for 15 mins at 2°C, and the supernatant was discarded. The bacterial pellets were resuspended in 4 mL of Buffer P1. 4 mL of Buffer P2 was added to the sample and was mixed thoroughly by vigorously inverting the sealed tube 4 to 6 times. The sample was incubated at room temperature for 5 mins. 4 mL of chilled buffer P3 was then added to the sample, mixed immediately and thoroughly by vigorously inverting the tube 4 to 6 times, and the sample was incubated on ice for 15 minutes. The sample was then centrifuged at 8000 rpm for 30 mins at 2°C. The supernatant containing the plasmid DNA was removed promptly to a new tube. The supernatant was centrifuged again at 8000 rpm for 15 mins at 2°C, and the supernatant containing the plasmid DNA was removed to a new tube promptly. The second centrifugation step was carried out to avoid applying the suspended or particulate material to the QIAGEN-tip. 4 ml of buffer QBT was applied to a QIAGEN-tip 100 for equilibration purpose, and the column was allowed to empty by gravity flow. The supernatant collected earlier was then applied to the QIAGEN-tip and allowed to enter the resin by gravity flow. The QIAGEN-tip was washed twice with 10 mL buffer QC. The DNA was then eluted with 5 mL buffer QF. 3.5 mL of RT isopropanol was added to the eluted DNA, mixed and centrifuged

immediately at 10000 rpm for 30 mins at 4°C. Following the centrifugation, the supernatant was decanted. The DNA pellets were washed with 2 mL of 70% ethanol kept at RT and centrifuged at 10000 rpm for 10 mins. The supernatant was carefully decanted without disturbing the pellets. The pellets were air-dried for 10 mins, and the DNA was re-dissolved in 10 µL of nuclease-free water. Nanodrop was used to measure the final concentration. For Midiprep, Thermo fisher scientific GeneJET Plasmid Midiprep kit (K0481) was used.

2.7 Embryo injections

The concentration of the plasmid purified using Midiprep was diluted down to 550 µg/µL using DNase and RNase-free water to make sure that the concentration used was optimal because of a high concentration of plasmid injected into the embryos usually prove to be lethal. The first step involves the preparation of injection needles. The needles to be used for injection were prepared using a flaming/brown micropipette puller, model P-87, and was used with the following settings: heat-590, time-170, vel-250, and pull-250. An 18 mm x 18 mm coverslip was broken into half and placed on a microscope slide. The broken edge of the coverslip was covered with halocarbon oil, and the slide was placed on the microscope. The unbroken needle tip and the broken edge of the coverslip were carefully brought into the same plane of focus. The tip of the needle was then broken to generate a beveled edge by moving the broken coverslip against the needle after pressure was applied to the syringe. To break the needle, halocarbon oil 700S was used, which also covered the margin. A total of 3 µL injection mix was added to the needle. The beveled tip was preferred over the blunt tip since they cause less damage to the embryo, thereby resulting in higher survival rates. Another essential component of this procedure: Fresh glue was prepared by adding double-sided scotch tape (Scotch 665) and 10 mL Heptane (enough to immerse the tape completely) in a

small vial. The vial was then sealed using parafilm (Bemis, Product number: #PM999) and left on a shaker overnight. The glue was made, keeping in mind that it has to be adhesive enough so that it is possible to mount the embryos while injecting them on the microscopic slide. However, it should not be super viscous so that it is difficult to pipette the glue on to the microscopic slide.

The flies BL-25709 (*y, w, nos phiC31 nls integrase; attP40, y+*) were expanded into multiple bottles. Young flies (approximately 2-3 days old) were then transferred into a cage and kept in an incubator overnight to speed up the process of egg-laying in order to get the maximum number of eggs on the day of injection. The cage was also lined with a regular paper in order to create more surface area for the flies to mate. The next day, a new collection cap containing grape-juice agar and yeast was added to the cage every 1 hour to reduce the possibility of collecting old eggs. The freshly-laid embryos were collected from the cap introduced after three hours from the beginning of this process for injection. Once the injection started, embryos were collected every 20 to 30 minutes to make sure that the embryos were as young as possible. The embryos were transferred to a freshly-prepared 50% bleach solution in a petri dish using a paintbrush and kept there for 45 seconds, which dechorionated the embryos. The dechorionated embryos were then washed with distilled water twice for 20 seconds each time. Since the entire procedure was conducted in an 18°C room, the growth of the embryos was slowed down. The embryos were lined up on grape-juice agar with their anterior and posterior part in the same direction. The embryos were transferred from the cap onto the injection slide by placing the tape on the embryos making sure that the posterior end was facing outwards for injection. The embryos were then placed in a desiccating chamber for 5 minutes. After the embryos were dry, halocarbon oil was used to submerge all the embryos and maximize the survival chances of the embryos after injection. The posterior of the embryo and the freshly-prepared needle were brought into the same focal plane, and the embryo was pierced by moving the stage towards the needle and not the other

way around. Optimum pressure was applied to inject the DNA solution, and the same procedure was repeated for every embryo on the slide. Vaseline was then applied encircling the newly-injected embryos, which were then covered with halocarbon oil. The slides containing the injected embryos were then placed in a humid chamber and kept in the 18°C incubator. After 24 hours, the L1 larvae were transferred to kitchen food, which was broken up by paintbrush to ensure proper and comfortable feeding¹²⁰.

2.8 RNA extraction of Whole-body samples

Five larvae were collected 42 hours after their L2/L3 molt for each replicate for a total of three replicates. The larvae were washed in 1% PBS for a total of three times, amounting to five minutes for every wash. The larvae were then transferred to 200 µL TRIzol for each replicate and flash-frozen in liquid nitrogen. This was followed by homogenizing the larvae with pestles that were pre-soaked in 1% Sodium dodecyl sulfate. The volume of the sample in the 1.5 mL tubes was then brought to 1 mL by adding more TRIzol. The entire volume of the samples was then vortexed thoroughly to ensure proper mixing followed by incubation at room temperature for 5 minutes. After the incubation, 200 µL of chloroform was added to the samples and shaken vigorously for 15 seconds. This was followed by another round of incubation at room temperature for 3 minutes. The samples were then centrifuged for 15 minutes at 4°C at 12000 rpm/ revolutions per minute. The upper, colorless, aqueous phase of the samples was then transferred to new 1.5 mL tubes. This was done without touching the interphase. 500 µL of isopropanol was then added to each sample, followed by inverting them five times to ensure homogenous mixing. The samples were then incubated at room temperature for 10 minutes, followed by centrifuging them for 15 minutes at 4°C at 12000 rpm. The supernatant was removed for each sample, and the pellets were then washed

with 1 mL of freshly prepared 70% ethanol and vortexed thoroughly followed by another round of centrifugation for 5 mins at 4°C at 12000 rpm. The supernatant for each sample was removed following the centrifugation, and the pellets were air-dried at room temperature for 5 to 10 minutes.

The air-dried pellets were then dissolved in 120 µL of RNAase free water at room temperature over the next 3 to 5 mins. 200 µL of chloroform was added to each of the samples and shaken vigorously by hand for 15 seconds, followed by incubation at room temperature for 3 minutes. The samples were then centrifuged for 15 mins at 4°C at 12000 rpm. The upper aqueous phase was then transferred to a new 1.5 mL centrifuge tube. 10 µL of 8M RNAase free LiCl solution was then added to the freshly collected aqueous phase for each sample and mixed thoroughly by inverting the tubes. 300 µL of 100% technical grade ethanol was then added to each sample and incubated on ice for the next 3 to 5 mins. The samples were then centrifuged at 0°C for 20 mins at 12000 rpm, followed by the removal of the supernatant. The pellets were then washed gently with 1 mL of 70% ethanol and centrifuged at 12000 rpm for 2 mins at 4°C. The supernatant was removed, and the pellets were air-dried at room temperature. The entire procedure outlined in this paragraph was repeated once more before dissolving the air-dried pellets in 10 µL of RNAase free water to obtain the final product. Nanodrop was then used to determine the final concentration of the finished product.

2.9 Verification of extracted RNA quality

The quality of the RNA extracted was measured using a 2100 Bioanalyzer instrument from Agilent and was used in combination with the Agilent RNA 6000 Nano kit. The entire procedure was demonstrated by Troy Locke from MBSU.

2.10 cDNA synthesis

RNA samples were bioanalyzed (an optional procedure) and standardized to 1 µg/µL before proceeding to cDNA synthesis. 9 µL of RNAase free water was added to a 0.2 mL PCR tube for each RNA sample. A master mix was prepared to contain the following components: 2 µL of 10X Reverse Transcriptase buffer, 0.8 µL of 25X dNTP mix (100 µM), 2 µL of 10X random primers and 4.2 µL of PCR grade water totaling 9 µL for each reaction. 1 µL of RNA sample was added to each of the 0.2 mL tubes containing 9 µL of RNAase free water. 9 µL of the master mix was added to each tube, followed by the addition of 1 µL of reverse transcriptase to each reaction tube. The different components in the 0.2 mL PCR tube were then mixed thoroughly by centrifuging them for 30 seconds, followed by vigorous shaking for 20 seconds. The samples were then run in the thermocycling program mentioned in table 2.9. The volume of each reaction was measured precisely using a pipette after the reaction was complete and diluted 1/20 with PCR grade water. The cDNA samples were then stored at 4°C until further use. The High-Capacity cDNA Reverse Transcription Kit was ordered from Thermo Fisher Scientific (catalog number: 4368814).

2.11 Validating qPCR primers

The primers that have been used for the qPCR experiments were designed by Roche's online primer design database¹²¹ by previous members of the lab and ordered through Integrated DNA technologies¹²². The sole purpose of conducting the primer validation experiment is to validate the accuracy and specificity of the ordered primers. Third instar whole body larval cDNA that was extracted from *w¹¹¹⁸* was serially diluted into samples of the following concentrations: ¼, 1/16,

1/64, 1/256, and 1/1024 using 20 μL of cDNA and 60 μL of RNAase free water every time. Both the forward and reverse primers of a particular gene were mixed to generate a single primer master mix having a final concentration of 3.2 μM . The following reagents were then mixed for each dilution: 5 μL of SYBR Green master mix (Thermo Fisher Scientific, catalog number: 4344463), 2.5 μL of the primer master mix and 2.5 μL of cDNA totaling a volume of 10 μL . All of the dilutions were prepared in triplicates. The standard curve was generated on a QuantStudio™ 6 Flex Real-Time PCR system. The software generates a real-time standard curve, amplification plot, and melt curve, which were subsequently analyzed and compared to *rp49* since it has a stable expression because of being transcribed continuously throughout the experiment.

2.12 Preparation of Grape food plates

700 mL of Milli Q water was thoroughly mixed with 30 grams of agar by a magnetic stirrer present in an already autoclaved flask. The solution was then autoclaved for an hour. After the autoclaving was done, the solution was cooled for the next 40 to 45 minutes. During this period, 0.5 gram of methyl paraben was mixed with 20 mL of 100% ethanol in a 50 ml tube and put on a shaker for homogenous mixing. The methyl paraben solution along with 295 mL of Minute maid grape punch was then added to the autoclaved solution, and the entire flask containing the solution was shaken vigorously to ensure homogenous mixing. The grape punch mixture was then poured onto small and large caps and also Petri dishes for experimental purposes. The caps and Petri dishes were then stored at 4°C for long-term storage.

2.13 Extracting DNA from adult flies

Sixty young adult flies (1-2 days after their eclosion) were selected and added to a 1.5 ml tube followed by flash freezing them in liquid nitrogen. 3 to 4 pestles were then put into liquid nitrogen and used to grind the flies manually, making sure that the flies are grind to a homogenous powder. 200 μ L of DNAzol was then added to the tube containing the fine powder followed by further grinding using a pestle with a mixer for 15 seconds. The step mentioned in the last line was then repeated two more times. 400 μ L of DNAzol was further added to bring the total volume up to 1000 μ L and vortexed for 15 seconds, and the sample was left at room temperature for 5 mins. The pestles were rinsed properly in the DNAzol before being discarded. The sample was then centrifuged at 13000 rpm for 15 mins at 4°C. Following the centrifugation, the green viscous supernatant was transferred to a new tube using a cut pipette tip for easy collection. 600 μ L to 800 μ L of chloroform was then added to the sample to ensure a 1:1 ratio and inverted for 2 to 3 times to ensure homogenous mixing. The sample was then spun at 13000 rpm for 2 mins at 4°C followed by transferring the upper phase (green viscous phase) into a new 1.5 mL tube. 500 μ L of 100% ethanol was added to the sample and mixed properly by shaking on a shaker for 3 minutes at room temperature. The sample was then centrifuged for 2 mins at 13000 rpm at 4°C. This particular centrifugation yielded DNA pellets along with polysaccharides and proteins and so the supernatant was discarded. 800 μ L of 70% ethanol was added to the sample and the tube was inverted for 3 to 4 times. The sample was then centrifuged for 1 minute at 13000 rpm at 4°C and the supernatant was discarded followed by air drying the pellets for 3 minutes at room temperature. 100 μ L of RNAase free water was added to the sample and the pellet was dissolved by shaking and using P10 pipette tips for 25 minutes on the shaker under the fume hood. 200 μ L of chloroform was

added to the sample and mixed by inverting for 3 to 4 times. The sample was then centrifuged for 2 minutes at 13000 rpm at 4°C, and the upper phase was transferred to a new 1.5 ml tube using a P100 pipettor. 4 µL of 5M sodium chloride was added to the sample and mixed by pipetting. 500 µL of 100% ethanol was added to the sample and mixed by shaking on a shaker for 3 minutes at room temperature. The sample was then centrifuged at 13000 rpm for 2 minutes at 4°C, and the supernatant was discarded. 800 µL of 70% ethanol was added to the pellet and mixed properly by inverting the tube for 3 to 4 times. The sample was then centrifuged for 1 minute at 13000 rpm and 4°C followed by discarding the supernatant, and the pellets were air-dried for 3 minutes at room temperature. 200 µL of 8 mM sodium hydroxide solution was added to the sample, and the DNA pellets were dissolved to yield the final product. The DNA concentration was then measured using Nanodrop (Thermo Scientific, Nanodrop 1000 Spectrophotometer). DNA was extracted for the following fly lines: $y^1v^1P(\text{nos-PhiC31.NLS};)X$; $P(\text{carryP})attP40(II)$ (#25709), $y^2cho^2v^1$ (TBX-0004) and $y^2cho^2v^1; sco/Cyo$ (TBX-0007).

2.14 Purification of PCR products

200 µL of 100% ethanol was added to 20 µl of the target PCR product and mixed properly by pipetting up and down. The sample was then kept at -20°C for 45 minutes. After 45 minutes, the sample was centrifuged at 12000 rpm at 4°C for 10 minutes, and the supernatant was discarded. 500 µL of 75% ethanol was added to the sample, and the sample was then centrifuged for 1 minute at room temperature. The supernatant was discarded, and the pellet was air-dried for 5 to 10 minutes. 50 µL of nuclease-free water was added to the air-dried pellet, which yielded the final product. The DNA concentration was then measured using Nanodrop.

2.15 Preparation of Competent cells

The preparation of competent cells is a multi-day process where day 1 involves growing the bacterial DH5 α cultures. Following transformation, a single bacterial colony was aseptically picked up from a plate that was incubated for approximately 18 hours at 37°C. The bacterial colony was then transferred into 5 mL of LB broth. The culture was then incubated for approximately 16 hours at 37°C with vigorous shaking (250-300 rpm). 100 μ L of the DH5 α culture was added to 100 mL of LB broth, placed on a shaker and shaken moderately at room temperature overnight. The OD of the culture was measured at a wavelength of 600 nm using a spectrophotometer every 30 minutes the next day (day 2) until the OD was 0.5. The culture vessel was then transferred to an ice water bath for 10 minutes. The cells were harvested by centrifugation at 2500 rpm for 10 minutes at 4°C in a 50 mL falcon tube. The medium was poured off, and the tube was dried by inverting it on a paper towel for 2 minutes. The cells were then resuspended gently by swirling them in 80 mL of ice-cold Inoue transformation buffer. The cells were harvested again by centrifuging them at 2500 rpm for 10 minutes at 4°C. The medium was dried off, and the tube was dried gently on paper towels for 2 minutes. The cells were gently resuspended in 20 mL of Inoue transformation buffer kept at 0°C. 1.5 mL of DMSO was added and swirled to mix the bacterial suspension. The suspension was stored on ice for 10 minutes. 50 μ L aliquots of tubes were then quickly dispensed into chilled, sterile microfuge tubes. The resulting competent cells were then snap-frozen by placing the microfuge tubes in liquid nitrogen, and the stock was stored at -80°C. Whenever the competent cells were needed for experimental purposes, the microfuge tubes were removed from -80°C, thawed in ice, and used immediately. The entire procedure was conducted following the instructions from Inoue, *et al.* (1990)¹²³.

2.16 Preparation of PBS

A stock solution of 10X PBS was prepared by mixing 25.6 grams of $\text{Na}_2\text{HPO}_4 \cdot 7\text{H}_2\text{O}$, 80 grams of NaCl, 2 grams of KCL, and 2 grams of KH_2PO_4 . The total volume of the mixture was brought to 1 liter by mixing with distilled water. The solution was then autoclaved for 40 minutes. 50 mL of the 10X PBS stock solution was then added to 450 mL of distilled water to prepare 1X PBS, and the solution was autoclaved to obtain the final product.

2.17 Preparation of Antibiotics

One gram of Ampicillin (catalog number 69-53-4) in powder form was measured and added to 20 mL of Milli Q water. Ample time was given to make sure that the Ampicillin completely dissolved in the Milli Q water. The resulting solution was then filter sterilized using a 0.22 μm filter and aliquoted into twenty 1.5 mL Eppendorf tubes (Thermo Scientific, Catalog number: 69715). The final concentration of the stock solution was 75 mg/mL. The stock solution was then stored at -20°C for long-term storage.

2.18 Immunofluorescence

The technique used in this thesis was adopted from Cell Signaling technology¹²⁴. The GFP-Flag tagged line of *Zfp8* from VDRC was used for this experiment. The larvae were dissected 42 hours after their L2/L3 molt. Post dissection, the ring glands were fixed in 4% formaldehyde for 20 minutes. This was followed by washing the samples in 1X PBST for 3 X 10 minutes. The samples were then stained in DAPI, followed by washing them in 1X PBST for 3 X 10 minutes.

The samples were then blocked in blocking buffer for 60 minutes. While blocking, the primary antibody was prepared by diluting in antibody dilution buffer. For the primary mouse anti-FLAG antibody (NEB 8146S), the dilution used was 1:1600. For the primary mouse anti-GFP antibody (Life Tech GF28R), the dilution used was 1:400. The samples were then incubated overnight in the diluted primary antibody at 4°C. The following day, the samples were washed in 1X PBS for 5 minutes for a total of 3 times. The samples were then incubated in diluted secondary antibody for 2 hours at room temperature in the dark. The dilution used for the secondary antibody was 1:1000 (Goat Anti-Mouse IgG H&L (Alexa Fluor® 488)). Following the incubation in the dark, the samples were washed in 1X PBS for 5 minutes for a total of 3 times. The samples were then fixed in slides and stored at 4°C protected from light.

2.19 ImageJ

ImageJ software (Schneider et al., 2012, Abramoff et al., 2004) was used to calculate the pixel intensity of the ring glands under study. Since the images had RGB values, the results were calculated using brightness values. RGB pixels were converted to brightness values using the formula: $\text{Value} = (\text{Red} + \text{Green} + \text{Blue}) / 3$. In other words: the higher the brightness value, the higher the intensity of red autofluorescence. After selecting the area of the ring gland, the software generated the mean brightness value for that sample. I decided to choose the brightness value of 10000 as the standard for determining whether the ring gland under consideration was displaying high-intensity red autofluorescence or low-intensity red autofluorescence. Any sample that had a brightness value of over 10000 was considered to display high-intensity red autofluorescence, and anything below 10000 was considered to display low-intensity red autofluorescence. The decision to choose the brightness value of 10000 as the standard for differentiating high-intensity and low-

intensity red autofluorescence was arbitrary. However, it resulted in a data-set that corroborates the rescue data, thereby signifying its biological relevance. All the images were studied under the same experimental conditions (Exposure time: 3 seconds).

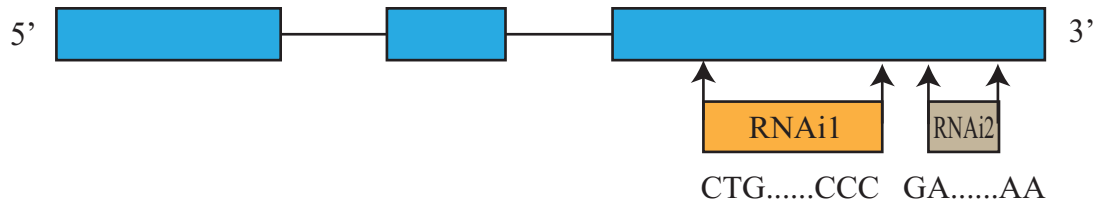


Figure 2.1: Illustration of *Zfrp8* transcription unit: The blue rectangles represent the exons and the lines joining the exons represent the introns of the transcription unit of *Zfrp8*. The orange rectangle represents the region of *Zfrp8* that is targeted by RNAi1 (VDRC id:11521) and the grey rectangle represents the region that is targeted by RNAi2 (BDSC id: 36581). The nucleotides underneath RNAi1 and RNAi2 denote the starting and ending nucleotides of the targeted region.

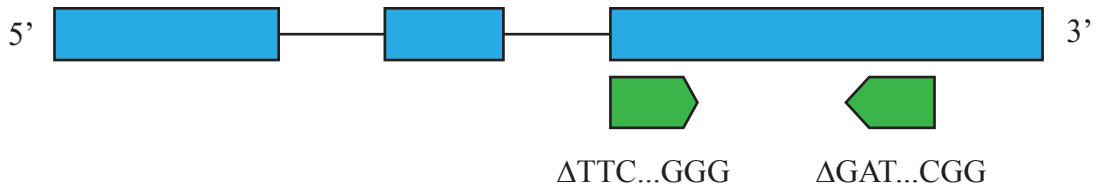


Figure 2.2: Illustration of the transgenic 2xgRNA line constructed: The blue rectangles represent the exons and the lines joining the exons represent the introns of the transcription unit of *Zfrp8*. The green arrows located beneath the third rectangle from the left or Exon 3 refer to the *Zfrp8* Knockout gRNA1 and gRNA2 respectively. The nucleotides underneath gRNA1 and gRNA2 denote the starting and ending nucleotides of the deleted region.

Table 2.1: *Drosophila melanogaster* lines used for the experiments conducted in this thesis:
The fly lines were obtained from Vienna *Drosophila* research center (VDRC), Bloomington *Drosophila* stock center (BDSC), Michael O'Connor's lab and Ruth Steward's lab:

Genotype	Flybase ID	Source
<i>w¹¹¹⁸</i>	FBst0005905	BDSC
<i>y,w,nos phiC31 nls integrase;attP40,y+</i>	FBti0077396	BDSC
<i>phantom22-Gal4</i>	N/A	Michael O'Connor
<i>w¹¹¹⁸;P{GD4600}v11521</i>	FBst0450284	VDRC
<i>y¹v¹;P{TRiP.HMJ02095}attp40</i>	FBst0042528	BDSC
<i>y¹sc[*]v¹sev²1;P{TRiP.GL00541}attP2</i>	FBst0036581	BDSC
<i>PBac{fTRG00630.sfGFP-TVPTBF}VK00033</i>	FBst0491649	VDRC
<i>Df(2R)SM206</i>	N/A	Ruth Steward

Table 2.2: Primers used for qPCR, cloning and sequencing:

Primer	Sequence	Description
PCR		
<i>Zfp8</i> Forward	5'-CTG CCA GGA GGC CCA AAA TG-3'	
<i>Zfp8</i> Reverse	5'-GAT GAG AAG CTC CTC CAC GTA G-3'	
<i>Zfp8</i> _pCFD5 Forward	5'-TTC GAT TCC CGG CCG ATG CAG ATC ACG AAT ACC GTC AAA AGT TTT AGA GCT AGA AAT AGC-3'	Clone two gRNAs
<i>Zfp8</i> _pCFD5 Reverse	5'-CTA TTT CTA GCT CTA AAA CGC CGT TCC CTG CCT AAA GAA TGC ACC AGC CGG GAA TCG AAC-3'	Clone two gRNAs
Sequencing		
tRNA Forward	5'-ATA GTA CCC TGC CAC GGT AC-3'	Screening for positive cloning
pCFDseq Reverse	5'-GCA CAA TTG TCT AGA ATG CAT AC-3'	Screening for positive cloning
qPCR		
<i>rp49</i> Forward	5'-TCC TTG ACC TGC CAA AAC T-3'	
<i>rp49</i> Reverse	5'-AAT GAT CTA TAA CAA AAT CCC CTG A-3'	
<i>nvd</i> Forward	5'-CCC TCA CCT AGG AGC CAA CT-3'	
<i>nvd</i> Reverse	5'-GGC ATA TAA CAC AGT CGT CAG C-3'	
<i>plm</i> Forward	5'-GGC ATC ATG GGT GGA TTT-3'	
<i>plm</i> Reverse	5'-CAA GGC CTT TAG CCA ATC G-3'	
<i>spok</i> Forward	5'-CGG TGA TCG AAA CAA CTC AC-3'	
<i>spok</i> Reverse	5'-CGA GCT AAA TTT CTC CGC TTT-3'	
<i>dib</i> Forward	5'-GTG ACC AAG GAG TTC ATT AGA TTT C-3'	
<i>dib</i> Reverse	5'-CCA AAG GTA AGC AAA CAG GTT AAT-3'	

Table 2.3: Reagents required to set up PCR reactions for double gRNA cloning

Reagents	μL
Nuclease-free water	10.75
5X Q5 reaction buffer	5
5X Q5 high GC enhancer buffer	5
10 mM dNTPs	0.5
10 μM forward primer	1.25
10 μM reverse primer	1.25
pCFD5 plasmid (10 ng/ μL)	1
Q5 high fidelity DNA polymerase (NEB M0491S)	0.25
Total	25

Table 2.4: Thermocycling conditions for PCR

Step	T $^{\circ}\text{C}$	Time
1	98	3 min
2	98	30 sec
3	Annealing Temperature (72 $^{\circ}\text{C}$)	30 sec
4	72	15 sec
5	72	2 min
6	4	Forever
Steps 2 to 4 are repeated 35 times		

Table 2.5: Reagents required for Gibson reaction

Reagents	μL
PCR fragment PCR fragment: backbone= 5:1	1
pCFD5 backbone (50 ng/ μL -100 ng/ μL)	1
1.33X Gibson master mix	6
The reaction is incubated in a thermocycler for 4 hrs.	

Table 2.6: Reagents required to digest plasmid with BbsI restriction enzyme

Reagents	μL
10X CutSmart Buffer	2
gRNA plasmid	9.2
BbsI HF	1
Nuclease-free water	7.8
Total	10

Table 2.7: Reagents required to do DpnI digestion

Reagents	μL
FastDigest Buffer	6
PCR product	45
DpnI	3
Nuclease-free H ₂ O	6
Total	60

Table 2.8: Reagents used for cDNA synthesis:

Reagents	μL
RNAase free water	9
Master Mix for 1 reaction	
10X RT Buffer	2
25X dNTP mix (100 μM)	0.8
10X Random primers	2
PCR grade water	4.2
RNA sample/0.2 ml tube	1
Reverse transcriptase (RTase)	1

Table 2.9: Thermocycling conditions for cDNA synthesis:

Step	Temperature (°C)	Time
1	25	10 mins
2	37	120 mins
3	85	5 mins
4	4	Hold

Table 2.10: Reagents used to prepare competent cells

Reagents/Solutions	Amount
DMSO	
PIPES	15.1 g
Milli-Q H ₂ O	80 ml
KOH or HCl	Until pH is 6.7
MnCl ₂ .4H ₂ O	10.88 g
CaCl ₂ .2H ₂ O	2.20 g
KCl	18.65 g
LB	
Distilled H ₂ O	950 mL
Tryptone	10 g
NaCl	10 g
Yeast extract	5 g
Agar	15 g

Chapter 3

Results

3. Results:

3.1 Loss-of-*Zfrp8* through RNA interference and mutation results in developmental defects

The King-Jones lab, in collaboration with Dr. Michael B. O'Connor and Dr. Kim F. Rewitz's lab, conducted a *Drosophila* genome-wide *in-vivo* RNAi screen targeting a total of 12,500 RNAi lines to determine the genes that are responsible for regulating steroid production. The primary screen conducted by triggering RNAi, specifically in the prothoracic gland, resulted in the identification of 1,906 genes potentially responsible for steroidogenesis. The secondary screen was then conducted exclusively in the King-Jones lab on approximately 800 genes that came out of the primary screen and survived to L3. The secondary screen was utilized to observe the effects on the ring glands when the candidate genes were knocked down, specifically in the prothoracic gland. *Zfrp8* is one such gene that came out of the secondary screen. My primary objective was to investigate the role of *Zfrp8* concerning iron homeostasis, heme regulation, as well as ecdysone biosynthesis. When the secondary screen was conducted in the King-Jones lab, it was observed that the PG-specific depletion of *Zfrp8* caused developmental defects, namely, major third instar arrest. Ecdysone is the primary steroid hormone in insects and is responsible for the developmental transitions from one stage to another, eventually resulting in metamorphosis leading to the formation of a fully-grown adult *Drosophila*. The developmental defects are quite common when ecdysone production is deficient in the fruit fly. For example, *Neverland* is one of the Halloween enzymes responsible for the conversion of dietary cholesterol to 7-dehydrocholesterol which is the first step of the ecdysteroid biosynthesis pathway. When *Neverland* is knocked down in the prothoracic gland using RNA interference, larvae exhibit a major arrest of both molting as well as growth. PG-specific RNAi or somatic CRISPR/Cas9 against *Coprox*, *Ppox*, and *FeCH*, resulted in

developmental defects or delays. For example, *Ppox* mutants resulted in major third instar arrests. Similarly, PG-specific RNAi of *Coprox* and *FeCH* displayed both first instar and second instar arrests as well as third instar arrests, respectively. The cytochrome P450 enzymes bind to heme in a non-covalent manner, which explains the reason behind the developmental defects that we notice when specific components of the heme biosynthesis pathway are disrupted while the Rieske electron oxygenase, Neverland, requires an Fe-S cluster to function. This suggests the possibility that the developmental defects or delays that are observed in the loss-of-*Zfrp8* animals could be due to reduced ecdysone production or a decrease in heme production, which, in turn, ends up affecting ecdysone production.

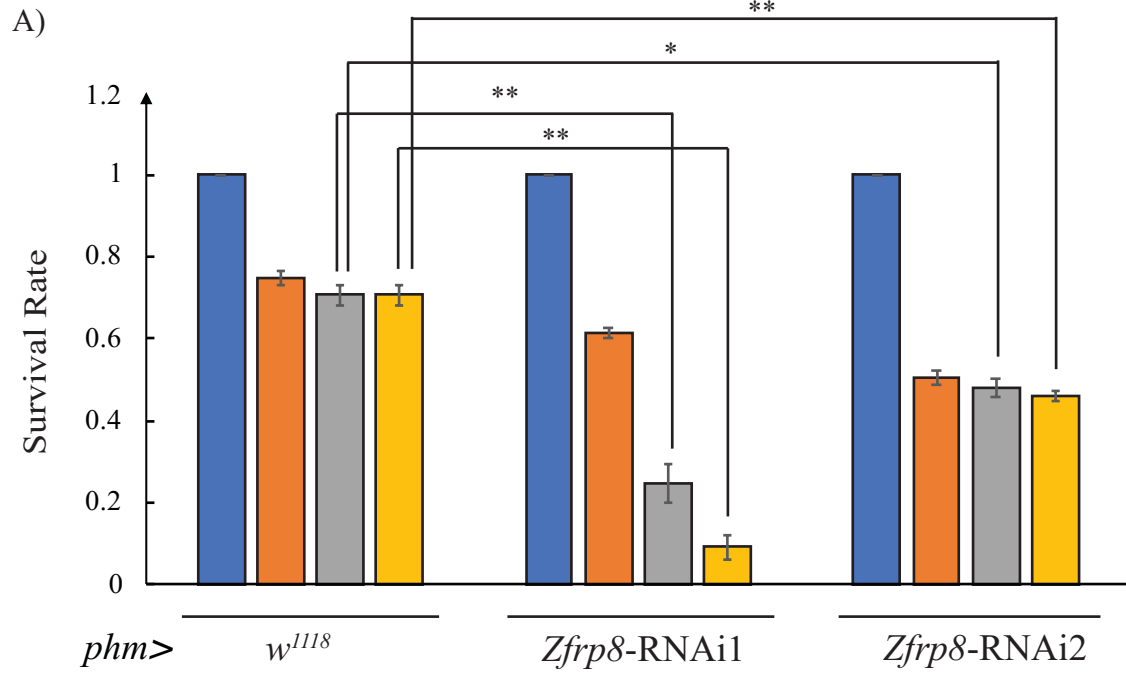
In order to observe the developmental phenotypes associated with PG-specific *Zfrp8*-RNAi, I had access to one VDRC RNAi line, two BDSC RNAi lines, and one *Zfrp8* mutant that was requested from Ruth Steward's lab. I used only BDSC id: 36581 because both the BDSC lines targeted almost the same region having an overlap of 20 base pairs. The BDSC line (BDSC id: 36581) targeted an overall region of 21 base pairs. The VDRC line (VDRC id: 11521) targeted a region of 373 base pairs. The VDRC line and the BDSC lines targeted different regions and hence are independent RNAi lines. The purpose of using independent RNAi lines is to minimize off-target effects. The off-target effects refer to the direct effect on the expression of genes by the short-interfering RNAs or siRNAs other than the genes they are intended to target¹²⁵. From here onwards, I will be referring to the VDRC line as *Zfrp8*-RNAi1 and the BDSC line as *Zfrp8*-RNAi2. In order to observe developmental defects generated when *Zfrp8* is knocked down specifically in the prothoracic gland, I used a prothoracic gland specific-*GAL4* driver (denoted as *phantom*>*GAL4* or *phm*>) to express the RNAi solely in the prothoracic gland and not the whole body. I used *phm*>*w*¹¹¹⁸ as my control to determine and compare the effects of *Zfrp8* with *w*¹¹¹⁸, and the effects were solely focused on the prothoracic gland. The reason I used *phm*>*w*¹¹¹⁸ as my control is

because of the normal development and ring gland size of the aforementioned animals where w^{1118} is a loss-of-function allele of the *white* gene. I set up a cross between virgin *phantom* females and *Zfrp8*-RNAi1 males to generate *PG>Zfrp8*-RNAi1 embryos. The embryos were grown on Nutrifly food, which is the primary diet for flies in King-Jones lab and was devoid of any added supplements. Similar to the results of the screen and shown in Figure 3.1.A, 9% of the *PG>Zfrp8*-RNAi1 animals reached adulthood, compared with 71% in controls ($P = 0.003$; one-tailed T-test). Another important observation was that the *PG>Zfrp8*-RNAi1 larvae achieved the transition from the second instar to third instar a full day late compared to the control. This resulted in the body size of *PG>Zfrp8*-RNAi1 adults being bigger compared to the control (*PG>w¹¹¹⁸*) because of the prolonged feeding period (Figure 3.1.B). For the *PG>Zfrp8*-RNAi2 animals, 46% of their embryos were able to reach adulthood. This was surprising since I was expecting a much lower percentage of adults to eclose similar to *PG>Zfrp8*-RNAi1, which meant that the developmental defect in this RNAi line was minimized, which was further supported by statistical analysis with a significant p-value of 0.006 for a one-tailed t-test. Apart from the RNAi lines, I also had access to a mutant line generated in Ruth Steward's lab: *Df(2R)SM206*, which has been reported to affect the expression of *Zfrp8* in the *Drosophila* genome¹²⁶. The *Zfrp8* mutant is balanced over CyO, GFP: so, while determining the homozygous embryos, I chose the eggs that were not showing any green autofluorescence under UV exposure. After transferring the eggs to the Nutrifly diet, I observed that none of the transferred animals survived beyond the first instar larval stage. This clearly points to the fact that *Zfrp8* is essential for the normal development of *Drosophila*, and loss-of-*Zfrp8* results in the inability of the affected animals to progress beyond the larval stages.

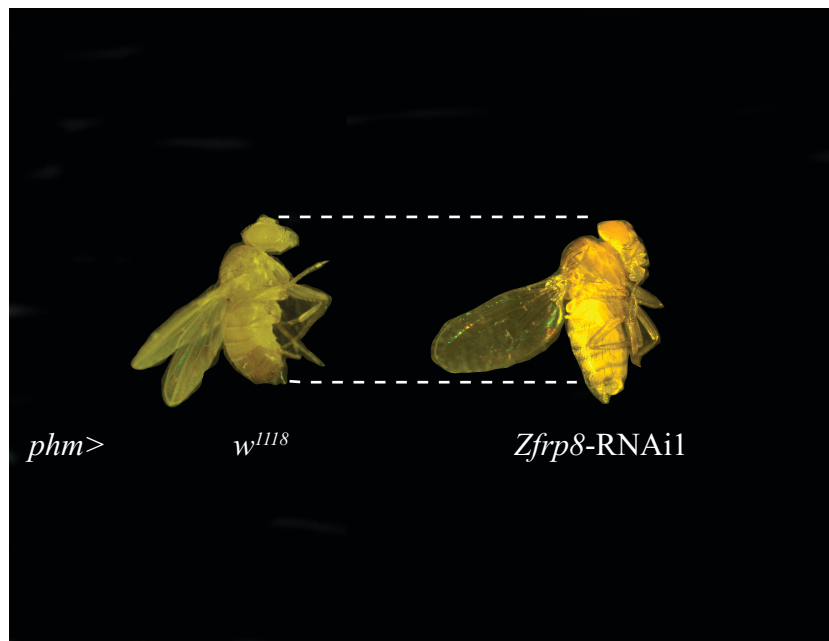
3.1.1 Loss-of-*Zfrp8* results in accumulation of heme precursors in the prothoracic gland

URO III or Uroporphyrinogen III is the first heme precursor with an intact tetrapyrrole ring structure in the heme biosynthesis pathway. Although the porphyrinogens are colorless compounds, on exposure to air and light have the ability to spontaneously convert to porphyrins, which have a characteristic dark red color and the ability to fluoresce. The ability to fluoresce is critical from the perspective of the work that we are doing because protoporphyrins can be detected as red autofluorescence upon their exposure to UV light. It means that any disruption in the heme biosynthesis pathway, starting from the formation of URO III, could be detected in the form of red autofluorescence. Knocking down *Alas* in the prothoracic gland results in the accumulation of heme precursors but not red autofluorescence in the prothoracic gland upon exposure to UV light because the accumulated heme precursors are not protoporphyrins. Since I hypothesized that the developmental defects in the *PG>Zfrp8-RNAi* are due to defects in the heme biosynthesis pathway, I used the theory as mentioned above to try and establish if knocking down *Zfrp8* results in red autofluorescence in the prothoracic gland. For this purpose, I generated *PG>Zfrp8-RNAi1* embryos. Since it is not possible to surgically separate the prothoracic gland from the ring gland since the ring gland is a fused structure, I dissected the brain-ring gland complex 42 hrs after their L2/L3 molt and viewed under a confocal microscope. The dissected ring gland was then exposed to UV light to observe if there was any red autofluorescence. Consistent with my hypothesis, all of the ring glands that I dissected displayed red autofluorescence, pointing to the possibility that knocking down *Zfrp8* in a PG-specific manner does disrupt the heme biosynthesis pathway and resulted in the accumulation of heme precursors. Synonymous with the rescue experiments data, knocking down *Zfrp8-RNAi2* in a PG-specific manner showed no red autofluorescence on being exposed to UV shown in Figure 3.1.C. Since the homozygous mutant stock did not reach third

instar larvae while I was working with the line, it was not possible to dissect the ring glands and expose them to UV light to determine if they are displaying red autofluorescence or not. It is too early to conclude whether the developmental defects displayed by the *PG>Zfrp8-RNAi1* animals and the *zfrp8* mutant was caused by a disruption in the heme and ecdysone pathway. Hence, more experiments need to be conducted in order to gather substantial evidence towards modifying my hypothesis. This led me to the question as to whether it was possible to rescue the developmental delays and the accumulation of heme precursors in the prothoracic gland of the *PG>Zfrp8-RNAi1* animals by supplementing their diet with heme related compounds as well as intermediates of the ecdysone biosynthesis pathway.



B)



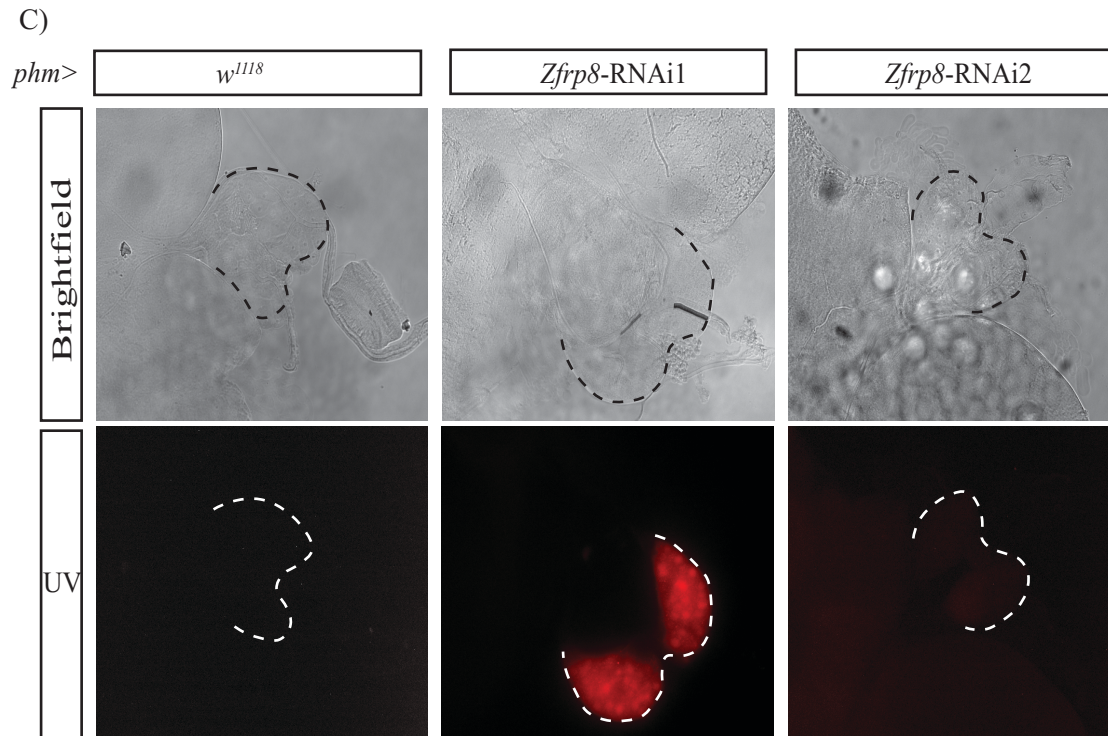


Figure 3.1: *PG*>*Zfrp8*-RNAi1 affected development whereas *PG*>*Zfrp8*-RNAi2 did not: A) *PG*>*Zfrp8*-RNAi1 and *PG*>*Zfrp8*-RNAi2 were grown on Nutrifly media while *PG*>*w¹¹¹⁸* acted as the control and was also grown on Nutrifly media. *PG*>*Zfrp8*-RNAi1 resulted in major 3rd instar larval arrest while *PG*>*Zfrp8*-RNAi2 did not display severe developmental defects compared to the *PG*>*Zfrp8*-RNAi1 animals. *PG*>*Zfrp8*-RNAi1 and *PG*>*Zfrp8*-RNAi2 are independent lines. The survival rate for each developmental stage was determined by normalizing the corresponding stage to the number of eggs that were collected. A student's t-test was conducted to determine the significance relative to *phm*>*w¹¹¹⁸*. ** for $P \leq 0.01$ and * for $P \leq 0.05$. Blue bars represent eggs (N=50); orange, grey and yellow bars represent L3, pupae and adults respectively. Error bars represent the standard error of mean. B) The adults were collected 10 days after egg laying (AEL) and their growth recorded, *phm*>*Zfrp8*-RNAi1 adult is larger in size compared to the *phm*>*w¹¹¹⁸* adult. C) Brain ring gland complexes viewed with a confocal microscope 42 hours after L2/L3 molt. The prothoracic glands are outlined in a dotted black line for the brightfield panel and in a dotted white line for the UV panel. Heme precursors display red autofluorescence on exposure to UV light. *phm*>*Zfrp8*-RNAi1 animals displayed visible red autofluorescence under UV light while no red autofluorescence was observed for *phm*>*Zfrp8*-RNAi2 and *phm*>*w¹¹¹⁸* animals.

3.2 Iron supplementation fails to rescue the developmental defects of *PG>Zfrp8-RNAi1* animals

If knocking down *Zfrp8* is responsible for reducing the cellular heme levels specifically in the prothoracic gland; this would explain the developmental delay in the *PG>Zfrp8-RNAi1* animals as well as the display of the phenotypes such as the accumulation of protoporphyrin in the prothoracic gland, which are similar to the symptoms (related to low iron levels) displayed by patients suffering from porphyria. Disrupting heme biosynthesis reduces cellular heme levels, which leads to developmental delays and accumulation of heme precursors in the prothoracic gland. Heme biosynthesis genes such as *Alas*, *Updo*, and *Ppox* when knocked down specifically in the prothoracic gland resulted in developmental defects similar to what I observed in *PG>Zfrp8-RNAi1* animals and this further led me to believe that the developmental defects observed in the *PG>Zfrp8-RNAi1* larvae could be caused by a reduction in cellular heme levels. I hypothesized that the developmental defects could be alleviated by supplementing iron to the Nutrifly food since the incorporation of iron into protoporphyrin IX leads to the production of heme and completes the heme biosynthesis pathway. If feeding iron to *PG>Zfrp8-RNAi1* animals leads to the rescue of the aforementioned developmental defects, it would mean that the defect was in the heme biosynthesis pathway. For this purpose, I used Ferric Ammonium Citrate (FAC) as the iron substitute. Before I start reporting the results, I would like to introduce two terms: food control and fly control. When I mention food control, I am talking about the *phm>Zfrp8-RNAi1* larvae being fed with Nutrifly food and in the experimental group, Nutrifly food with specific added supplements (FAC in this case). I introduced the term food control since both the control and the experimental group are the same but are reared on different food supplements to observe the developmental effect that the added supplemental has on the *PG>Zfrp8-RNAi1* animals. When I

mention fly control, I am talking about the *phm>w¹¹¹⁸* larvae and the *phm>Zfrp8-RNAi1* larvae, both fed with the same supplement. Since there are two different genotypes at play here but are being fed the same food supplement: hence the term fly control.

Based on the work done by Nhan Huynh, one of the graduate students in the King-Jones lab, PG-specific depletion of *AGBE*, one of the genes that came out of the screen resulted in third instar delay. More importantly, the developmental delay was completely rescued by dietary iron supplementation¹²⁷. However, none of the developmental defects displayed by knocking down the heme biosynthesis genes such as *Ppox*, *Urod* and *FeCH* specifically in the prothoracic gland were rescued by dietary iron supplementation. This led me to believe that there is a possibility that the developmental defects displayed by loss-of-*Zfrp8*, could be rescued by dietary iron supplementation. I generated the *PG>Zfrp8-RNAi1* embryos, which were then grown on 1 mM dietary iron supplemented Nutrifly food. Surprisingly, iron supplementation was unable to rescue the developmental defects that were displayed by the *PG>Zfrp8-RNAi1* animals. For the *PG>Zfrp8-RNAi1* animals that were grown without iron supplementation, 24% of the embryos developed into adults, whereas the *PG>Zfrp8-RNAi1* animals that were grown on food that contained iron as a supplement, 19% of the embryos developed into adults. Therefore, iron failed to rescue the developmental defects, in fact, the number of adults was significantly lower ($P = 0.4$, one-tailed t-test). Similarly, if we consider fly control i.e., when the *PG>w¹¹¹⁸* animals were grown with iron supplementation, 27% of the embryos went on to become adults as evident from Figure 3.2.A. On comparing the growth rate with *PG>Zfrp8-RNAi1* animals fed with iron, there was no rescue and the decline in eclosion is also not drastic. When I conducted a statistical analysis for both food control and fly control, the results were not significant based on the p-value (P value for food control = 0.4, P value for fly control = 0.1).

Iron supplementation also failed to remove the excess heme precursors that accumulated in the prothoracic gland for the *PG>Zfrp8-RNAi1* animals. In order to determine the amount of red autofluorescence on exposure to UV in the *PG>Zfrp8-RNAi1* animals supplemented with iron, I collected the eggs and staged the embryos during their transition from the second instar to their third instar. After dissecting the embryos 42 hrs after their L2/L3 molt, when I exposed the ring glands to UV, 100% of the ring glands displayed red autofluorescence (Figure 3.2.B), which indicates that iron feeding failed to remove the protoporphyrins that accumulated in the prothoracic gland because of a defective heme biosynthesis pathway and also corroborates the rescue data. If iron feeding had been able to rescue the developmental defects observed in *PG>Zfrp8-RNAi1* animals, it would have been evident that a lack of cellular or mitochondrial iron is responsible for disrupting the heme production which resulted in the defects mentioned above.

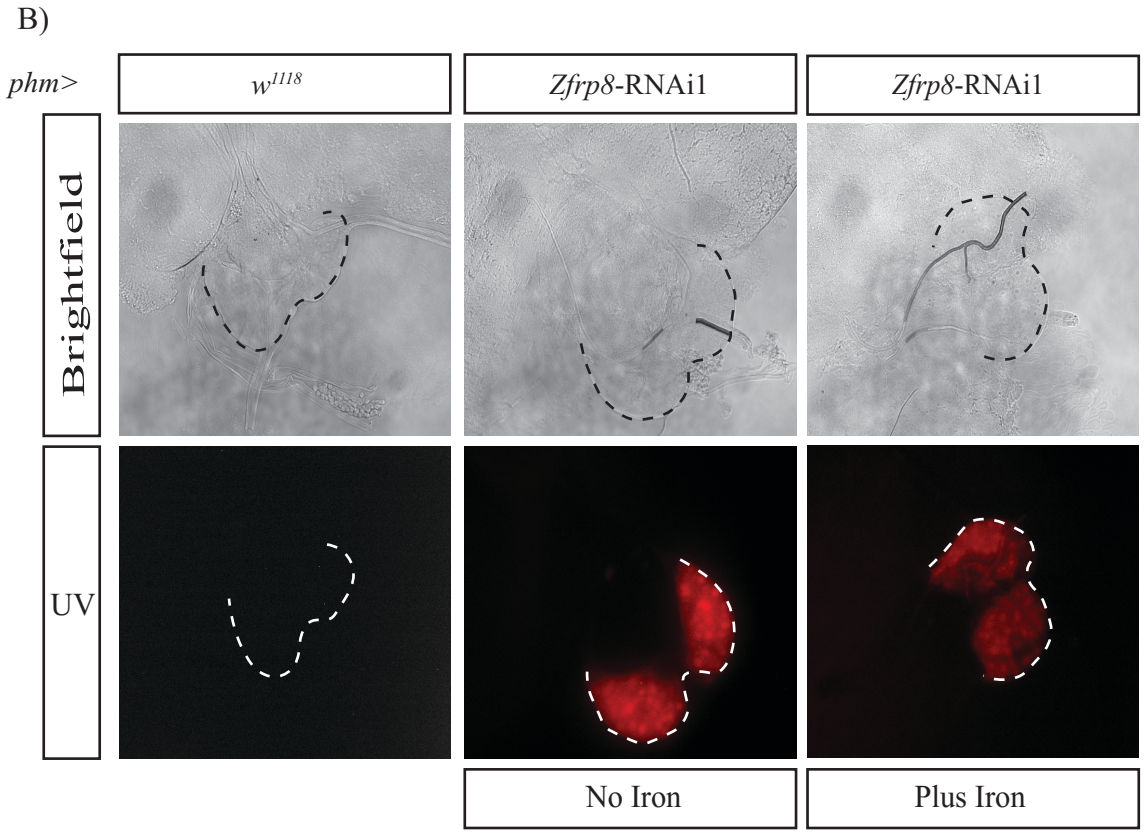
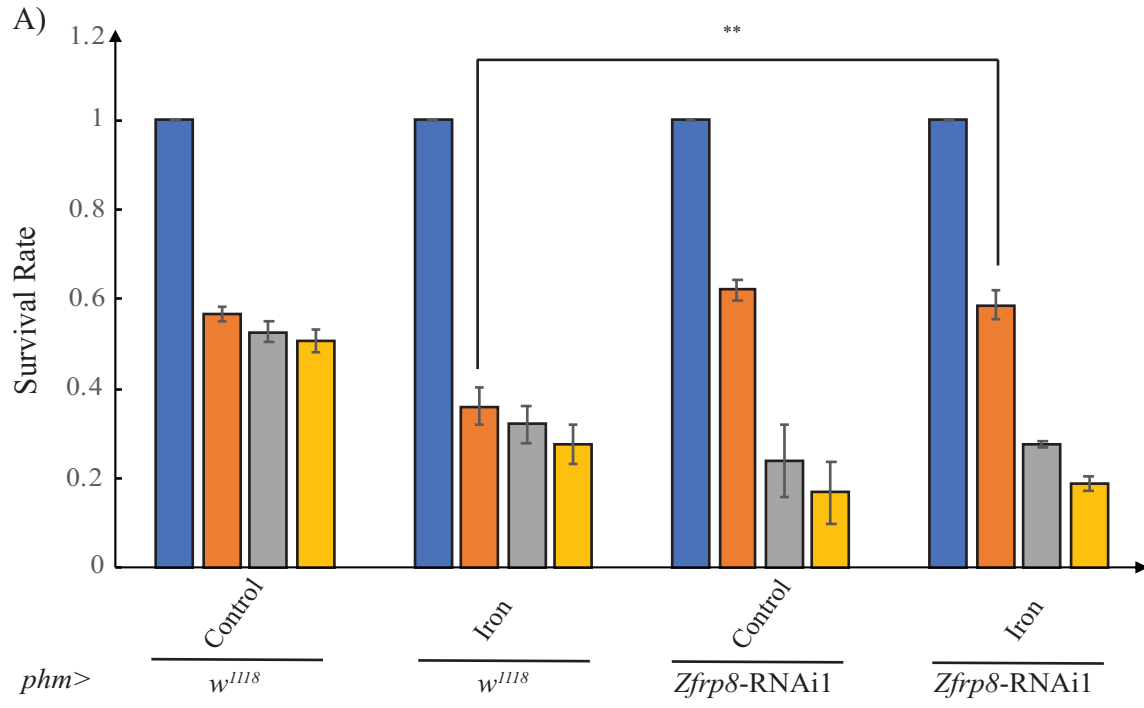


Figure 3.2: Iron supplementation fails to rescue *PG>Zfrp8-RNAi1* animals: A) *PG>w¹¹¹⁸* and *PG>Zfrp8-RNAi1* animals grown on control media and 1 mM iron-supplemented diet. Relative to both control media and control fly, iron supplementation fails to rescue the *PG>Zfrp8-RNAi1* animals. The survival rate for each developmental stage was determined by normalizing the corresponding stage to the number of eggs that were collected. A student's t-test was conducted to determine the significance relative to *phm>w¹¹¹⁸* supplemented with iron. ** for $P \leq 0.01$ and * for $P \leq 0.05$. Blue bars represent eggs (N=50); orange, grey and yellow bars represent L3, pupae and adults respectively. Error bars represent the standard error of mean. B) Brain ring gland complexes viewed with a confocal microscope 42 hours after L2/L3 molt. The prothoracic glands are outlined in a dotted black line for the brightfield panel and in a dotted white line for the UV panel. Heme precursors display red autofluorescence on exposure to UV light. *phm>Zfrp8-RNAi1* animals displayed visible red autofluorescence under UV light clearly suggesting the accumulation of heme precursors and the inability of iron to rescue the developmental defects.

3.3 Hemin supplementation fails to rescue the developmental defects of *PG>Zfrp8-RNAi1* animals

I hypothesized that knocking down *Zfrp8* using the RNA interference reduces heme levels in the prothoracic gland, which is also supported by the fact that *PG>Zfrp8-RNAi1* results in developmental delay concerning the third instar larvae as well as red autofluorescence in the prothoracic gland on exposure to UV. Based on experiments done by previous members of the King-Jones lab, we learned that *PG>Ppox-RNAi2* where the RNAi transgene is located in the second chromosome displayed third instar arrest whereas *PG>Ppox-RNAi3* (RNAi transgene is located in the third chromosome), displayed a two-day delay when I used puparium formation in control (*PG>w¹¹¹⁸*) as a reference. As I reported in the previous section, *PG>Zfrp8-RNAi1* displayed major third instar arrest, which is similar to the phenotype displayed by *PG>Ppox-RNAi2*. Moreover, *PG>Zfrp8-RNAi1* displayed a one-day delay relative to the L2/L3 molt, which is less severe when compared to the two-day delay displayed by *PG>Ppox-RNAi3*. This comparison is important since *Ppox* is one of the genes involved in the heme biosynthetic pathway and the developmental defects observed in *Drosophila* on knocking down *Ppox*, specifically in the prothoracic gland can be attributed to reduced heme production. When *PG>Zfrp8-RNAi1* larvae show similar developmental defects or delays as *PG>Ppox-RNAi2* and 3, it points to the possibility that reduced heme levels could again be the reason behind these developmental defects or delays. We know that the cytochrome P450 enzymes require iron to function in order to generate biologically active ecdysone, which is responsible for the developmental transitions in the fruit fly. Based on my hypothesis, *PG>Zfrp8-RNAi1* leads to reduced heme levels, which ultimately affects the functioning of the P450 enzymes and leads to reduced ecdysone generation. The reduced ecdysone levels in the prothoracic gland explain the rationale behind the developmental

delays, more specifically, the major arrest of the third instar larvae since ecdysone fails to trigger the developmental transitions when needed. In order to figure out if the developmental delay when *Zfrp8* is specifically knocked down in the prothoracic gland is due to the reduction in the cellular heme levels, I decided to increase the cellular heme levels in the prothoracic gland. For this purpose, I used hemin as a supplement by adding it to the Nutrifly food and growing the *PG>Zfrp8-RNAi1* larvae on the said supplement and observed if hemin was able to rescue the developmental delays in the *PG>Zfrp8-RNAi1* larvae. As already determined by Dr. Brian Phelps, a previous graduate student in King-Jones lab, the hemin concentration that I used was 1 mM since it is the optimal concentration and is also easy to prepare.

Previous work indicated that both *PG>Ppox-RNAi2* and *PG>Ppox-RNAi3* larvae are partially rescued when supplemented with hemin, but not the *Ppox* mutant (Phelps and Soltani, personal communication). This led me to believe that if *PG>Ppox-RNAi* lines could be either completely or partially rescued by hemin, *PG>Zfrp8-RNAi1* could also be rescued by hemin either partially or completely. I generated *PG>Zfrp8-RNAi1* eggs, which were then grown on 1 mM hemin supplemented Nutrifly food. Surprisingly, even when supplemented with hemin, the developmental delay caused in the *PG>Zfrp8-RNAi1* larvae was not rescued. With respect to control food, I did not observe a significant decline in the number of adults that eclosed. For the *phm>Zfrp8-RNAi1* animals not supplemented with hemin, 21% of the embryos went on to become adults, but for the same animals when fed with hemin, 19% of the embryos went on to become adults (Figure 3.3.A). However, with respect to control flies the decline was significant which was also evident from the p-value of 0.004 (one-tailed t-test) when the calculation was done with respect to the adults that eclosed. For the *phm>w¹¹¹⁸* embryos that were reared on a hemin supplemented diet, 47% of the embryos went on to become fully-grown adults (Figure 3.3.A). I

did not try hemin supplementation with *PG>Zfrp8-RNAi2* larvae because they neither showed any kind of developmental delay nor red autofluorescence in the prothoracic gland.

I also collected eggs for dissection purposes and staged the larvae during their transition from second instar to third instar. The larvae undergoing the L2/L3 molt were transferred to a fresh plate and were dissected after 42 hrs. All of the ring glands that I dissected showed strong red autofluorescence which means that hemin feeding failed to remove the accumulation of heme precursors generated because of a defective heme biosynthesis pathway and consistent with the rescue data (Figure 3.3.B). Combining these data, I was able to conclude that hemin feeding failed to rescue the developmental delay as well as the accumulation of heme precursors.

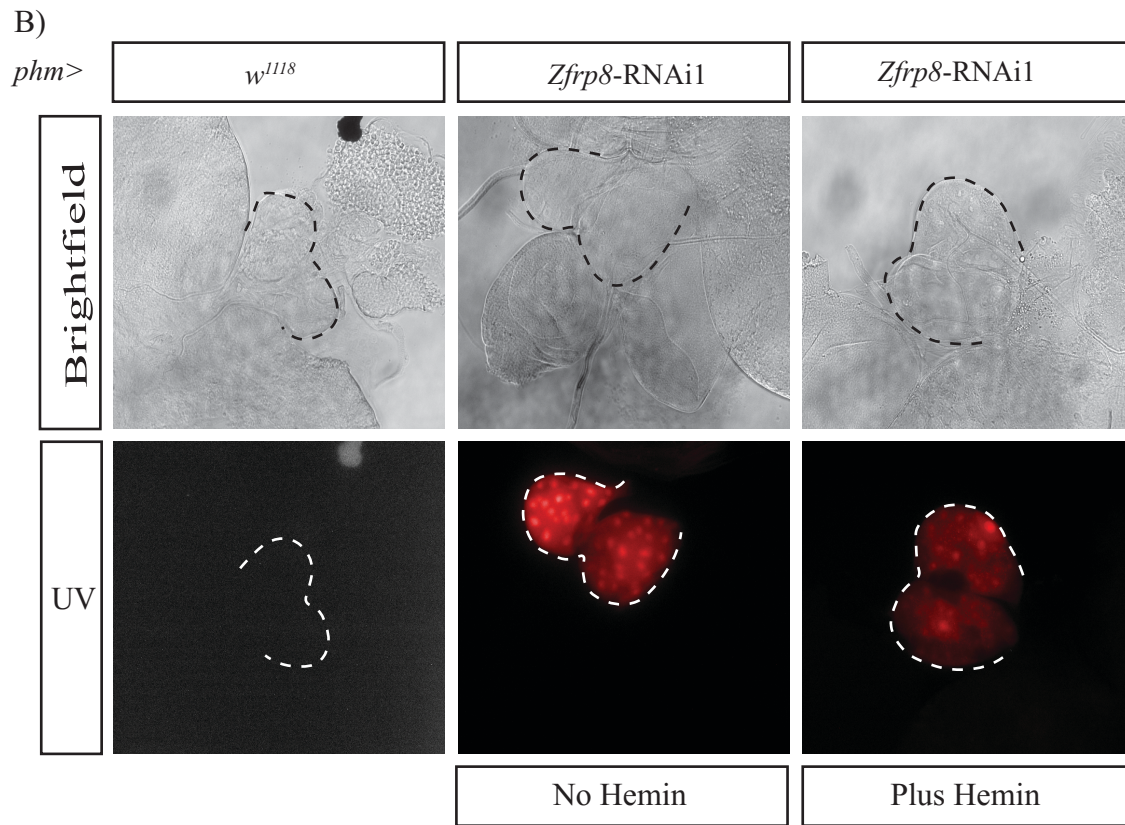
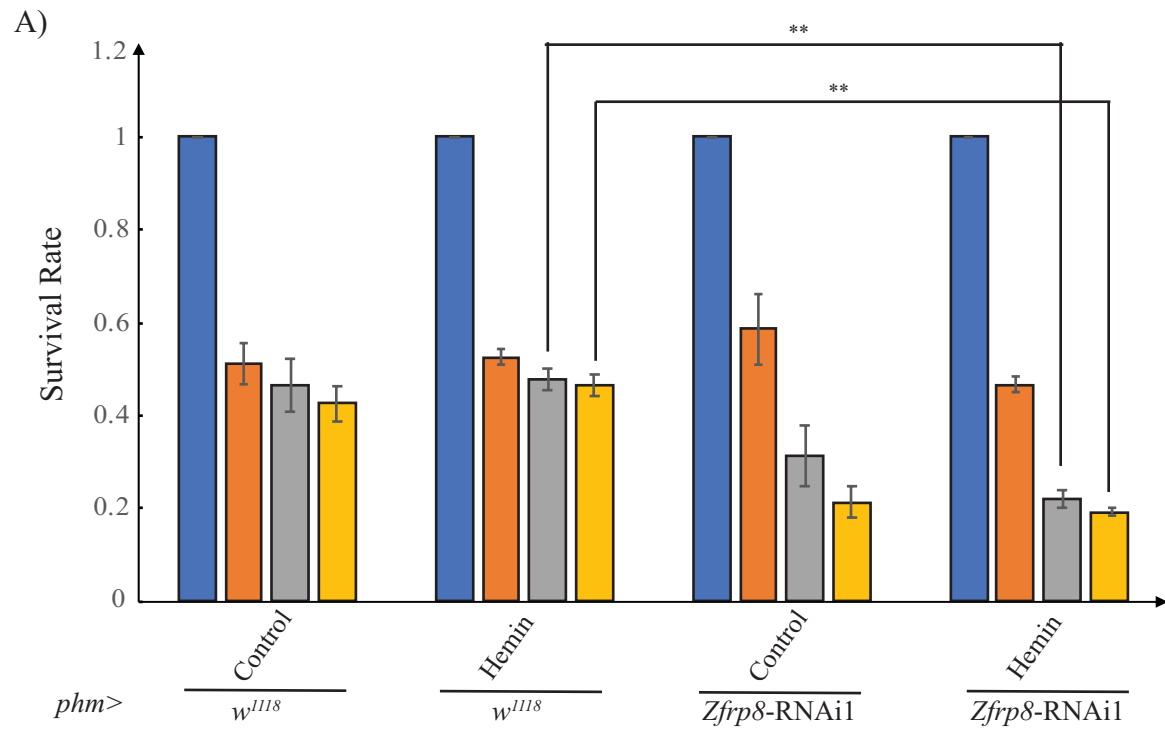


Figure 3.3: Hemin supplementation fails to rescue *PG>Zfrp8-RNAi1* animals: A) *PG>w¹¹¹⁸* and *PG>Zfrp8-RNAi1* animals grown on control media and 1 mM Hemin-supplemented diet. Relative to both control media and control fly, hemin supplementation fails to rescue the *PG>Zfrp8-RNAi1* animals. The survival rate for each developmental stage was determined by normalizing the corresponding stage to the number of eggs that were collected. A student's t-test was conducted to determine the significance relative to *phm>w¹¹¹⁸* supplemented with hemin. ** for $P \leq 0.01$ and * for $P \leq 0.05$. Blue bars represent eggs (N=50); orange, grey and yellow bars represent L3, pupae and adults respectively. Error bars represent the standard error of mean. B) Brain ring gland complexes viewed with a confocal microscope 42 hours after L2/L3 molt. The prothoracic glands are outlined in a dotted black line for the brightfield panel and in a dotted white line for the UV panel. Heme precursors display red autofluorescence on exposure to UV light. *phm>Zfrp8-RNAi1* animals displayed visible red autofluorescence under UV light clearly suggesting that accumulation of heme precursors and the inability of hemin to rescue the developmental defects.

3.4 Iron chelation fails to rescue the developmental defects of *PG>Zfrp8-RNAi1* animals

In humans, mitochondrial iron accumulation is associated with neurodegenerative disorders such as Friedrich's Ataxia or FRDA^{128,129}. FRDA leads to the reduction in the transcript levels of the *frataxin* gene^{130,131}, which encodes a mitochondrial protein and has been implicated in a variety of functions, which includes storing iron, heme biogenesis as well as protecting mitochondria from oxidative damage. The *Drosophila frataxin* homolog is essential for the proper development of the flies, and when knocked down using the RNA interference technique causes phenotypes similar to the human disease as well as results in tissue-specific toxicity and loss of intracellular iron homeostasis¹³²⁻¹³⁴. We already know that heme is vital for systemic iron homeostasis in mammals. When heme biosynthesis is disrupted in mammals upon downregulation of *Alas2* in bone marrow erythroblasts, it leads to insufficient protoporphyrin IX production. We know that incorporation of iron into protoporphyrin IX in the final step of the heme biosynthesis pathway results in the production of heme. Since protoporphyrin IX is produced in limited quantities, the iron that is available is not used up, resulting in the accumulation of excess iron in the mitochondria, which leads to oxidative stress-induced cell damage. This leads to the possibility that excess iron could be one of the reasons behind the developmental defects that we have observed due to the loss-of-genes that were identified in the screen. My objective was to determine if excess iron was responsible for the developmental defects that we have observed and for that purpose, I depleted the iron resources that were already present in the *PG>Zfrp8-RNAi1* animals by introducing an iron chelator. Accordingly, I generated *PG>Zfrp8-RNAi1* embryos, which were then transferred to a diet supplemented with 100 μ M BPS, which acts as the iron chelator. Concerning the food control, when the *PG>Zfrp8-RNAi1* animals were grown without supplementing their diet with an iron chelator, 13% of the embryos eclosed as adults. In contrast, for the *PG>Zfrp8-RNAi1*

animals that were grown on an iron chelator supplemented diet, 10% of the embryos developed into adults (Figure 3.4.A). Therefore, supplementing iron chelator to the *PG>Zfrp8-RNAi1* animals significantly decreased their overall survival rate, which is supported by statistical analysis with a p-value of 0.001 for a one-tailed t-test. When the *PG>w¹¹¹⁸* animals were grown on an iron chelator supplemented diet, 53% of the embryos became adults, as evident from Figure 3.4.A. It is quite evident that concerning both food and fly control; there is a decrease in survival rate with respect to the number of adults reflecting the fact that reducing the iron stores in the *PG>Zfrp8-RNAi1* animals further complicates their developmental defects rather than alleviating the problems.

I was curious to examine if supplementing the diet of the *PG>Zfrp8-RNAi1* animals would affect the accumulation of heme precursors in the prothoracic gland. For this purpose, I dissected larvae 42 hrs after they underwent their L2/L3 molt and exposed the dissected ring glands under UV light. All of the ring glands that I dissected showed visible red autofluorescence, clearly pointing to the fact that iron chelation did not affect the protoporphyrin accumulation in the prothoracic gland (Figure 3.4.B). Combining the rescue data along with the detection of red autofluorescence, it is evident that iron chelation does not rescue but instead exacerbates the developmental defects that are displayed by the *PG>Zfrp8-RNAi1* animals.

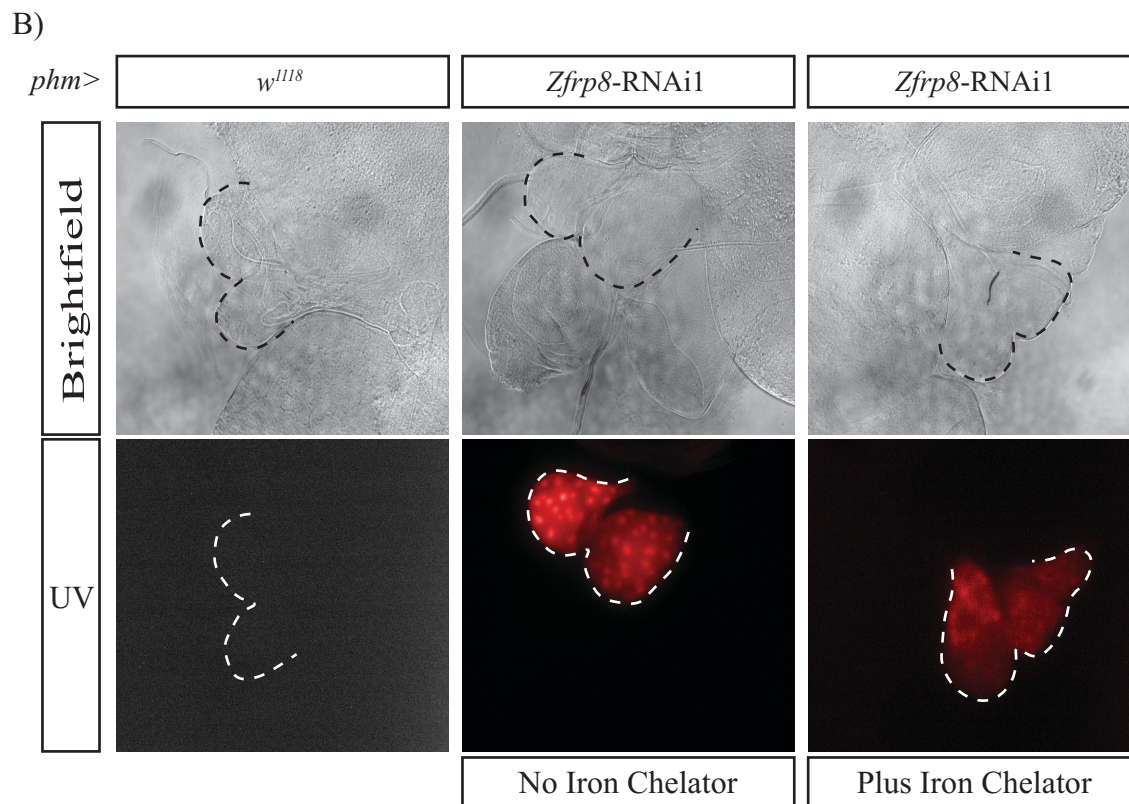
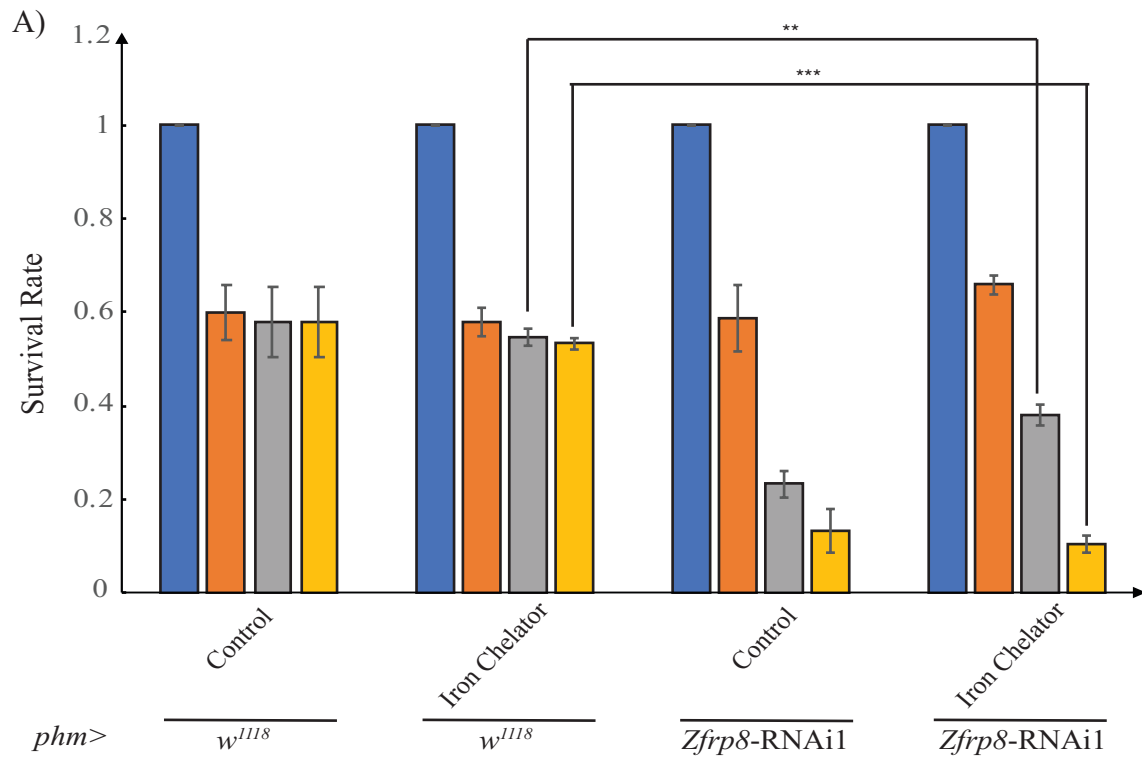


Figure 3.4: Iron chelator supplementation fails to rescue *PG>Zfrp8-RNAi1* animals:

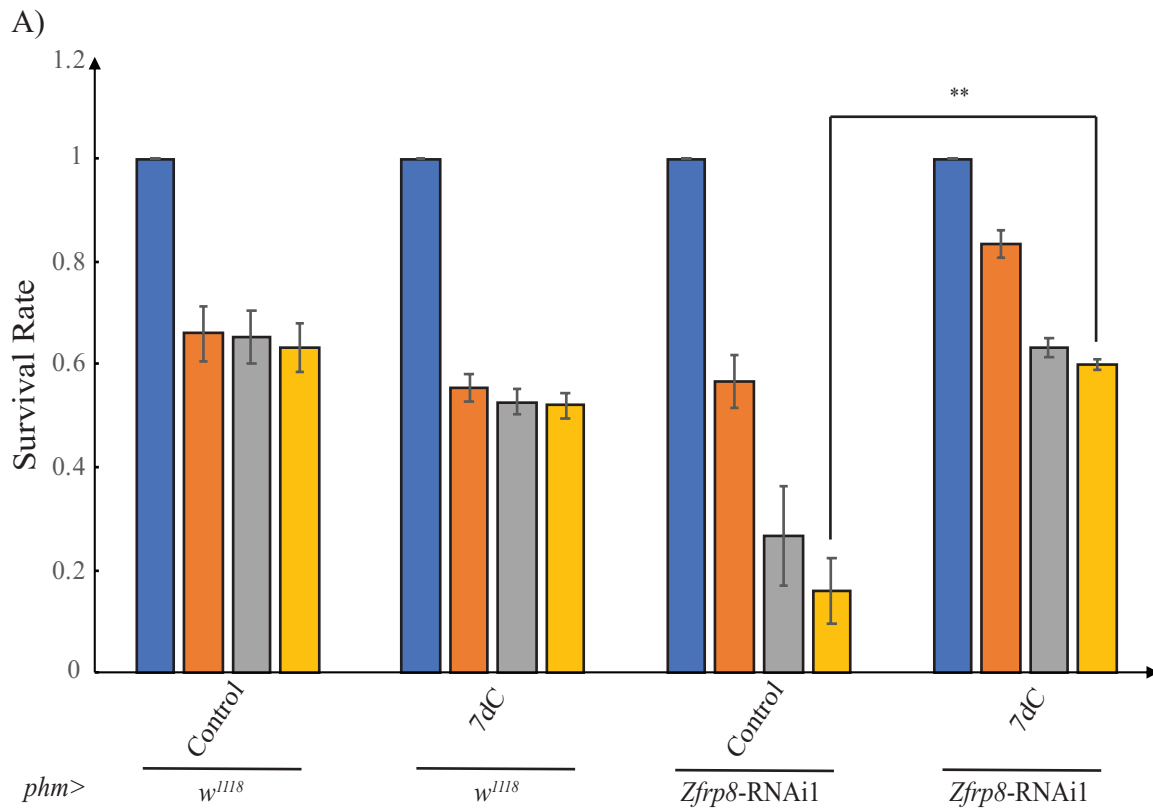
A) *PG>w¹¹¹⁸* and *PG>Zfrp8-RNAi1* animals grown on control media and 100 μ M iron chelator-supplemented diet. Relative to both control media and control fly, supplementing the diet with iron chelator fails to rescue the *PG>Zfrp8-RNAi1* animals. The survival rate for each developmental stage was determined by normalizing the corresponding stage to the number of eggs that were collected. A student's t-test was conducted to determine the significance relative to *phm>w¹¹¹⁸* supplemented with iron chelator. *** for $P \leq 0.001$ and ** for $P \leq 0.01$. Blue bars represent eggs (N=50); orange, grey and yellow bars represent L3, pupae and adults respectively. Error bars represent the standard error of mean. B) Brain ring gland complexes viewed with a confocal microscope 42 hours after L2/L3 molt. The prothoracic glands are outlined in a dotted black line for the brightfield panel and in a dotted white line for the UV panel. Heme precursors display red autofluorescence on exposure to UV light. *phm>Zfrp8-RNAi1* animals displayed visible red autofluorescence under UV light clearly suggesting that accumulation of heme precursors and the inability of iron chelator to alleviate the developmental defects.

3.5 7-dehydrocholesterol or 7-dC supplementation results in a significant rescue of *PG>Zfrp8*-RNAi1 animals

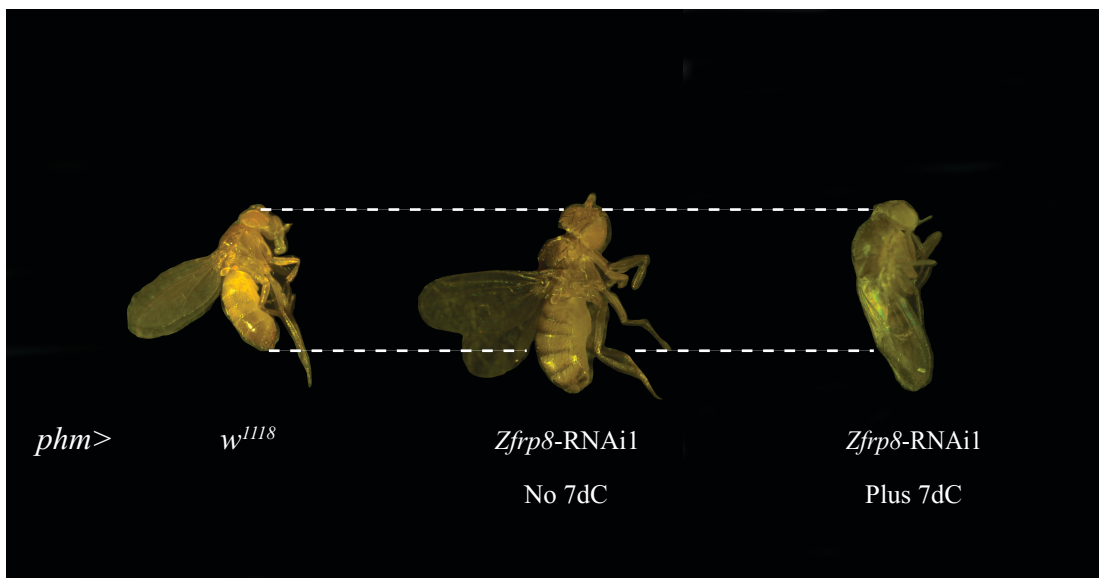
I have reported in the previous sections that knocking down *Zfrp8* in the prothoracic gland, specifically using RNA interference, resulted in the developmental delay of the L2/L3 molt by an entire day compared to the control (*PG>w¹¹¹⁸*). The knockdown also resulted in the accumulation of heme precursors in the prothoracic gland resulting in red autofluorescence. *Neverland*, a Rieske-electron oxygenase responsible for the conversion of dietary cholesterol to 7-dehydrocholesterol in the ecdysone biosynthesis pathway, when knocked down specifically in the prothoracic gland, resulted in prolonged first-instar larvae phenotype. The *PG>Nvd*-RNAi animals showed an apparent arrest concerning growth in body size when compared to the control animals approximately 48 hours after egg-laying. The *PG>Nvd*-RNAi animals also stopped their feeding in a gradual manner around 72 hrs after egg-laying and completely stopped moving. This was followed by 98% of the animals dying in the form of first-instar larvae before the 108 hrs mark after egg laying (Yoshiyama et al., 2006). Based on experiments done by previous members in the King-Jones lab, it has been shown that knocking down *Neverland* in the prothoracic gland resulted in weak autofluorescence, which is a less severe phenotype when compared to *PG>Zfrp8*-RNAi1 and signaled the accumulation of heme precursors in the prothoracic gland. Although the exact mechanism responsible for this phenotype is not clear. We know that if *Neverland* is knocked down in the prothoracic gland, it will lead to a decline in the production of the biologically active hormone, 20-hydroxyecdysone which, in turn, will affect the developmental transitions of *Drosophila* from one stage to another and result in developmental defects similar to what we noticed in the *PG>Nvd*-RNAi and *PG>Zfrp8*-RNAi1 animals. More interestingly, 7-dehydrocholesterol was able to rescue the *PG>Nvd*-RNAi animals to adulthood (Figure 6:

Yoshiyama et al., 2006). This led me to believe that *Zfrip8* could somehow fit into the ecdysone biosynthesis pathway, and based on these results and observations, I hypothesized that 7-dehydrocholesterol would be able to rescue the developmental defects of the *PG>Zfrip8-RNAi1* animals^{135,136}. I generated *PG>Zfrip8-RNAi1* embryos which were then transferred onto the target supplements. Since sterols are soluble in laboratory-grade ethanol but are not soluble in water, the control food contains 1 mL of 95% ethanol to make sure that the ethanol itself has no effects on the growth pattern of the concerned animals. The *PG>Zfrip8-RNAi1* embryos were grown on Nutrifly food supplemented with 0.1 mg/mL 7-dehydrocholesterol. For the *PG>Zfrip8-RNAi1* embryos that were grown without 7-dC supplementation, only 16% of the embryos went on to become adults. In contrast, the *PG>Zfrip8-RNAi1* that were supplemented with 7-dC, 60% of the embryos developed into normal-looking adults. With respect to the food control, there was a significant increase in the survival rate for the *PG>Zfrip8-RNAi1* animals. The significance is also reflected in the statistics with a p-value of 0.01 when I conducted a one-tailed t-test (Figure 3.5.A). Therefore, we could say that 7-dehydrocholesterol can significantly rescue the developmental defects of the *PG>Zfrip8-RNAi1* animals, although the rescue cannot be termed as a complete rescue. For the *PG>w¹¹¹⁸* animals that were supplemented with 7-dC, 52% of the embryos went on to become adults. If we compare this to the *PG>Zfrip8-RNAi1* animals grown on a 7-dC supplemented diet with a survival rate of 60%, the increase is not significant, which was also corroborated by the one-tailed t-test with a p-value of 0.07 (Figure 3.5.A). The comparatively larger body size of *PG>Zfrip8-RNAi1* adults was rescued by 7-dC feeding (Figure 3.5.B). I did not try 7-dC feeding with *PG>Zfrip8-RNAi2* because it was not associated with developmental defects. I also collected fresh embryos for dissection and staged the larvae during their transition from the second instar to the third instar. The larvae undergoing the L2/L3 molt were transferred to a fresh plate and were dissected after 42 hrs. Interestingly, I observed a range of visible red

autofluorescence for all the ring glands that I dissected. In order to determine the intensity of the red autofluorescence, I used ImageJ¹³⁷⁻¹³⁹ software as described in section 2.19 to help me determine the pixel intensity of the ring glands that I have studied. After the calculations with ImageJ, 4 out of 24 (16.67%) of the ring glands were classified as displaying high-intensity red-autofluorescence while the rest 20 (83.33%) were classified as displaying low-intensity red autofluorescence as shown in Figure 3.5.C. Combining these data, I would like to conclude that although 7-dC feeding results in the significant rescue of *PG>Zfrp8-RNAi1* animals but falls short of resulting in complete rescue of the tested animals. These results also suggest the possibility that *Zfrp8* might be regulating the iron and heme homeostasis through a yet unknown mechanism but not the conventional heme biosynthesis pathway as well as ecdysone biosynthesis through the ecdysone biosynthetic pathway.



B)



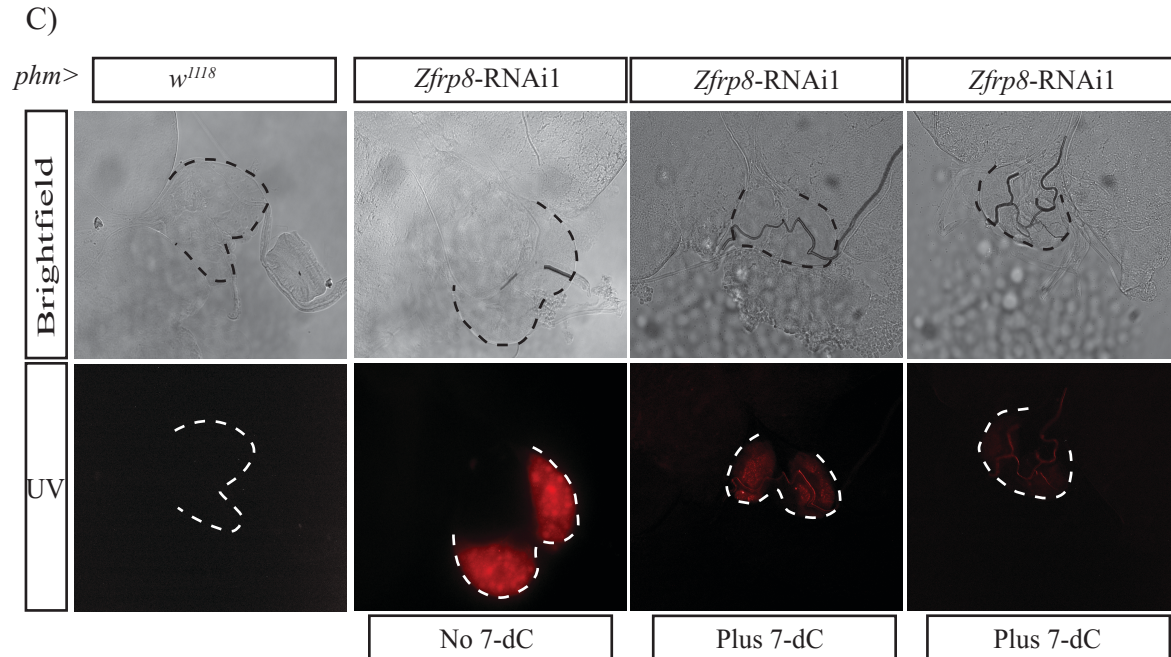


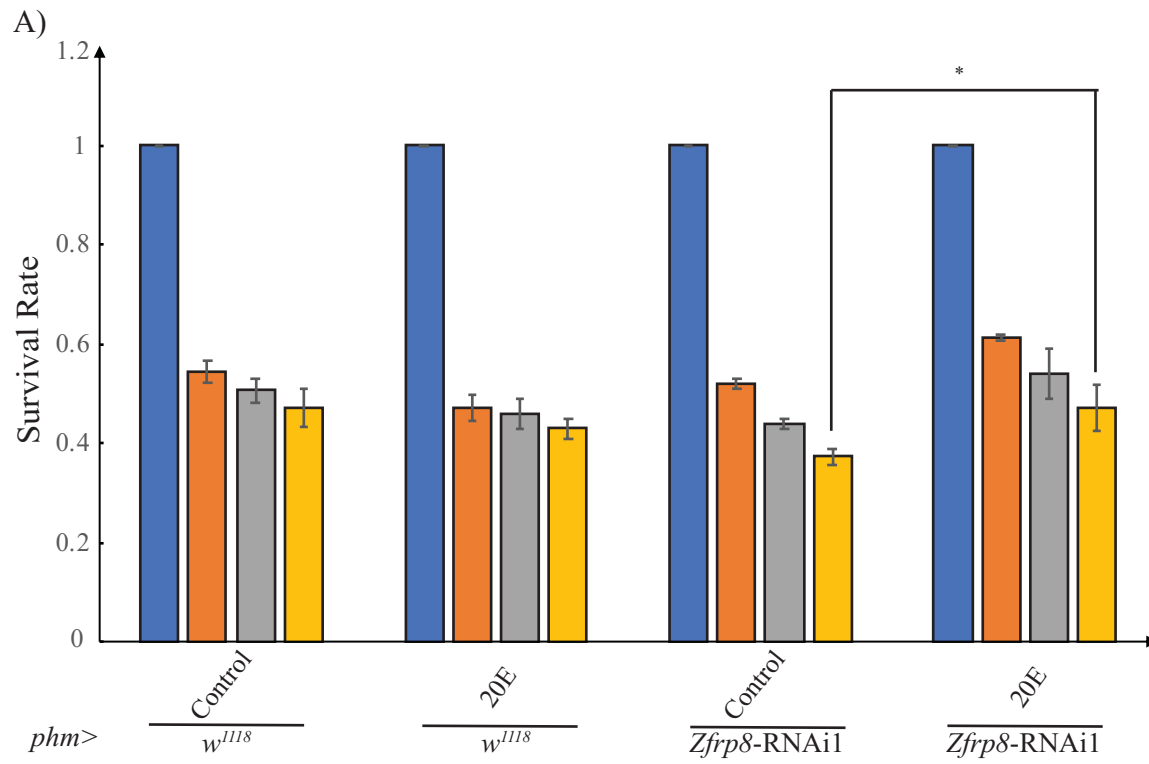
Figure 3.5: 7-Dehydrocholesterol or 7-dC supplementation results in significant, but not complete rescue of *PG>Zfrip8*-RNAi1 animals: A) *PG>w¹¹¹⁸* and *PG>Zfrip8*-RNAi1 animals grown on control media and 0.1 mg/mL 7dC-supplemented diet. Relative to control media and not control fly, 7-dC supplementation results in significant rescue of *PG>Zfrip8*-RNAi1 animals although 7-dC fails to completely rescue the *PG>Zfrip8*-RNAi1 animals. The survival rate for each developmental stage was determined by normalizing the corresponding stage to the number of eggs that were collected. A student's t-test was conducted to determine the significance relative to *phm>Zfrip8*-RNAi1 grown on control media. ** for $P \leq 0.01$. Blue bars represent eggs (N=50); orange, grey and yellow bars represent L3, pupae and adults respectively. Error bars represent the standard error of mean. B) The adults were collected 10 days after egg laying (AEL) and their growth recorded. Although *phm>Zfrip8*-RNAi1 adult is larger in size compared to the *phm>w¹¹¹⁸* adult, supplementing the diet of *phm>Zfrip8*-RNAi1 with 7-dC results in the reduction of the body size and the size becomes similar to that of the *PG>w¹¹¹⁸* animals. C) Brain ring gland complexes viewed with a confocal microscope 42 hours after L2/L3 molt. The prothoracic glands are outlined in a dotted black line for the brightfield panel and in a dotted white line for the UV panel. The third panel from the left comprises the prothoracic gland displaying high-intensity red autofluorescence and the fourth panel from the left shows the prothoracic gland displaying low-intensity red autofluorescence. The higher percentage of low-intensity fluorescing ring glands clearly suggests that 7-dC feeding results in significant removal of the accumulated heme precursors from the prothoracic gland.

3.6 20-hydroxyecdysone or 20E supplementation rescues the developmental defects of *PG>Zfrp8-RNAi1* animals, but not as efficiently as 7-dC feeding

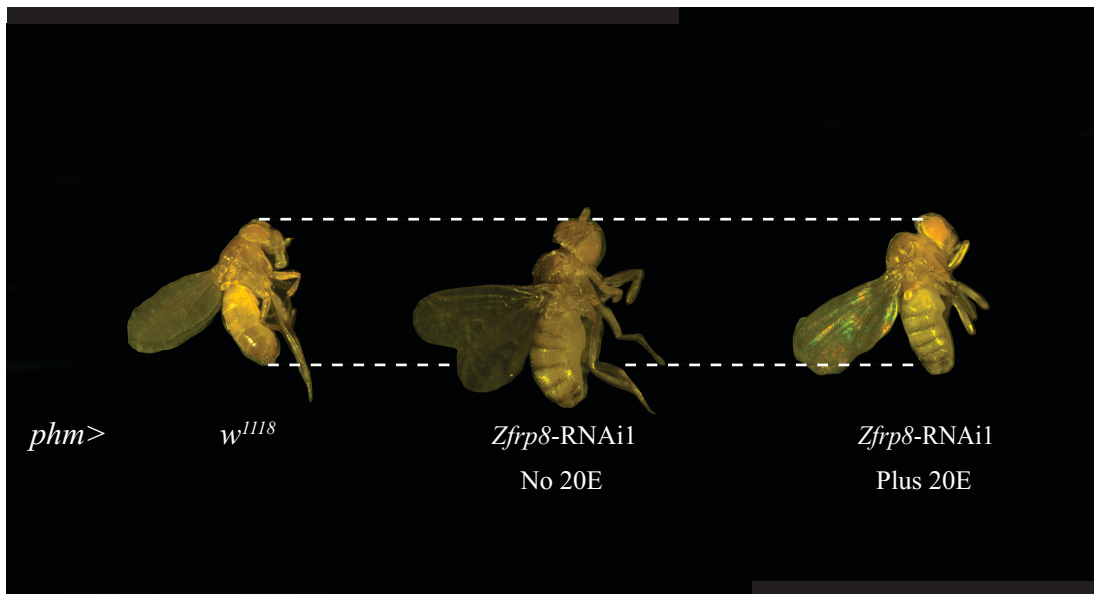
Ecdysone levels are high during the late third instar larval stages when the pupae prepare itself to undergo the puparium formation. There is a surge in the ecdysone level during this time point, which pushes the third instar larvae to undergo metamorphosis once there are enough nutrients available for the larvae to survive metamorphosis. Since the relationship between ecdysone and heme has been already established, it is crucial to figure out whether knocking down the genes involved in the heme biosynthesis pathway and the ecdysone biosynthesis pathway also affects the ecdysone levels in the larvae especially when a high amount of ecdysone is required to enter metamorphosis. Niwa et al., 2014¹⁴⁰ conducted experiments in which they knocked down *Neverland* in the prothoracic gland and found that animals are in a persistent first instar stage. Their data proved that ecdysteroids are downregulated in *PG>Nvd-RNAi* animals, which points to the fact that knocking down *Neverland* fails to produce the required amount of ecdysone since ecdysone is the end product of the ecdysone biosynthesis pathway and leads to the delay or arrest of the developmental transitions. In order to test whether knocking down heme biosynthesis genes affects the ecdysteroid titers, Brian Phelps from King-Jones lab investigated the ecdysteroid titers in *Ppox* mutant larvae to determine if the ecdysone levels are downregulated when *Ppox* is non-functional. As expected, the ecdysone levels in *Ppox* mutant larvae were significantly downregulated compared to the control (*PG>w¹¹¹⁸*) larvae. This established the fact that because *Ppox* was mutated, it led to a significant decrease in the production of heme. Since the cytochrome P450 enzymes require heme to function, reduced levels of heme affected the functional activity of cytochrome P450 enzymes, which eventually led to ecdysone not being produced and affecting the developmental transitions of the concerned animals. I hypothesized that *PG>Zfrp8-RNAi1*

animals would also have reduced ecdysone titers since *Zfrip8* has reduced ecdysone and heme levels and would show a certain degree of rescue on 20-hydroxyecdysone supplementation^{141,142}. For this purpose, I generated *PG>Zfrip8-RNAi1* embryos which were then transferred to a diet supplemented with 20-hydroxyecdysone. For the *PG>Zfrip8-RNAi1* animals that were growing without 20E supplementation, 37% of the embryos went on to become adults and the *PG>Zfrip8-RNAi1* animals that were supplemented with 20E, 47% of the embryos eclosed as fully-grown adults. Therefore, with respect to the food control, there is a rescue ($p=0.04$, one-tailed t-test) (Figure 3.6.A). For the *PG>w¹¹¹⁸* animals that were supplemented with 20-hydroxyecdysone, 43% of the embryos became adults (Figure 3.6.A). Therefore, when it came to the fly control, the rescue cannot be considered significant since the p-value was greater than 0.05 although there was a slight increase in the survival percentage when the *PG>w¹¹¹⁸* animals supplemented with 20E are compared to the *PG>Zfrip8-RNAi1* animals supplemented with 20E. As is evident from Figure 3.6.B, the large body size of the *PG>Zfrip8-RNAi1* animals is almost rescued back to the size of the control (*PG>w¹¹¹⁸*) flies by 20E-feeding.

To determine the accumulation of heme precursors in the ring gland after supplementing the *PG>Zfrip8-RNAi1* animals with 20E, I collected the eggs and staged the larvae to determine the L2/L3 molt. The larvae were then transferred to a fresh food plate and dissected 42 hrs after the L2/L3 molt. Similar to 7dC-supplemented samples, the 20E-supplemented samples also displayed a range of visible red autofluorescence, and hence I employed the same principle as I did with 7-dC samples. Based on ImageJ analysis, 8 out of 30 (26.67%) of the ring glands were classified as displaying high-intensity red autofluorescence while the rest 22 (73.33%) of the ring glands were classified as displaying low-intensity red autofluorescence as shown in Figure 3.6.C. Based on this, the conclusion was that 20E-feeding does rescue the *PG>Zfrip8-RNAi1* animals, but the rescue is not as strong as 7-dC feeding.



B)



C)

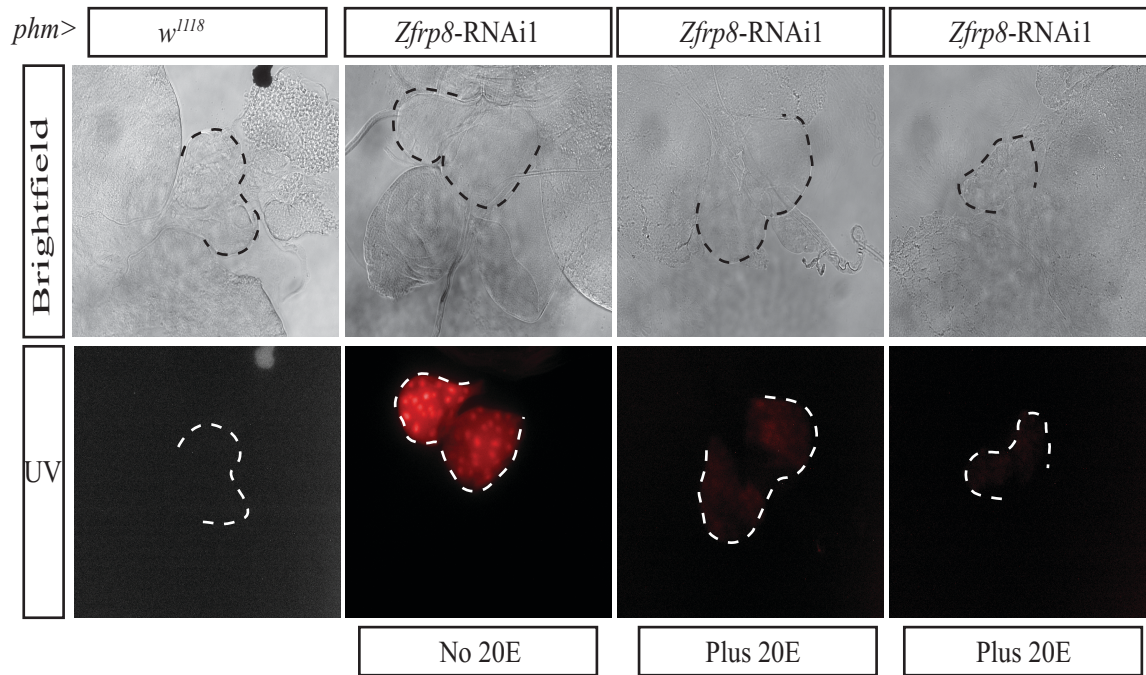


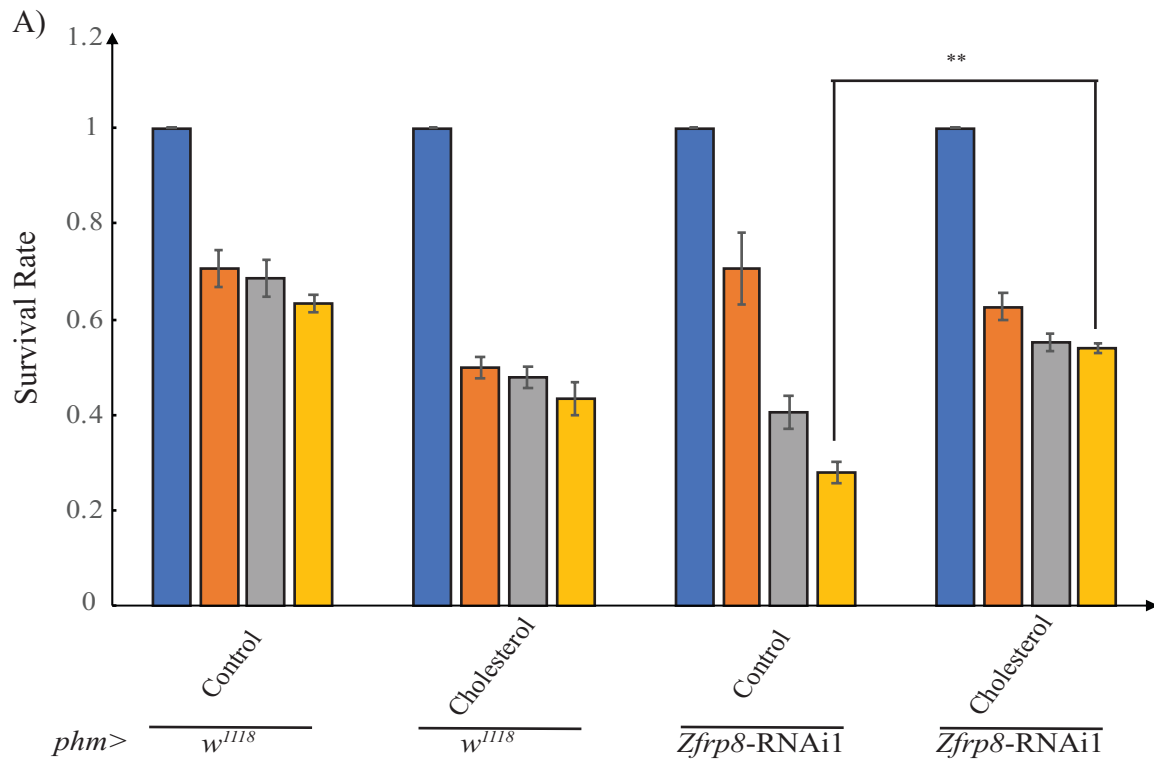
Figure 3.6: 20-hydroxyecdysone or 20E supplementation results in rescue of *PG*>*Zfip8*-RNAi1 animals, but less significant compared to 7dC: A) *PG*>*w¹¹¹⁸* and *PG*>*Zfip8*-RNAi1 animals grown on control media and 0.33 mg/mL 20E-supplemented diet. Relative to control media and not control fly, 20E results in the rescue of *PG*>*Zfip8*-RNAi1 animals but not as significant compared to 7dC. The survival rate for each developmental stage was determined by normalizing the corresponding stage to the number of eggs that were collected. A student's t-test was conducted to determine the significance relative to *phm*>*Zfip8*-RNAi1 grown on control media. * for $P \leq 0.05$. Blue bars represent eggs (N=50); orange, grey and yellow bars represent L3, pupae and adults respectively. Error bars represent the standard error of mean. B) The adults were collected 10 days after egg laying (AEL) and their growth recorded. Although *phm*>*Zfip8*-RNAi1 adult is larger in size compared to the *phm*>*w¹¹¹⁸* adult, supplementing the diet of *phm*>*Zfip8*-RNAi1 with 20E results in the reduction of the body size and the size becomes similar to that of the *PG*>*w¹¹¹⁸* (control) animals. C) Brain ring gland complexes viewed with a confocal microscope 42 hours after L2/L3 molt. The prothoracic glands are outlined in a dotted black line for the brightfield panel and in a dotted white line for the UV panel. The third panel from the left comprises the prothoracic gland displaying high-intensity red autofluorescence and the fourth panel from the left shows the prothoracic gland displaying low-intensity red autofluorescence. The higher percentage of low-intensity fluorescing ring glands compared to the high-intensity fluorescing ring glands suggests that 20E was successful in removing majority of the accumulated heme precursors although the efficiency was less compared to that of 7dC.

3.7 Cholesterol supplementation rescues the developmental defects of *PG>Zfrp8-RNAi1* animals, but less efficiently than 7-dC

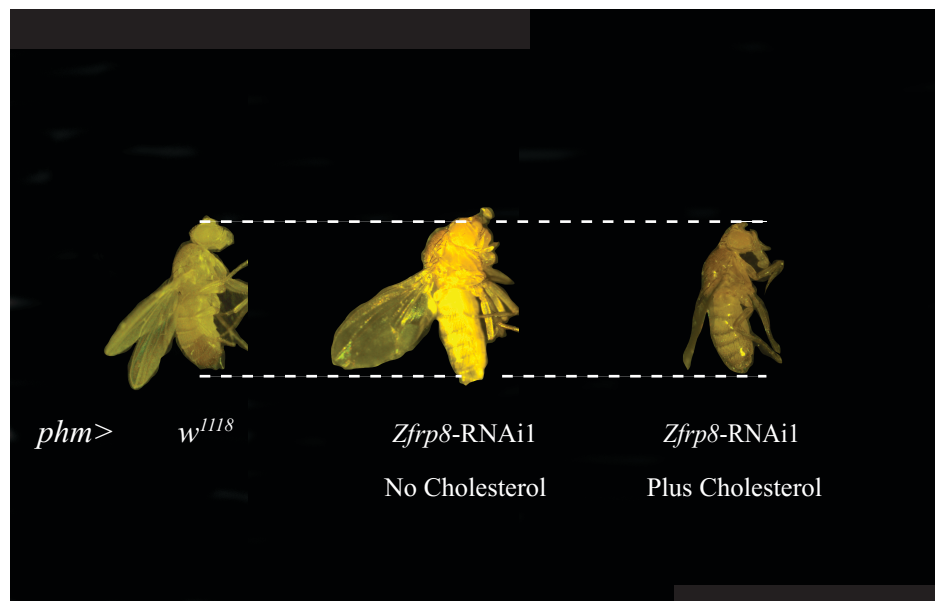
It is very important for the proper regulation of cholesterol metabolism as well as homeostasis concerning steroidogenesis in both vertebrates as well as invertebrates¹⁴³. Since cholesterol comes before 7-dehydrocholesterol in the ecdysone biosynthesis pathway and *PG>Nvd-RNAi* showed rescue with 7-dehydrocholesterol but not with cholesterol, I treated cholesterol supplementation as a negative control. As we know, *Drosophila* is a cholesterol auxotroph, which means that *Drosophila* cannot synthesize cholesterol on its own and needs to uptake cholesterol from the diet. If the fruit flies are surviving on low- or no-cholesterol diet, it is not possible for the animals to proceed to the point of metamorphosis and they usually end up dying in the larval stages. Since embryos do not uptake any form of sterols from the food, it is believed that cholesterol, as well as its derivatives, are maternally deposited in order to survive the process of embryogenesis and hence *Drosophila* on a low- or no-cholesterol diet do not die in the embryonic stages. Based on experiments conducted in the King-Jones lab, none of the development defects or delays displayed on knocking down the heme biosynthesis genes and the ecdysone biosynthesis genes specifically in the prothoracic gland have been rescued with cholesterol supplementation. Therefore, it made me curious whether the developmental defects displayed by the *PG>Zfrp8-RNAi1* animals could be rescued by cholesterol supplementation^{144,145}. For this purpose, I generated *PG>Zfrp8-RNAi1* embryos, which were then transferred to a diet that was supplemented cholesterol. For the *PG>Zfrp8-RNAi1* animals that were grown without being supplemented with cholesterol, 28% of the embryos went on to complete their full developmental cycle and eclose as adults whereas, for the *PG>Zfrp8-RNAi1* animals that were being supplemented with cholesterol, 54% of the embryos went to become fully-grown adults. Therefore, with respect to the food control, I have observed a

significant increase in survival rate which is also backed up by statistical analysis with a p-value of 0.002 for a one-tailed t-test (Figure 3.7.A). Similarly, for the *PG>w¹¹¹⁸* animals that were grown on a diet supplemented with cholesterol, 48% of the embryos went on to become adults (Figure 3.7.A). Therefore, with respect to the fly control, the increase in survival rate was not significant, given that the p-value generated was greater than 0.05. Feeding the *PG>Zfip8-RNAi1* animals with 20E rescued their large body size back to normal, as evident from Figure 3.7.B.

In order to determine whether feeding the *PG>Zfip8-RNAi1* animals with cholesterol, which is the starting component of the ecdysone biosynthetic pathway, results in the removal of the accumulated heme precursors, I collected the *PG>Zfip8-RNAi1* embryos and staged them during their transition from L2 to L3. The freshly transitioned larvae were then transferred to a fresh food cap and then dissected after 42 hrs. Similar to 7-dC and 20E, I observed a range of visible red autofluorescence and applied the same principle as before. After analyzing the samples with ImageJ, 7 out of the 30 (23.33%) ring glands under study were classified as displaying high-intensity red autofluorescence while the rest 23 (76.67%) were classified as displaying low-intensity red autofluorescence as shown in Figure 3.7.C. Combining these results, I concluded that cholesterol can rescue the *PG>Zfip8-RNAi1* animals to a certain degree, although it is less compared to 7-dC feeding. Based on the feeding experiments conducted with the components of the ecdysone biosynthesis pathway, this suggests that *Zfip8* regulates the iron or heme homeostasis through an unknown mechanism or pathway yet to be identified which in turn leads to the production of functional ecdysone through the ecdysone biosynthetic pathway, but further experiments need to be conducted to come to a more solid conclusion and determine the exact mechanisms behind the interaction as mentioned above.



B)



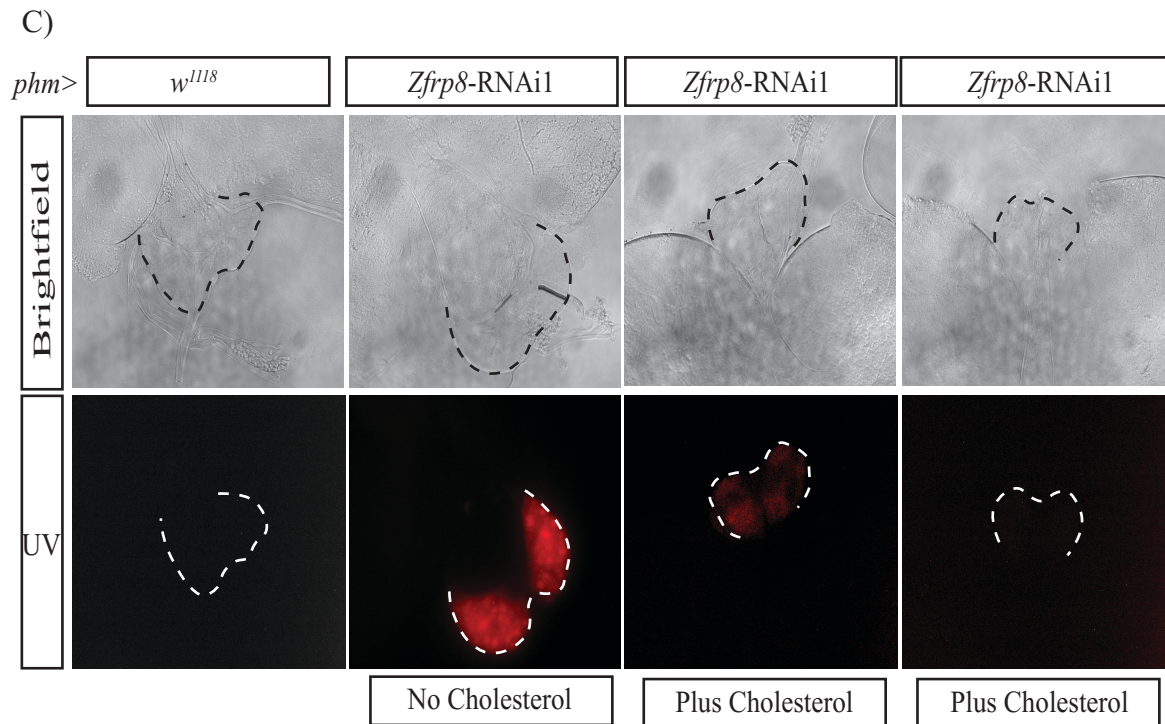


Figure 3.7: Cholesterol supplementation results in rescue of *PG>Zfzp8*-RNAi1 animals, but to a lesser degree compared to 7dC: A) *PG>w¹¹¹⁸* and *PG>Zfzp8*-RNAi1 animals grown on control media and 0.02 mg/mL Cholesterol-supplemented diet. Relative to control media and not control fly, Cholesterol results in the rescue of *PG>Zfzp8*-RNAi1 animals but not as significant compared to 7dC. The survival rate for each developmental stage was determined by normalizing the corresponding stage to the number of eggs that were collected. A student's t-test was conducted to determine the significance relative to *phm>Zfzp8*-RNAi1 grown on control media. ** for $P \leq 0.01$. Blue bars represent eggs (N=50); orange, grey and yellow bars represent L3, pupae and adults respectively. Error bars represent the standard error of mean. B) The adults were collected 10 days after egg laying (AEL) and their growth recorded. Although *phm>Zfzp8*-RNAi1 adult is larger in size compared to the *phm>w¹¹¹⁸* adult, supplementing the diet of *phm>Zfzp8*-RNAi1 with 20E results in the reduction of the body size and the size becomes similar to that of the *PG>w¹¹¹⁸* (control) animals. C) Brain ring gland complexes viewed with a confocal microscope 42 hours after L2/L3 molt. The prothoracic glands are outlined in a dotted black line for the brightfield panel and in a dotted white line for the UV panel. The third panel from the left comprises the prothoracic gland displaying high-intensity red autofluorescence and the fourth panel from the left shows the prothoracic gland displaying low-intensity red autofluorescence. The higher percentage of low-intensity fluorescing ring glands compared to the high-intensity fluorescing ring glands gives rise to the conclusion that Cholesterol supplementation succeeded in removing the majority of the accumulated heme precursors from the prothoracic gland.

3.8 Loss-of-*Zfrip8* results in downregulation of ecdysteroidogenic genes in whole-body samples

As I have already mentioned, knocking down *Zfrip8* specifically in the prothoracic gland leads to developmental delays, leading to *PG>Zfrip8-RNAi1* animals undergoing the transition from the second instar to the third instar a day later compared to the control (*PG>w¹¹¹⁸*). Since 20-hydroxyecdysone is the molting hormone in *Drosophila* and is also responsible for the developmental transitions from one stage to another stage, I hypothesized that developmental delays or defects on knocking down *Zfrip8* or other genes identified in the screen specifically in the prothoracic gland would be caused by the downregulation of 20-hydroxyecdysone as well as the other components of the ecdysone biosynthesis pathway. I observed the expression level of the different Halloween genes when *Zfrip8* was knocked down, specifically in the prothoracic gland. In order to achieve this, I normalized the expression of a target gene to the expression of a reference gene, *rp49*, in this case, which has a stable expression¹⁴⁶. For this experiment, I focused on the Halloween genes, namely *phantom*, *disembodied*, *spookier*, and *Neverland* since these four Halloween genes have been reported to be selectively expressed in the prothoracic gland cells of *Drosophila* during the larval developmental stages^{147,148}. Even if the whole third instar larvae were my sample and not specific tissues, it would not affect the overall result of the relative expression of the genes since they are produced only in the PG cells. For this purpose, I generated *PG>Zfrip8-RNAi1* embryos. The embryos were kept on a diet of Nutrifly food without any added supplements. The larvae were staged during their transition from the second instar to the third instar and collected 42 hrs after their transition. The relative fold change determines how many times a particular gene is upregulated or downregulated compared to the control. Since *rp49* represents the baseline in this experiment, it is showing a relative fold change of 1 because it is

being compared to its expression. The other Halloween genes that were under consideration in this experiment were all downregulated in the *PG>Zfrp8-RNAi1* animals, as evident from Figure 3.8. The *phm* was the least downregulated, and this could be mainly because *phantom* is upregulated by approximately 300 times in the prothoracic gland during the late third instar larval stage, even in control samples. *Dib* was the most downregulated in this study, followed by *Nvd* and *Spok* in increasing order. The result mentioned above points to the fact that knocking down *Zfrp8* specifically in the prothoracic gland results in the downregulation of the genes involved in the ecdysone biosynthetic pathway and conducting the experiment specifically on prothoracic gland would result in more concrete evidence with respect to my hypothesis.

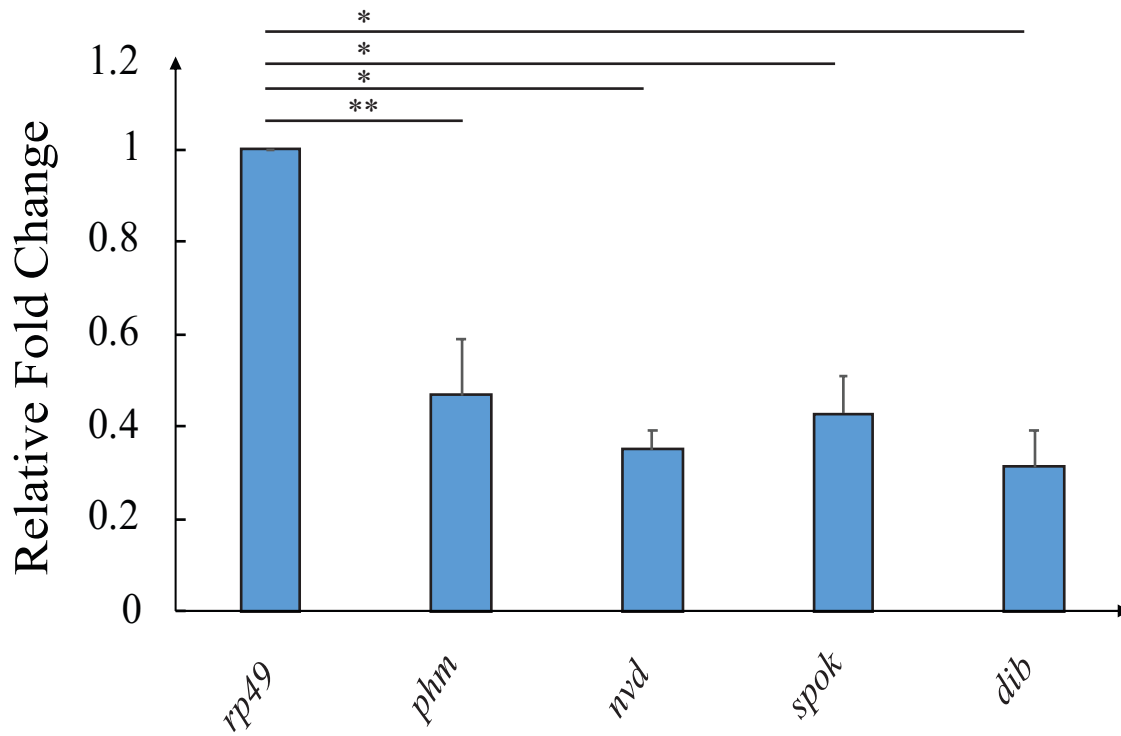


Figure 3.8: *Zfrp8*-RNAi reduced the expression of ecdysteroidogenic genes: qPCR was conducted to determine the expression of ecdysteroidogenic genes in the whole body after *Zfrp8* was knocked down using RNAi technique. Samples were dissected 42 hrs after the L2/L3 molt. Samples were normalized to control, *rp49*. ** for $P \leq 0.01$ and * for $P \leq 0.05$. Error bars represent the standard error of mean.

3.9 *Zfrp8* localization in the prothoracic gland

Zfrp8 localizes both in the nucleus and cytoplasm of the *Drosophila* ovary. However, no literature reported the subcellular localization of *Zfrp8* in the prothoracic gland. I had access to a transgenic *Zfrp8* line that was tagged with both Flag and GFP. This particular line contained the strong 3xP3-dsRed marker, which is an eyeless derived promoter fragment and results in strong dsRed expression specifically in the developing eye and in the brain¹⁴⁹. This led me to use a green fluorophore conjugated secondary antibody, thereby making it easier to view the tagged *Zfrp8* without any interference. I set up a cross between siblings of the transgenic *Zfrp8* line since *Zfrp8* is not overexpressed in V318625, and hence I was not able to take advantage of the *GAL4-UAS* system. The embryos were collected and staged during their transition from L2 to L3, and the larvae were dissected 42 hrs after their L2/L3 molt to maintain consistency. Following the procedure mentioned in section 3.18, images of the sample were recorded in a confocal microscope. Virgin *phm* flies were crossed with *w¹¹¹⁸* males, which acted as a negative control for this experiment since *phm>w¹¹¹⁸* animals lack GFP. On analyzing the data, I was not able to detect *Zfrp8* in the prothoracic gland, which is evident from the green panel of Figure 3.9. Based on the data from Flybase, the expression of *Zfrp8* in *Drosophila* is low over its entire life cycle. It is especially low during the L3 wandering stage, which is when I dissected my samples thereby corroborating the result that I got. This makes it challenging to determine the subcellular localization of *Zfrp8* in the prothoracic gland itself, making it mandatory to conduct further experiments to come to a definitive conclusion.

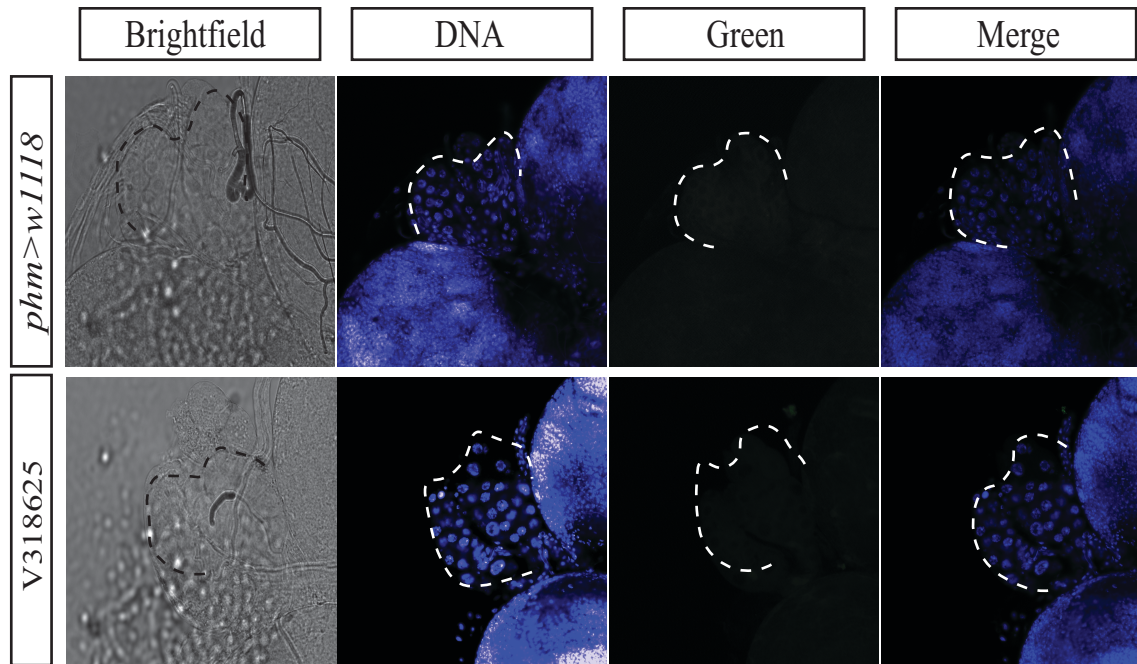


Figure 3.9: Transgenic GFP-tagged *Zfp8* did not show any localization in the prothoracic gland: To determine the localization of *Zfp8* in prothoracic gland, a primary antibody (1:400) was used in conjunction with a green fluorescent protein secondary-antibody (1:1000). Brain ring-gland complexes were dissected from the control (*phm*>*w¹¹¹⁸*) as well as the experimental sample: transgenic GFP-tagged *Zfp8*. The brain-ring gland complexes were dissected 42 hrs after the L2/L3 molt. If *Zfp8* would have been detected, the green panel would have displayed autofluorescence. The prothoracic glands are outlined in a dotted black line for the brightfield panel and in a dotted white line for the blue, green and merge channels. V318625 refers to the VDRC id of the fly line under study with the genotype of V318625 being PBac {fTRG00630.sfGFP-TVPTBF}VK00033.

Chapter 4

Discussion

4. Discussion:

4.1 The importance of *Zfrp8* with respect to the proper development of *Drosophila*

RNA interference, one of the most widely used techniques to disrupt the function of a particular gene, has been the core methodology of my thesis. I have employed the RNAi technique in conjunction with the GAL4/UAS system to knockdown *Zfrp8*, the gene being investigated in this thesis, specifically in the prothoracic gland. I focused on the prothoracic gland because that is the production site for ecdysone, the major steroid hormone in insects. I generated the *PG>Zfrp8-RNAi1* animals, which helped me to study the effects of knocking down *Zfrp8* in the prothoracic gland, more specifically, how the knockdown affected the development of the animals as mentioned above. Based on data from the VDRC website, *Zfrp8-RNAi1* (VDRC id: 11521) has no predicted off-target sites, which lends more credibility to the results that I generated. Only 9% of the embryos became fully-grown adults compared to the control (*PG>w¹¹¹⁸*) where approximately 71% of the embryos went on to become fully-grown adults. The L2/L3 transition was also delayed by an entire day compared to the control. Because of the 24-hr delay in the transition from L2 to L3 for the *PG>Zfrp8-RNAi1* animals, their corresponding adults were bigger compared to the control because of the prolonged feeding period. The prothoracic gland of the *PG>Zfrp8-RNAi1* animals also displayed red autofluorescence 42 hrs after their L2/L3 molt. *Zfrp8-RNAi2* targeted a different region of *Zfrp8*, however the treated animals did not display any developmental defects and their prothoracic glands did not display any red autofluorescence. The body size of the *PG>Zfrp8-RNAi2* animals was similar to the control animals (data not shown) since their transition from L2 to L3 was not delayed by a day but happened at the same time as the control. The purpose of experimenting with multiple RNAi lines is to validate the results since the

siRNAs may target a different gene and also contributed to the phenotype^{150,151}. I also had access to a mutant *Zfrp8* line *Df(2R)SM206* that was requested from Ruth Steward's lab by Dr. Qiuxiang Ou, a previous member of the King-Jones lab. It was also reported by Ruth Steward's lab that homozygous *Zfrp8* null-allele, *Df(2R)SM206* resulted in severe growth and developmental delays with most larvae perishing in the larval stages. However, it was not specified which larval stage the animals died. The few animals that were able to survive until pupariation were found to be smaller in size compared to their heterozygous siblings. Approximately 2% of the embryos went on to become adults but were reported to have poor viability as well as poor female fertility. As I already reported, when I was working with the homozygote, it did not survive behind the first instar larval stage. *Df(2R)SM183*, another mutant created by the Steward lab, affects both *tamo* and *Zfrp8* expression and hence cannot be relied upon for studying the developmental effects on the *Zfrp8* gene itself. Both the homozygous and hemizygous larvae of the *Zfrp8^{M-1-1}* mutant, which was identified in an Ethyl methanesulphonate (EMS) screen conducted by the Steward lab displayed approximately 5% adult survival. Unfortunately, the *Zfrp8^{M-1-1}* mutant died even before I received it. Combining the results from the RNAi lines and the mutants, it points to the fact that *Zfrp8* is essential for the development of *Drosophila*. The red autofluorescence caused by the accumulation of heme precursors suggests the possibility that the developmental defects displayed by the *PG>Zfrp8-RNAi1* and the mutant animals are because of a disruptive heme biosynthesis pathway. The defective heme pathway also leads to a reduction in the cellular heme and iron levels, which then downregulates the activity of the Halloween enzymes because they require iron to function. This leads to the possibility that the developmental defects could be caused because of a malfunctioning ecdysone biosynthesis pathway. Because of the off-target effects of RNAi and other factors that I already mentioned in section 1.7, I generated *Zfrp8* CRISPR KO construct to validate the phenotypes that were displayed by the RNAi lines and the mutants. The *Zfrp8* CRISPR

KO construct was sequence-verified, and I had access to a control gRNA line termed “no target pCFD5” which ensured the construct that I generated was trustworthy. The CRISPR construct that I generated to knock down *Zfjp8* must be injected successfully since the injections did not work out for me, unfortunately. This could have happened because of the following reasons: i) The broken needles that were generated did not have a sharp enough tip and ended up damaging the embryos, thereby decreasing their overall survival rates. ii) The embryos prepared to undergo injection need to be placed in a desiccation chamber, which is critical for their survival. The desiccation time depends on the temperature and humidity of the room in which the injections are being carried out. It is quite possible that the injected embryos were not desiccated for the required time or underwent desiccation longer than required, which affected their survival rates. iii) Not enough pressure was applied to the syringe that was attached to the needle, and therefore the DNA solution was not injected into the embryos. This could have happened for some of the embryos, but not all since the pressure is maintained manually while injecting and is not pre-determined automatically. iv) Post injections, the injected embryos are covered with halocarbon oil. If excess oil is not removed, inhibition of oxygen exchange to the embryos results in asphyxia or the excess oil leads the embryos to flow off their slide resulting in further desiccation, which contributes to their decline in survival rates. Once the injections are complete, and the transgenic flies are generated successfully, it would be interesting to see the developmental effects of the *Zfjp8* transgene when expressed specifically in the prothoracic gland. I expect that the transgenic *Zfjp8* CRISPR knockouts would result in larval lethality similar to that of the *Zfjp8* mutants. If the transgenic animals make it to the third instar larval stage, they would also display visible red autofluorescence in the prothoracic gland on exposure to UV. My expectation arises from the fact that a similar approach for the Halloween genes *phm* and *dib* also resulted in their gRNA lines phenocopying their respective mutant animals (Huynh et al., 2018). In order to determine the

efficiency of the 2xgRNA line with respect to disrupting the expression of *Zfrp8*, the *Zfrp8*-gRNA line needs to be crossed with the *act-Cas9* line which will allow to target *Zfrp8* in a ubiquitous manner. The resulting phenotype should be similar to that of the *Zfrp8* mutant animals. The *Zfrp8* gene region should also be sequenced in the genomic region extracted from the dissected ring glands of the transgenic animals to further verify that the observed phenotypes were due to the disruption of *Zfrp8*. The genomic DNA extracted from the adjacent brain will serve as a control. qPCR needs to be conducted on the *Zfrp8*-2xgRNA line to determine the downregulation of *Zfrp8* compared to the control. All of these results together would completely validate the role of *Zfrp8* regarding its involvement concerning iron or heme homeostasis as well as ecdysone biosynthesis.

4.2 *Zfrp8* does not feed into the heme biosynthesis pathway

We already know that iron is essential for the basic functioning of nearly all organisms on earth. Although iron is a trace element, it is essential for carrying out erythropoiesis and is also essential for DNA synthesis and repair, mitochondrial function, and also carries out many enzymatic reactions that are required for cell survival^{152,153}. Since I hypothesized that the developmental defects caused in the *PG>Zfrp8-RNAi1* animals are caused by disruptions in the heme biosynthesis pathway, it is possible that feeding these animals with iron as well as heme supplements would reverse the developmental defects that we have noticed. Incorporation of iron into protoporphyrin IX in the final step of the heme biosynthesis pathway leads to the formation of heme, so if there is a lack of cellular or mitochondrial iron levels, it will lead to the disruption of heme production. More importantly, the developmental defects displayed by the loss-of-*AGBE* were completely rescued with dietary iron supplementation. I decided to supplement the *PG>Zfrp8-RNAi1* embryos with dietary iron with the expectation that the developmental defects would be rescued, but unfortunately, dietary iron was not able to rescue the observed phenotype. Supplementing the *PG>Zfrp8-RNAi1* animals with dietary iron also failed to remove the accumulation of protoporphyrins in the prothoracic gland. This points to the possibility that lack of cellular or mitochondrial iron, which results in the disruption of the heme production that I mentioned earlier in this section, does not happen in the final step of the heme biosynthesis pathway but somewhere before that. It also gives rise to the idea that *Zfrp8* probably does not participate in cellular iron homeostasis. According to my proposed hypothesis, disruption in the heme biosynthesis pathway leads to reduced heme production, and thereby a lack of heme results in the developmental defects. Since dietary iron failed to rescue the observed defects, I turned my attention towards supplementing the *PG>Zfrp8-RNAi1* animals with exogenous heme in the form

of hemin. Hemin supplementation would bypass all the steps in the heme biosynthesis pathway, and if I observe any degree of rescue in the *PG>Zfrp8-RNAi1* animals, it would suggest that *Zfrp8* indeed feeds into the heme biosynthesis pathway in one way or the other. Surprisingly, hemin supplementation also failed to rescue the developmental delays or defects that I have observed in the *PG>Zfrp8-RNAi1* animals. Hemin supplementation also failed to remove the excess heme precursors that accumulated in the prothoracic gland. Based on the dietary iron and hemin supplementation experiments, I was trying to determine if lack of cellular or mitochondrial iron and heme deficiency is responsible for the developmental delays in the *PG>Zfrp8-RNAi1* animals. Since both the supplements failed to rescue the developmental defects, I turned my attention towards another probable cause that could result in the effects mentioned above: iron overload. For this purpose, I decided to implement BPS as an iron chelator. Supplementing the diet of the *PG>Zfrp8-RNAi1* animals with an iron chelator had no effect whatsoever on the developmental defects as well as the accumulation of heme precursors in the concerned animals. These experiments point to the fact that *Zfrp8* does not feed into the heme biosynthesis pathway directly, but in an indirect manner or mechanism that is yet to be ascertained.

4.3 *Zfrp8* feeds into a yet-to-be ascertained pathway to produce heme required for ecdysone synthesis but may not feed into the conventional ecdysone biosynthesis pathway

Since the iron and heme supplements failed to rescue the developmental defects that have been observed in the *PG>Zfrp8-RNAi* animals, indicating that *Zfrp8* does not feed into the heme biosynthesis pathway for the production of heme but rather in a yet-to-be ascertained pathway. I focused my attention on the ecdysone biosynthesis pathway. The Halloween enzymes, including the cytochrome P450 monooxygenases except for *shroud*, require iron to function. The cytochrome P450 monooxygenases bind to heme in a non-covalent manner whereas *Neverland*, which is a Rieske-electron oxygenase, requires a Fe-S cluster in its catalytic center. During the late third instar larval stage before the onset of metamorphosis, there is a surge in ecdysone levels, which is critically important to start the process of puparium formation. As I reported earlier in section 1.5, the expression of the cytochrome P450 genes responsible for producing ecdysone is increased by 40 to 180 times during this transition (Ou et al., 2016). This increase in expression also corresponds to the high demand for iron and heme since iron is required for the proper functioning of the Halloween enzymes. If there is a reduction in cellular or mitochondrial iron and heme levels, it would eventually affect the working of the Halloween enzymes and result in a highly decreased production of ecdysone. Since 20-hydroxyecdysone is the primary molting hormone in *Drosophila*, reduced ecdysone production would disrupt the onset of metamorphosis by delaying or arresting the transition. Based on previous work done in the King-Jones lab, disrupting the function of *Neverland*, which converts dietary cholesterol to 7-dC specifically in the prothoracic gland resulted in weak autofluorescence because of accumulated heme precursors and this led me to test this theory by adding different components of the ecdysone biosynthesis pathway namely 7-dehydrocholesterol, 20-hydroxyecdysone and cholesterol as a supplement to the fly food and

observe if these added supplements would be able to rescue the developmental defects of the *PG>Zfrp8-RNAi1* animals. If I am able to observe significant rescue for any of the ecdysone-related supplements, I would be able to state that *Zfrp8* feeds into the ecdysone biosynthetic pathway. I started with 7-dehydrocholesterol, which also acts as my positive control and managed to rescue 60% of the embryos to adulthood, which was significant when compared to the food control. On supplementing the *PG>Zfrp8-RNAi1* animals with 20-hydroxyecdysone, I observed that 47% of the embryos became adults which is significant based on statistical analysis. Since Cholesterol acted as a negative control, I was not expecting a significant rescue, but to my surprise, 54% of the embryos went on to become adults, which is a significant rescue based on statistical analysis. With respect to the different intensities of visible red autofluorescence observed as per ImageJ analysis when the *PG>Zfrp8-RNAi1* animals were supplemented with Cholesterol, 20E, and 7-dC, this could be attributed to the fact that the supplements were able to induce significant rescue but not complete rescue. Hence, the higher the rescue, the greater the percentage of ring glands displaying low-intensity autofluorescence, which signifies better removal of the accumulated heme precursors from the prothoracic gland. The fact that 7dC works so much better than the molting hormone 20E itself could be attributed to the utilization of 7dC as a dietary precursor. 7dC generates a time-dependent fluctuation of ecdysteroids by operating through a series of biosynthesis enzymes downstream of Neverland^{154,155}. There is a possibility that 7dC feeds into an alternate signaling pathway which is responsible for regulating heme metabolism or production and thereby dietary supplementation of 7dC results in the movement of the signal into the yet-to-be identified signaling pathway which in turn significantly reduces the red autofluorescence present in the prothoracic gland of the *PG>Zfrp8-RNAi1* animals. The fact that rescuing the ecdysone pathway results in the reduction of red autofluorescence in the prothoracic gland is because of the association of 20E with *E75*, a heme sensor and a crucial 20E response

gene that is responsible for affecting 20E ecdysteroid titer^{156,157}. Rescuing the pathway leads to the increased production of 20-hydroxyecdysone, which in turn rapidly induces the expression of *E75*¹⁵⁸. Since heme is responsible for maintaining the stability of the *E75* ligand-binding domain, the availability of heme is proportional to the levels of *E75* expression. With the increase in *E75* induction, the heme availability is also increased, which translates to the reduction in red autofluorescence in the prothoracic gland. Based on the results and observations, it could be concluded that all the three supplements that came out of the ecdysone biosynthesis pathway helped to rescue the developmental defects of the *PG>Zfrp8-RNAi1* animals by a significant degree but not completely, and this is pretty strong evidence suggesting that *Zfrp8* feeds into the ecdysone biosynthesis pathway although further experiments need to be conducted to discover the underlying mechanisms responsible for the interaction as mentioned above.

With respect to my revised predicted model, *Zfrp8* does not act through the conventional heme biosynthesis pathway, which results in the production of heme but instead through an unidentified pathway that needs to be identified to get a better view of the overall predicted model. The significant rescue of *PG>Zfrp8-RNAi1* animals by components of the ecdysone biosynthetic pathway proves that *Zfrp8* acts through the ecdysone biosynthesis pathway, but the fact that the sterol components are not able to induce a complete rescue in the affected animals could be because heme is not produced as required for the cytochrome P450 enzymes which results in minor downregulation of the ecdysteroidogenic genes (needs to be confirmed by further experiments). It is highly possible that 7-dC feeds into an alternate signaling pathway which is in charge of regulating iron or heme metabolism or production.

4.4 Establishing parallels between *PDCD2* and *Zfrp8*

Programmed Cell Death Protein 2 or *PDCD2*, the vertebrate ortholog of *Zfrp8*, is highly conserved and was originally identified in rat thymocytes that were undergoing programmed cell death^{159,160}. *PDCD2*, located on chromosome 6q27 situated in a region known to be involved in translocations and deletions in leukemias and lymphomas, suggests that *PDCD2* might play a role in determining hematopoietic cell fate decisions^{161,162}. The function of *PDCD2* is still not defined, and its expression has been recorded during embryonic development and in normal adult tissues¹⁶³⁻¹⁶⁵. *PDCD2* expression is enriched in mouse embryonic, hematopoietic, and neural stem cells. *PDCD2* also plays a role in zebrafish hematopoiesis. *PDCD2* has been reported to be highly expressed in human cancer cells, which suggests that continued expression of the protein likely points toward the possibility of clinical relapse in patients suffering from acute leukemia¹⁶⁶. Loss-of-*PDCD2* results in the induction of p53 and p53 direct target genes such as p21 and involves the reduction of downstream genes responsible for promoting cell cycle. p53 or tumor protein regulates the cell cycle, thereby functioning as a tumor suppressor¹⁶⁷. When *PDCD2* is knocked down in embryonic stem cells, it leads to a failure in S-phase entry since the induction of p53 and p53 target genes are usually associated with cell cycle arrest as well as apoptosis. The depletion of *PDCD2* in embryonic stem cells also resulted in a substantial elongation of the G1 phase of the cell cycle, usually short in wildtype embryonic stem cells¹⁶⁸⁻¹⁷⁰, another observation that points to the inability of *PDCD2*-depleted embryonic stem cells to enter the S-phase resulting in a significant defect in growth. It is highly likely that *PDCD2* controls the cell cycle of embryonic stem cells, and it does so by mediating through the p53 pathway¹⁷¹, although the mechanism underlying this interaction is yet-to-be elucidated. Since *Zfrp8* and *PDCD2* are highly conserved, it is expected that *Zfrp8* KO would result in significant upregulation of p53, which would, in turn,

result in cell cycle arrest and explain the reason behind the larval lethality that we have observed in the *Zfrp8* mutants. It would be particularly interesting to observe the effects of the cell cycle arrest on the prothoracic gland compared to the rest of the *Drosophila* body since PG is a polytene tissue and our primary focus. Literature review shows that conditions responsible for arresting cell growth also result in the blockage of endocycle progression, thereby suggesting that these two processes are maintained on a tight regulatory linkage¹⁷². *PDCD2* is required for the proliferation of both mouse embryonic fibroblasts or MEFs as well as embryonic stem cells which clearly outlines the effects of *PDCD2* on the proliferation of both pluripotent as well as more differentiated cells. Protein-protein interactions determined by STRING¹⁷³ (<https://string-db.org/cgi/network.pl?taskId=ufWISnvu2Swg>) reports the interaction of *PDCD2* with quite a few regulators of the ubiquitin pathway including ubiquitin-specific peptidases USP49 and USP43¹⁷⁴ as well as the ubiquitin ligase, Parkin^{175,176} thereby establishing the role of *PDCD2* in the regulation of p53 ubiquitination. Based on the interactions of *Zfrp8*, as shown by STRING, *Zfrp8* interacts with CG11583 and CG6712, where both are ribosome biogenesis proteins. Ubiquitin and ubiquitin-like proteins are known to play a role in ribosome biogenesis where the nuclear ubiquitin-proteasome system is responsible for controlling the supply of ribosomal proteins in order to assemble new ribosomal subunits in the nucleolus¹⁷⁷⁻¹⁸¹. If the ribosomal proteins are knocked out, it results in the disruption of ribosome biogenesis, which in turn triggers a p53-dependent response¹⁸². It would be exciting to determine the role of *Zfrp8* in the aforementioned interaction. *PDCD2* physically interacts with Host Cell Factor 1 (HCF-1)¹⁸³⁻¹⁸⁶ and HCF-1 is known to function as a coactivator or corepressor with respect to the regulation of multiple phases of the cell cycle. The amino acid region ranging from 150 to 200 for *PDCD2* was reported to specifically interact with all the known species of HCF-1 that were tested, ranging from humans through *C.elegans* (Scarr et al.,2002), suggesting that this particular function of *PDCD2* could be

conserved. Similarly, the region between amino acids 1910 and 2005 was determined to be responsible for the binding of HCF-1 to PDCD2. The association between the proteins mentioned above remains critical for the suppression of HCF-1, which in turn stimulates cell division. Loss-of-*PDCD2* results in the inhibition of erythroid differentiation of K562 leukemia cells by upregulating transcription factors responsible for sustaining multilineage progenitors and downregulates erythroid-specific signals. K562 cells were chosen because they resemble bipotent megakaryocytic-erythroid progenitors or MEPs and have been utilized to study erythroid as well as megakaryocytic differentiation¹⁸⁷⁻¹⁸⁹.

4.5 Future directions:

4.5.1 Determining the upregulation of ecdysteroidogenic titers in the presence of sterol supplements

We know by now that *PG>Zfrip8*-RNAi1 animals show no rescue whatsoever with dietary iron and hemin supplementation but show a significant rescue with 7-dehydrocholesterol, 20-hydroxyecdysone as well as cholesterol. Based on my hypothesis, the developmental delays in the *PG>Zfrip8*-RNAi1 animals are due to the reduced production of ecdysone, which ultimately affected the transition of the concerned animals from one developmental stage to another- the L2/L3 molt in this case. This hypothesis was further supported by the fact that the *PG>Zfrip8*-RNAi1 animals showed a significant rescue with the components of the ecdysone biosynthesis pathway when compared to the food control. I am predicting that *PG>Zfrip8*-RNAi1 animals have reduced ecdysteroidogenic titers in their whole body, and this effect will be more pronounced specifically in the prothoracic gland since it is responsible for producing ecdysone. qPCR would be conducted to observe the ecdysteroidogenic titers in the *PG>Zfrip8*-RNAi1 animals without any added supplements. If the data confirms a reduction in ecdysteroidogenic titers, for both the whole body and the prothoracic gland the next experiment would be to observe the ecdysteroidogenic titers when the *PG>Zfrip8*-RNAi1 are fed with the sterol supplements, the supplements that have shown a certain degree of rescue in the experiments that I have conducted. I expect that the ecdysteroidogenic titers will be upregulated in the sterol supplemented animals compared to the animals growing without sterol supplementation.

4.5.2 Determining the efficiency of the 2xgRNA line

Once the *Zfrp8* 2xgRNA line has been created and successfully verified, it would also be essential to observe the ecdysone levels in the transgenic flies, and I am expecting the ecdysone titers to be downregulated similar to the *PG>Zfrp8-RNAi1* flies which would also determine the efficiency of the *Zfrp8* 2xgRNA lines. All the rescue experiments that were conducted with dietary iron, hemin, an iron chelator, 7-dehydrocholesterol, 20-hydroxyecdysone and cholesterol on the *PG>Zfrp8-RNAi1* animals should also be conducted on the *Zfrp8* 2xgRNA line to verify that knocking down *Zfrp8* specifically in the prothoracic gland via two independent methods generates the same results. It would also be interesting to see the ecdysteroidogenic titers in the whole body as well as prothoracic gland for the *Zfrp8* 2xgRNA transgenic flies. I am expecting the ecdysteroidogenic titers to be downregulated in the somatic CRISPR/Cas9 line. The sterol supplements 7-dehydrocholesterol, 20-hydroxyecdysone and cholesterol that were able to rescue the *PG>Zfrp8-RNAi1* animals to a certain degree should also be able to rescue the *Zfrp8* 2xgRNA flies, although it would be difficult to predict if the degree of rescue would be amplified or downregulated in the CRISPR line compared to the RNAi line. The ecdysteroidogenic titers in the *Zfrp8* 2xgRNA fly rescued with sterol supplements should also be upregulated compared to the *Zfrp8* 2xgRNA flies that were growing without sterol supplementation. The ecdysteroidogenic titers would be calculated 42 hrs post L2/L3 molt.

4.5.3 Elucidating the interaction of *Zfrp8* with piRNA pathway proteins

PIWI-interacting RNAs or piRNAs are 23 to 31 nucleotide small RNAs that are associated with Piwi family Argonaute or AGO proteins but produced by Dicer-independent mechanisms¹⁹⁰⁻¹⁹². piRNAs, just like *Zfrp8*, are known to regulate the activity of transposable elements, thereby protecting the genome integrity during oocyte development as well as germ stem cell differentiation¹⁹³⁻¹⁹⁸. *Zfrp8* has also been shown to dominantly enhance or suppress the ovary or egg phenotypes of most of the piRNA pathway mutants. For example, loss of one copy of *Zfrp8* resulted in the significant enhancement of the egg phenotypes of *vasa*, *AGO3*, and *Spindle-E (spn-E)*¹⁹⁹ mutants. Furthermore, the nuclear localization of *Zfrp8* is strongly reduced in the mutants, which is consistent with this result. These two results strongly suggest that *Zfrp8* is regulated in part by the piRNA pathway genes. It has also been established that *Mael*, one of the piRNA pathway component acts antagonistically to *Zfrp8* whereby its perinuclear accumulation is dependent on *Zfrp8* as well as the egg phenotype of *mael* is suppressed by the loss of one copy of *Zfrp8* which is opposite to the effects observed in the case of *vasa* and *spn-E* mutants^{200,201}. Co-immunoprecipitation experiments have further validated the interaction by proving that *Zfrp8* and *Mael* are found in the same complex (Minakhina et al., 2014). Since the genetic interaction of *Zfrp8* with piRNA pathway genes has already been discovered, it would be interesting to see if depleting the piRNA biosynthesis genes by utilizing a germline-specific *GAL4* driver to achieve gene-specific knockdown²⁰²⁻²⁰⁴ would result in abnormal subcellular localization of *Zfrp8* specifically in the prothoracic gland. It would also be imperative to observe the accumulation of heme precursors in the prothoracic gland on germline-specific knockdown of the piRNA biosynthesis genes. If there is visible red autofluorescence, it would suggest the possibility that the piRNA genes might be responsible for regulating cellular iron or heme metabolism which in turn results

in the regulation of ecdysone thereby providing further ground that *Zfrp8* and piRNA genes might be working together to carry out the aforementioned regulation. If the germline-specific depletion of the piRNA pathway genes fails to display significant red autofluorescence in the prothoracic gland under UV exposure, it would mean that disrupting the piRNA pathway genes specifically in the germline does not result in heme-related phenotypes but is a unique feature of *Zfrp8*. It would also be interesting to observe the localization of *Zfrp8* when supplemented with 7dC, 20E and Cholesterol, specifically in the prothoracic gland in the presence of *vasa*, *AGO3*, and *Spindle-E* or *spn-E* mutants. Another interesting experiment would be to conduct qPCR in order to observe if the piRNA pathway genes are upregulated or downregulated when *Zfrp8* is knocked down specifically in the prothoracic gland, the reverse experiment could also be conducted whereby the piRNA pathway genes are knocked down in the germline, and the expression of *zfrp8* would be observed. The experiments, as mentioned above, would shed light on how the interaction between *Zfrp8* and the piRNA pathway genes are regulated or maintained with respect to iron/heme homeostasis as well as ecdysone production. Since there is no existing report connecting piRNA pathway genes with iron or heme homeostasis as well as ecdysone biosynthesis, it would provide an answer to the following question: If the piRNA pathway genes are taking part in such a regulation, are they doing it with the help of *Zfrp8*? The probable answer to this question will help the future investigators to figure out if this is the alternative pathway that I have predicted in my revised model.

4.5.4 Validating the interaction between *Zfrp8* and piRNA pathway proteins in S2 cells

In order to further validate the experimental results that I have got using the *Drosophila* fly lines from different stock centers, the next approach would involve employing the embryonic line S2 since it has been stably transformed and is known to produce a large number of variants that are good enough to mimic the experimental conditions in order to generate the corresponding results²⁰⁵. Experiments involving cell line is also known to complement the genetic as well as developmental experiments done on the fly lines. The embryonic line S2 will be ordered from the *Drosophila* Genomics Resource Center or DGRC²⁰⁶. Using the cell culture approach, the genetic interaction between *Zfrp8* and the piRNA pathway proteins could be further validated. Co-immunoprecipitation experiments under different conditions, namely in the presence of iron-supplemented conditions, heme-supplemented conditions, sterol-supplemented conditions, could be carried out to determine if the interaction between *Zfrp8* and the piRNA pathway proteins are enhanced or suppressed in the presence of different supplements. This would further help us understand the interaction mentioned above and if this interaction is affected by an increase in iron, heme, or sterol levels.

4.6 Conclusions:

Zfrp8 is essential for maintaining hematopoietic stem cells in *Drosophila melanogaster*, where hematopoiesis refers to the conversion of immature precursor cells to mature red blood cells²⁰⁷. Loss-of-*Zfrp8* leads the stem cells, whether it be hematopoietic, follicle, or germline, to lose their ability to self-renew, and they start behaving like mature prohemocytes. Apart from that, before my work, there have been no reports of linking *Zfrp8* directly with iron/heme homeostasis as well as ecdysone production. My model illustrates that *Zfrp8*, one of the 34 genes that came out of the genetic screen, participates in the production of heme through the heme biosynthesis pathway. The produced heme then acts as a co-factor for the cytochrome P450 enzymes, which enables them to function properly and results in the formation of 20-hydroxyecdysone or the biologically active form of ecdysone through the ecdysone biosynthesis pathway. The developmental defects displayed by the *PG>Zfrp8-RNAi* animals include the major arrest of the third instar larvae and the visible red autofluorescence of the prothoracic gland under UV exposure. The mutant *Df(2R)SM206* also did not survive beyond the first instar larval stage. These results together suggest that knocking down *Zfrp8* or the loss-of-*Zfrp8* results in the disruption of either the heme biosynthetic pathway or the ecdysone biosynthetic pathway or both which results in the developmental defects that we have already observed. This led me to use dietary iron, hemin, iron chelator as well as Cholesterol, 20E and 7-dC as supplements to try and rescue the developmental defects associated with the *PG>Zfrp8-RNAi* animals. Iron, hemin, and iron chelator supplementation failed to rescue the developmental defects of the concerned animals. In contrast, the sterol supplementations resulted in the significant rescue of the *PG>Zfrp8-RNAi* animals with 7-dC resulting in the most significant rescue. Neither of the supplements was able to display complete rescue of the affected animals. Knocking down *Zfrp8* also resulted in the downregulation

of the ecdysteroidogenic genes under study, namely *phm*, *dib*, *spok*, and *nvd*. This led me to update my predicted model (Figure 4), whereby I stated that *Zfrp8* does play a part in heme production but not through the conventional heme biosynthesis pathway but through a pathway or mechanism that has been still not identified. The biosynthesized heme then acts as a co-factor for the P450 enzymes, which then produces ecdysone. The inability of the sterol supplements to completely rescue the *PG>Zfrp8*-RNAi animals could be attributed to the fact that there could be a shortage of heme production through the yet-to-be-identified pathway which results in the downregulation of the cytochrome P450 genes. Further experiments need to be conducted in order to map out the detailed interaction or the underlying mechanisms that are at play here.

On a different note, it would be interesting to figure out whether *zfrp8* plays a role with respect to causing porphyria. Since knocking down *Zfrp8* results in protoporphyrin accumulation in the prothoracic gland, which is equivalent to what is observed in patients suffering from porphyria, caused due to a dysfunctional heme biosynthetic pathway leading to a reduction in cellular iron or heme levels. However, based on my revised model, *Zfrp8* does not act through the heme biosynthesis pathway, but through a still unidentified pathway, it would be imperative to figure out the intermediates/components involved in that alternate pathway and if disrupting that pathway by knocking down or knocking out the components of that pathway also results in porphyria-like phenotypes. That would provide a strong argument towards proving the involvement of *Zfrp8* with respect to causing porphyria. Since *Zfrp8* has been reported to be involved in a complex with a piRNA pathway protein, it would make sense to determine the physical interactors of *Zfrp8* utilizing mass-spectrometry^{208,209} both by collecting ring gland and by the cell-culture approach to gain further validation. More importantly, if those physical interactors are responsible for affecting the involvement of *Zfrp8* concerning heme homeostasis and ecdysone production, that would open up a new avenue on this particular topic.

On taking into consideration, the work done in my thesis sheds light on the behavior of *Zfrp8* with respect to iron/heme homeostasis and ecdysone production suggesting for the first time the involvement of *Zfrp8* in a yet-to-be-identified pathway leading to heme biosynthesis resulting in functional cytochrome P450s which lead to ecdysone production. The significant rescue demonstrated by 7-dC supplementation suggests the possibility that the gene studied in this thesis, *Zfrp8*, might not feed into the conventional ecdysone biosynthesis pathway but may branch off into a separate pathway after 7-dC which in turn regulates the iron or heme metabolism.

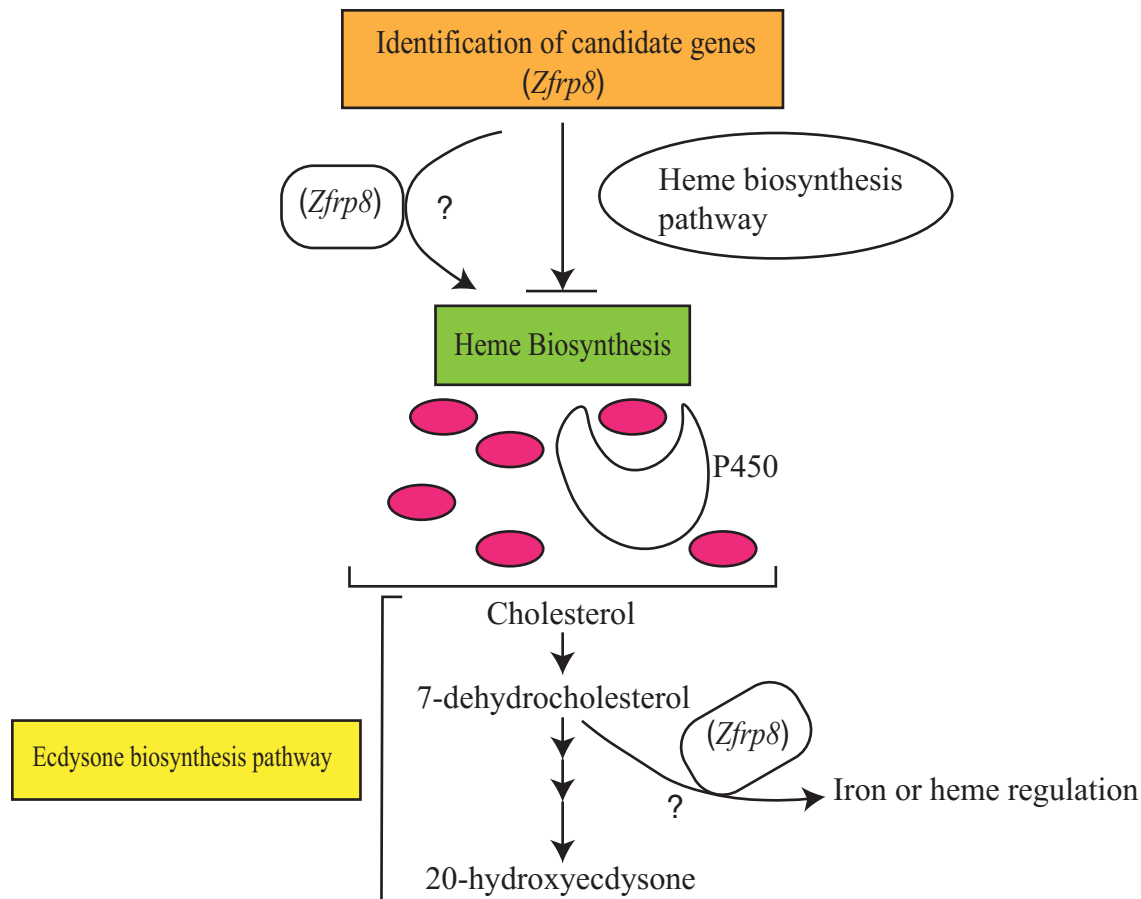


Figure 4: Updated proposed model linking *Zfrp8* to iron/heme homeostasis and ecdysone production: The original hypothesis stated that *Zfrp8* acts through the heme biosynthesis pathway resulting in heme production. The produced heme acts as a co-factor for the cytochrome P450 enzymes, the P450s synthesize the steps of the ecdysone biosynthesis pathway resulting in the biologically active form of ecdysone. Based on the rescue experiments that I conducted, dietary iron and heme failed to rescue the developmental defects displayed by the *PG>Zfrp8-RNAi1* animals whereas the sterol supplements were able to rescue the affected animals by a significant margin. These results altogether led me to update my previously hypothesized model suggesting that *Zfrp8* does participate in heme production but not by the conventional heme biosynthesis pathway but by a yet-to-be identified pathway. The significant rescue demonstrated by 7-dC supplementation suggests that *Zfrp8* might feed into a separate pathway that regulates iron or heme metabolism but may not feed into the conventional ecdysone biosynthesis pathway. Further experiments need to be conducted to completely validate the model that I have proposed.

References

References:

- 1) Zubeldia-Brenner, L., Roselli, C. E., Recabarren, S. E., Deniselle, M. C. G., & Lara, H. E. (2016). Developmental and Functional Effects of Steroid Hormones on the Neuroendocrine Axis and Spinal Cord. *Journal of Neuroendocrinology*, *28*(7). doi: 10.1111/jne.12401
- 2) Diamond, M. (2009). Clinical implications of the organizational and activational effects of hormones. *Hormones and Behavior*, *55*(5), 621–632. doi: 10.1016/j.yhbeh.2009.03.007
- 3) Thornton, J., Zehr, J. L., & Loose, M. D. (2009). Effects of prenatal androgens on rhesus monkeys: A model system to explore the organizational hypothesis in primates. *Hormones and Behavior*, *55*(5), 633–644. doi: 10.1016/j.yhbeh.2009.03.015
- 4) Wallen, K. (2009). The Organizational Hypothesis: Reflections on the 50th anniversary of the publication of Phoenix, Goy, Gerall, and Young (1959). *Hormones and Behavior*, *55*(5), 561–565. doi: 10.1016/j.yhbeh.2009.03.009
- 5) Arnold, A. P. (2009). The organizational–activational hypothesis as the foundation for a unified theory of sexual differentiation of all mammalian tissues. *Hormones and Behavior*, *55*(5), 570–578. doi: 10.1016/j.yhbeh.2009.03.011
- 6) Guillette, L. J., Crain, D. A., Rooney, A. A., & Pickford, D. B. (1995). Organization versus Activation: The Role of Endocrine-Disrupting Contaminants (EDCs) during Embryonic Development in Wildlife. *Environmental Health Perspectives*, *103*, 157. doi: 10.2307/3432527
- 7) Desvergne, B., & Héligon, C. (2009). Steroid hormone pulsing drives cyclic gene expression. *Nature Cell Biology*, *11*(9), 1051–1053. doi: 10.1038/ncb0909-1051

- 8) Lightman, S. L., & Conway-Campbell, B. L. (2010). The crucial role of pulsatile activity of the HPA axis for continuous dynamic equilibration. *Nature Reviews Neuroscience*, *11*(10), 710–718. doi: 10.1038/nrn2914
- 9) Parent, A.-S., Teilmann, G., Juul, A., Skakkebaek, N. E., Toppari, J., & Bourguignon, J.-P. (2003). The Timing of Normal Puberty and the Age Limits of Sexual Precocity: Variations around the World, Secular Trends, and Changes after Migration. *Endocrine Reviews*, *24*(5), 668–693. doi: 10.1210/er.2002-0019
- 10) Lachelin, G., & Yen, S. (1978). Hypothalamic chronic anovulation. *American Journal of Obstetrics and Gynecology*, *130*(7), 825–831. doi: 10.1016/0002-9378(78)90017-0
- 11) Hoffenberg, R. (1974). Aetiology of hyperthyroidism. II. *Bmj*, *3*(5929), 508–510. doi: 10.1136/bmj.3.5929.508
- 12) Norman, A. (2003). HORMONES | Steroid Hormones. *Encyclopedia of Food Sciences and Nutrition*, 3166–3174. doi: 10.1016/b0-12-227055-x/00606-4
- 13) Rhen, T., & Cidlowski, J. A. (2009). Steroid Hormone Action. *Yen & Jaffes Reproductive Endocrinology*, 105–120. doi: 10.1016/b978-1-4160-4907-4.00005-x
- 14) Holst, J.P., Soldin, O.P., Guo, T., & Soldin, S.J. (2004). Steroid hormones: relevance and measurement in the clinical laboratory. *Clinics in laboratory medicine*, *24* 1, 105-18.
- 15) Hoffman, J. R., & Ratamess, N. A. (2006). Medical issues associated with anabolic steroid use: are they exaggerated?. *Journal of sports science & medicine*, *5*(2), 182–193.
- 16) Yesalis, C. E., & Bahrke, M. S. (2005). Anabolic Steroid and Stimulant Use in North American Sport between 1850 and 1980. *Sport in History*, *25*(3), 434–451. doi: 10.1080/17460260500396251

- 17) Pandey, U. B., & Nichols, C. D. (2011). Human Disease Models in *Drosophila melanogaster* and the Role of the Fly in Therapeutic Drug Discovery. *Pharmacological Reviews*, 63(2), 411–436. doi: 10.1124/pr.110.003293
- 18) Nijhout, H. F., Riddiford, L. M., Mirth, C., Shingleton, A. W., Suzuki, Y., & Callier, V. (2013). The developmental control of size in insects. *Wiley Interdisciplinary Reviews: Developmental Biology*, 3(1), 113–134. doi: 10.1002/wdev.124
- 19) Fernández-Moreno, M. A., Farr, C. L., Kaguni, L. S., & Garesse, R. (2007). *Drosophila melanogaster* as a Model System to Study Mitochondrial Biology. *Methods in Molecular Biology Mitochondria*, 33–49. doi: 10.1007/978-1-59745-365-3_3
- 20) Ou, Q., Zeng, J., Yamanaka, N., Brakken-Thal, C., O'Connor, M. B., & King-Jones, K. (2016). The Insect Prothoracic Gland as a Model for Steroid Hormone Biosynthesis and Regulation. *Cell reports*, 16(1), 247–262. <https://doi.org/10.1016/j.celrep.2016.05.053>
- 21) Albrecht, E. D. (2003). Steroid hormone regulation of angiogenesis in the primate endometrium. *Frontiers in Bioscience*, 8(4), d416–429. doi: 10.2741/1001
- 22) Chowen, J., Frago, L., & Argente, J. (2004). The regulation of GH secretion by sex steroids. *European Journal of Endocrinology*. doi: 10.1530/eje.0.151u095
- 23) Jurgens, G., Wieschaus, E., Nusslein-Volhard, C., & Kluding, H. (1984). Mutations affecting the pattern of the larval cuticle in *Drosophila melanogaster*. *Wilhelm Roux Archives of Developmental Biology*, 193(5), 283–295. doi: 10.1007/bf00848157
- 24) Jurgens, G., Wieschaus, E., Nusslein-Volhard, C., & Kluding, H. (1984). Mutations affecting the pattern of the larval cuticle in *Drosophila melanogaster*.*Genes and Evolution* (1984).
- 25) Nusslein-Volhard, C., & Wieschaus, E. Mutations affecting segment number and polarity in *Drosophila*. *Nature* 287, 795-801 (1980).

- 26) Gilbert, L. I., Rybczynski, R., & Warren, J. T. (2002). Control and Biochemical Nature of the Ecdysteroidogenic Pathway. *Annual Review of Entomology*, 47(1), 883–916. doi: 10.1146/annurev.ento.47.091201.145302
- 27) Iga, M., & Kataoka, H. (2012). Recent Studies on Insect Hormone Metabolic Pathways Mediated by Cytochrome P450 Enzymes. *Biological and Pharmaceutical Bulletin*, 35(6), 838–843. doi: 10.1248/bpb.35.838
- 28) Niwa, R., Namiki, T., Ito, K., Shimada-Niwa, Y., Kiuchi, M., Kawaoka, S., ... Shinoda, T. (2010). Non-molting glossy/shroud encodes a short-chain dehydrogenase/reductase that functions in the Black Box of the ecdysteroid biosynthesis pathway. *Development*, 137(12), 1991–1999. doi: 10.1242/dev.045641
- 29) Namiki, T., Niwa, R., Sakudoh, T., Shirai, K.-I., Takeuchi, H., & Kataoka, H. (2005). Cytochrome P450 CYP307A1/Spook: A regulator for ecdysone synthesis in insects. *Biochemical and Biophysical Research Communications*, 337(1), 367–374. doi: 10.1016/j.bbrc.2005.09.043
- 30) Ono, H., Rewitz, K. F., Shinoda, T., Itoyama, K., Petryk, A., Rybczynski, R., ... Oconnor, M. B. (2006). Spook and Spookier code for stage-specific components of the ecdysone biosynthetic pathway in Diptera. *Developmental Biology*, 298(2), 555–570. doi: 10.1016/j.ydbio.2006.07.023
- 31) Ou, Q., Magico, A., & King-Jones, K. (2011). Nuclear Receptor DHR4 Controls the Timing of Steroid Hormone Pulses During *Drosophila* Development. *PLoS Biology*, 9(9). doi: 10.1371/journal.pbio.1001160
- 32) Rewitz, K., Rybczynski, R., Warren, J., & Gilbert, L. (2006). The Halloween genes code for cytochrome P450 enzymes mediating synthesis of the insect moulting hormone. *Biochemical Society Transactions*, 34(6), 1256–1260. doi: 10.1042/bst0341256

- 33) Mcbrayer, Z., Ono, H., Shimell, M., Parvy, J.-P., Beckstead, R. B., Warren, J. T., ... Oconnor, M. B. (2007). Prothoracicotropic Hormone Regulates Developmental Timing and Body Size in *Drosophila*. *Developmental Cell*, *13*(6), 857–871. doi: 10.1016/j.devcel.2007.11.003
- 34) Riddiford, L. M., Truman, J. W., Mirth, C. K., & Shen, Y.-C. (2010). A role for juvenile hormone in the prepupal development of *Drosophila melanogaster*. *Development*, *137*(7), 1117–1126. doi: 10.1242/dev.037218
- 35) Mirth, C. K., Tang, H. Y., Makohon-Moore, S. C., Salhadar, S., Gokhale, R. H., Warner, R. D., ... Shingleton, A. W. (2014). Juvenile hormone regulates body size and perturbs insulin signaling in *Drosophila*. *Proceedings of the National Academy of Sciences*, *111*(19), 7018–7023. doi: 10.1073/pnas.1313058111
- 36) Wijesekera, T. P., Saurabh, S., & Dauwalder, B. (2016). Juvenile Hormone Is Required in Adult Males for *Drosophila* Courtship. *Plos One*, *11*(3). doi: 10.1371/journal.pone.0151912
- 37) Battersby, A. R. (2000). Tetrapyrroles: the pigments of life. *Natural Product Reports*, *17*(6), 507–526. doi: 10.1039/b002635m
- 38) Chiabrando, D., Vinchi, F., Fiorito, V., Mercurio, S., & Tolosano, E. (2014). Heme in pathophysiology: a matter of scavenging, metabolism and trafficking across cell membranes. *Frontiers in Pharmacology*, *5*. doi: 10.3389/fphar.2014.00061
- 39) Sawicki, K. T., Chang, H. C., & Ardehali, H. (2015). Role of heme in cardiovascular physiology and disease. *Journal of the American Heart Association*, *4*(1), e001138. <https://doi.org/10.1161/JAHA.114.001138>
- 40) Poulos T. L. (2014). Heme enzyme structure and function. *Chemical reviews*, *114*(7), 3919–3962. <https://doi.org/10.1021/cr400415k>

- 41) Ajioka, R. S., Phillips, J. D., & Kushner, J. P. (2006). Biosynthesis of heme in mammals. *Biochimica Et Biophysica Acta (BBA) - Molecular Cell Research*, 1763(7), 723–736. doi: 10.1016/j.bbamcr.2006.05.005
- 42) Neuberger, A., & Scott, J. J. (1953). Aminolævulinic Acid and Porphyrin Biosynthesis. *Nature*, 172(4389), 1093–1094. doi: 10.1038/1721093a0
- 43) Shemin, D., & Russell, C. S. (1953). δ -AMINOLEVULINIC ACID, ITS ROLE IN THE BIOSYNTHESIS OF PORPHYRINS AND PURINES¹. *Journal of the American Chemical Society*, 75(19), 4873–4874. doi: 10.1021/ja01115a546
- 44) Bishop, D. F., Henderson, A. S., & Astrin, K. H. (1990). Human δ -aminolevulinate synthase: Assignment of the housekeeping gene to 3p21 and the erythroid-specific gene to the X chromosome. *Genomics*, 7(2), 207–214. doi: 10.1016/0888-7543(90)90542-3
- 45) Sachs, P. (1931). Ein Fall von Akuter Porphyrie mit Hochgradiger Muskelatrophie. *Klinische Wochenschrift*, 10(24), 1123–1125. doi: 10.1007/bf01740238
- 46) Bogorad, L., & Granick, S. (1953). The Enzymatic Synthesis of Porphyrins from Porphobilinogen. *Proceedings of the National Academy of Sciences*, 39(12), 1176–1188. doi: 10.1073/pnas.39.12.1176
- 47) Bogorad, L. (1955). Intermediates in the Biosynthesis of Porphyrins from Porphobilinogen. *Science*, 121(3155), 878–879. doi: 10.1126/science.121.3155.878
- 48) Cornah, J. E., & Smith, A. G. (2009). Transformation of Uroporphyrinogen III into Protohaem. *Tetrapyrroles*, 74–88. doi: 10.1007/978-0-387-78518-9_4
- 49) Layer, G., Reichelt, J., Jahn, D., & Heinz, D. W. (2010). Structure and function of enzymes in heme biosynthesis. *Protein science : a publication of the Protein Society*, 19(6), 1137–1161. <https://doi.org/10.1002/pro.405>

- 50) Edel, Y., & Mamet, R. (2018). Porphyria: What Is It and Who Should Be Evaluated? *Rambam Maimonides Medical Journal*, 9(2). doi: 10.5041/rmmj.10333
- 51) Karim, Z., Lyoumi, S., Nicolas, G., Deybach, J.-C., Gouya, L., & Puy, H. (2015). Porphyrias: A 2015 update. *Clinics and Research in Hepatology and Gastroenterology*, 39(4), 412–425. doi: 10.1016/j.clinre.2015.05.009
- 52) Erwin A, Balwani M, Desnick RJ; Porphyrias Consortium of the NIH-Sponsored Rare Diseases Clinical Research Network. Congenital Erythropoietic Porphyria. 2013 Sep 12 [Updated 2016 Apr 7]. In: Adam MP, Ardinger HH, Pagon RA, et al., editors. GeneReviews® [Internet]. Seattle (WA): University of Washington, Seattle; 1993-2020. Available from: <https://www.ncbi.nlm.nih.gov/books/NBK154652/>
- 53) Cappellini, M. D., Brancaleoni, V., Graziadei, G., Tavazzi, D., & Pierro, E. D. (2010). Porphyrias at a glance: diagnosis and treatment. *Internal and Emergency Medicine*, 5(S1), 73–80. doi: 10.1007/s11739-010-0449-7
- 54) Poblete-Gutiérrez, P., Wiederholt, T., Merk, H. F., & Frank, J. (2006). The porphyrias: clinical presentation, diagnosis and treatment. *European journal of dermatology: EJD*, 16(3), 230–240.
- 55) Wardman, P., & Candeias, L. P. (1996). Fenton Chemistry: An Introduction. *Radiation Research*, 145(5), 523. doi: 10.2307/3579270
- 56) Kremer, M. L. (2003). The Fenton Reaction. Dependence of the Rate on pH. *The Journal of Physical Chemistry A*, 107(11), 1734–1741. doi: 10.1021/jp020654p
- 57) Danielsen, E. T., Moeller, M. E., Yamanaka, N., Ou, Q., Laursen, J. M., Soenderholm, C., Zhuo, R., Phelps, B., Tang, K., Zeng, J., Kondo, S., Nielsen, C. H., Harvald, E. B., Faergeman, N. J., Haley, M. J., O'Connor, K. A., King-Jones, K., O'Connor, M. B., & Rewitz, K. F. (2016). A Drosophila Genome-Wide Screen Identifies Regulators of Steroid

Hormone Production and Developmental Timing. *Developmental cell*, 37(6), 558–570.
<https://doi.org/10.1016/j.devcel.2016.05.015>

- 58) Mojica, F. J., Díez-Villaseñor, C., García-Martínez, J., & Soria, E. (2005). Intervening sequences of regularly spaced prokaryotic repeats derive from foreign genetic elements. *Journal of molecular evolution*, 60(2), 174–182. <https://doi.org/10.1007/s00239-004-0046-3>
- 59) Ishino, Y., Shinagawa, H., Makino, K., Amemura, M., & Nakata, A. (1987). Nucleotide sequence of the *iap* gene, responsible for alkaline phosphatase isozyme conversion in *Escherichia coli*, and identification of the gene product. *Journal of bacteriology*, 169(12), 5429–5433. <https://doi.org/10.1128/jb.169.12.5429-5433.1987>
- 60) Bolotin, A., Quinquis, B., Sorokin, A., & Ehrlich, S. D. (2005). Clustered regularly interspaced short palindrome repeats (CRISPRs) have spacers of extrachromosomal origin. *Microbiology (Reading, England)*, 151(Pt 8), 2551–2561. <https://doi.org/10.1099/mic.0.28048-0>
- 61) Pourcel, C., Salvignol, G., & Vergnaud, G. (2005). CRISPR elements in *Yersinia pestis* acquire new repeats by preferential uptake of bacteriophage DNA, and provide additional tools for evolutionary studies. *Microbiology (Reading, England)*, 151(Pt 3), 653–663. <https://doi.org/10.1099/mic.0.27437-0>
- 62) Garneau, J. E., Dupuis, M. È., Villion, M., Romero, D. A., Barrangou, R., Boyaval, P., Fremaux, C., Horvath, P., Magadán, A. H., & Moineau, S. (2010). The CRISPR/Cas bacterial immune system cleaves bacteriophage and plasmid DNA. *Nature*, 468(7320), 67–71. <https://doi.org/10.1038/nature09523>
- 63) Sontheimer, E. J., & Marraffini, L. A. (2010). Microbiology: slicer for DNA. *Nature*, 468(7320), 45–46. <https://doi.org/10.1038/468045a>

- 64) Brouns, S. J., Jore, M. M., Lundgren, M., Westra, E. R., Slijkhuis, R. J., Snijders, A. P., Dickman, M. J., Makarova, K. S., Koonin, E. V., & van der Oost, J. (2008). Small CRISPR RNAs guide antiviral defense in prokaryotes. *Science (New York, N.Y.)*, 321(5891), 960–964.
- 65) Gasiunas, G., Barrangou, R., Horvath, P., & Siksnys, V. (2012). Cas9-crRNA ribonucleoprotein complex mediates specific DNA cleavage for adaptive immunity in bacteria. *Proceedings of the National Academy of Sciences*, 109(39). doi: 10.1073/pnas.1208507109
- 66) Jinek, M., Chylinski, K., Fonfara, I., Hauer, M., Doudna, J. A., & Charpentier, E. (2012). A programmable dual-RNA-guided DNA endonuclease in adaptive bacterial immunity. *Science (New York, N.Y.)*, 337(6096), 816–821. <https://doi.org/10.1126/science.1225829>
- 67) Deveau, H., Garneau, J. E., & Moineau, S. (2010). CRISPR/Cas system and its role in phage-bacteria interactions. *Annual review of microbiology*, 64, 475–493. <https://doi.org/10.1146/annurev.micro.112408.134123>
- 68) Horvath, P., & Barrangou, R. (2010). CRISPR/Cas, the Immune System of Bacteria and Archaea. *Science*, 327(5962), 167–170. doi: 10.1126/science.1179555
- 69) Karginov, F. V., & Hannon, G. J. (2010). The CRISPR system: small RNA-guided defense in bacteria and archaea. *Molecular cell*, 37(1), 7–19. <https://doi.org/10.1016/j.molcel.2009.12.033>
- 70) Koonin, E. V., & Makarova, K. S. (2009). CRISPR-Cas: an adaptive immunity system in prokaryotes. *F1000 biology reports*, 1, 95. <https://doi.org/10.3410/B1-95>
- 71) Sorek, R., Kunin, V., & Hugenholtz, P. (2008). CRISPR--a widespread system that provides acquired resistance against phages in bacteria and archaea. *Nature reviews. Microbiology*, 6(3), 181–186. <https://doi.org/10.1038/nrmicro1793>

- 72) van der Oost, J., Jore, M. M., Westra, E. R., Lundgren, M., & Brouns, S. J. (2009). CRISPR-based adaptive and heritable immunity in prokaryotes. *Trends in biochemical sciences*, 34(8), 401–407. <https://doi.org/10.1016/j.tibs.2009.05.002>
- 73) Jansen, R., Embden, J. D., Gaastra, W., & Schouls, L. M. (2002). Identification of genes that are associated with DNA repeats in prokaryotes. *Molecular microbiology*, 43(6), 1565–1575. <https://doi.org/10.1046/j.1365-2958.2002.02839.x>
- 74) Mojica, F., Díez-Villaseñor, C., García-Martínez, J., & Almendros, C. (2009). Short motif sequences determine the targets of the prokaryotic CRISPR defence system. *Microbiology (Reading, England)*, 155(Pt 3), 733–740. <https://doi.org/10.1099/mic.0.023960-0>
- 75) Deveau, H., Barrangou, R., Garneau, J. E., Labonté, J., Fremaux, C., Boyaval, P., Romero, D. A., Horvath, P., & Moineau, S. (2008). Phage response to CRISPR-encoded resistance in *Streptococcus thermophilus*. *Journal of bacteriology*, 190(4), 1390–1400.
- 76) Zhang, Z., Zhang, Y., Gao, F., Han, S., Cheah, K. S., Tse, H. F., & Lian, Q. (2017). CRISPR/Cas9 Genome-Editing System in Human Stem Cells: Current Status and Future Prospects. *Molecular therapy. Nucleic acids*, 9, 230–241. <https://doi.org/10.1016/j.omtn.2017.09.009>
- 77) Mali, P., Yang, L., Esvelt, K. M., Aach, J., Guell, M., DiCarlo, J. E., Norville, J. E., & Church, G. M. (2013). RNA-guided human genome engineering via Cas9. *Science (New York, N.Y.)*, 339(6121), 823–826. <https://doi.org/10.1126/science.1232033>
- 78) Wang, H., Yang, H., Shivalila, C. S., Dawlaty, M. M., Cheng, A. W., Zhang, F., & Jaenisch, R. (2013). One-step generation of mice carrying mutations in multiple genes by CRISPR/Cas-mediated genome engineering. *Cell*, 153(4), 910–918. <https://doi.org/10.1016/j.cell.2013.04.025>

- 79) Cong, L., Ran, F. A., Cox, D., Lin, S., Barretto, R., Habib, N., Hsu, P. D., Wu, X., Jiang, W., Marraffini, L. A., & Zhang, F. (2013). Multiplex genome engineering using CRISPR/Cas systems. *Science (New York, N.Y.)*, *339*(6121), 819–823. <https://doi.org/10.1126/science.1231143>
- 80) Hwang, W. Y., Fu, Y., Reyon, D., Maeder, M. L., Tsai, S. Q., Sander, J. D., Peterson, R. T., Yeh, J. R., & Joung, J. K. (2013). Efficient genome editing in zebrafish using a CRISPR-Cas system. *Nature biotechnology*, *31*(3), 227–229. <https://doi.org/10.1038/nbt.2501>
- 81) Bassett, A. R., Tibbit, C., Ponting, C. P., & Liu, J. L. (2013). Highly efficient targeted mutagenesis of *Drosophila* with the CRISPR/Cas9 system. *Cell reports*, *4*(1), 220–228. <https://doi.org/10.1016/j.celrep.2013.06.020>
- 82) Gratz, S. J., Cummings, A. M., Nguyen, J. N., Hamm, D. C., Donohue, L. K., Harrison, M. M., Wildonger, J., & O'Connor-Giles, K. M. (2013). Genome engineering of *Drosophila* with the CRISPR RNA-guided Cas9 nuclease. *Genetics*, *194*(4), 1029–1035. <https://doi.org/10.1534/genetics.113.152710>
- 83) Yu, Z., Ren, M., Wang, Z., Zhang, B., Rong, Y. S., Jiao, R., & Gao, G. (2013). Highly efficient genome modifications mediated by CRISPR/Cas9 in *Drosophila*. *Genetics*, *195*(1), 289–291. <https://doi.org/10.1534/genetics.113.153825>
- 84) Huynh, N., Zeng, J., Liu, W., & King-Jones, K. (2018). A *Drosophila* CRISPR/Cas9 Toolkit for Conditionally Manipulating Gene Expression in the Prothoracic Gland as a Test Case for Polytene Tissues. *G3 (Bethesda, Md.)*, *8*(11), 3593–3605. <https://doi.org/10.1534/g3.118.200539>
- 85) Ohhara, Y., Kobayashi, S., & Yamanaka, N. (2017). Nutrient-Dependent Endocycling in Steroidogenic Tissue Dictates Timing of Metamorphosis in *Drosophila melanogaster*. *PLoS genetics*, *13*(1), e1006583. <https://doi.org/10.1371/journal.pgen.1006583>

- 86) Beck, K. L., Conlon, C. A., Kruger, R., & Coad, J. (2014). Dietary determinants of and possible solutions to iron deficiency for young women living in industrialized countries: a review. *Nutrients*, 6(9), 3747–3776. <https://doi.org/10.3390/nu6093747>
- 87) Kasai, S., Mimura, J., Ozaki, T., & Itoh, K. (2018). Emerging Regulatory Role of Nrf2 in Iron, Heme, and Hemoglobin Metabolism in Physiology and Disease. *Frontiers in veterinary science*, 5, 242. <https://doi.org/10.3389/fvets.2018.00242>
- 88) Iolascon, A., De Falco, L., & Beaumont, C. (2009). Molecular basis of inherited microcytic anemia due to defects in iron acquisition or heme synthesis. *Haematologica*, 94(3), 395–408. <https://doi.org/10.3324/haematol.13619>
- 89) Immenschuh, S., Vijayan, V., Janciauskiene, S., & Gueler, F. (2017). Heme as a Target for Therapeutic Interventions. *Frontiers in pharmacology*, 8, 146. <https://doi.org/10.3389/fphar.2017.00146>
- 90) Leitch H. A. (2016). Hematologic improvement with iron chelation therapy in acquired anemias. *European journal of haematology*, 96(6), 551–552. <https://doi.org/10.1111/ejh.12703>
- 91) Kontoghiorghe, C. N., & Kontoghiorghes, G. J. (2016). New developments and controversies in iron metabolism and iron chelation therapy. *World journal of methodology*, 6(1), 1–19. <https://doi.org/10.5662/wjm.v6.i1.1>
- 92) Yoshiyama, T. (2006). Neverland is an evolutionally conserved Rieske-domain protein that is essential for ecdysone synthesis and insect growth. *Development*, 133(13), 2565–2574. doi: 10.1242/dev.02428
- 93) Hu, Y., Flockhart, I., Vinayagam, A., Bergwitz, C., Berger, B., Perrimon, N., & Mohr, S. E. (2011). An integrative approach to ortholog prediction for disease-focused and other functional studies. *BMC Bioinformatics*, 12(1), 357. doi: 10.1186/1471-2105-12-357

- 94) Minakhina, S., Druzhinina, M., & Steward, R. (2007). Zfrp8, the Drosophila ortholog of PDCD2, functions in lymph gland development and controls cell proliferation. *Development*, *134*(13), 2387–2396. doi: 10.1242/dev.003616
- 95) Minakhina, S., & Steward, R. (2010). Hematopoietic stem cells in Drosophila. *Development (Cambridge, England)*, *137*(1), 27–31. <https://doi.org/10.1242/dev.043943>
- 96) Kokorina, N. A., Granier, C. J., Zakharkin, S. O., Davis, S., Rabson, A. B., & Sabaawy, H. E. (2012). PDCD2 knockdown inhibits erythroid but not megakaryocytic lineage differentiation of human hematopoietic stem/progenitor cells. *Experimental hematology*, *40*(12), 1028–1042.e3. <https://doi.org/10.1016/j.exphem.2012.08.004>
- 97) Barboza, N., Minakhina, S., Medina, D. J., Balsara, B., Greenwood, S., Huzzy, L., Rabson, A. B., Steward, R., & Schaar, D. G. (2013). PDCD2 functions in cancer cell proliferation and predicts relapsed leukemia. *Cancer biology & therapy*, *14*(6), 546–555. <https://doi.org/10.4161/cbt.24484>
- 98) Granier, C. J., Wang, W., Tsang, T., Steward, R., Sabaawy, H. E., Bhaumik, M., & Rabson, A. B. (2014). Conditional inactivation of PDCD2 induces p53 activation and cell cycle arrest. *Biology Open*, *3*(9), 821–831. doi: 10.1242/bio.20148326
- 99) Margolis, J., & Spradling, A. (1995). Identification and behavior of epithelial stem cells in the Drosophila ovary. *Development (Cambridge, England)*, *121*(11), 3797–3807.
- 100) Decotto, E., & Spradling, A. C. (2005). The Drosophila ovarian and testis stem cell niches: similar somatic stem cells and signals. *Developmental cell*, *9*(4), 501–510. <https://doi.org/10.1016/j.devcel.2005.08.012>

- 101) Wieschaus, E., & Szabad, J. (1979). The development and function of the female germ line in *Drosophila melanogaster*: a cell lineage study. *Developmental biology*, 68(1), 29–46. [https://doi.org/10.1016/0012-1606\(79\)90241-0](https://doi.org/10.1016/0012-1606(79)90241-0)
- 102) Lin, H., & Spradling, A. C. (1993). Germline stem cell division and egg chamber development in transplanted *Drosophila* germaria. *Developmental biology*, 159(1), 140–152. <https://doi.org/10.1006/dbio.1993.1228>
- 103) Morrison, S. J., & Spradling, A. C. (2008). Stem cells and niches: mechanisms that promote stem cell maintenance throughout life. *Cell*, 132(4), 598–611. <https://doi.org/10.1016/j.cell.2008.01.038>
- 104) Losick, V. P., Morris, L. X., Fox, D. T., & Spradling, A. (2011). *Drosophila* stem cell niches: a decade of discovery suggests a unified view of stem cell regulation. *Developmental cell*, 21(1), 159–171. <https://doi.org/10.1016/j.devcel.2011.06.018>
- 105) Spradling, A., Fuller, M. T., Braun, R. E., & Yoshida, S. (2011). Germline stem cells. *Cold Spring Harbor perspectives in biology*, 3(11), a002642. <https://doi.org/10.1101/cshperspect.a002642>
- 106) Bozzetti, M. P., Specchia, V., Cattenoz, P. B., Laneve, P., Geusa, A., Sahin, H. B., Di Tommaso, S., Friscini, A., Massari, S., Diebold, C., & Giangrande, A. (2015). The *Drosophila* fragile X mental retardation protein participates in the piRNA pathway. *Journal of cell science*, 128(11), 2070–2084. <https://doi.org/10.1242/jcs.161810>
- 107) Megosh, H. B., Cox, D. N., Campbell, C., & Lin, H. (2006). The Role of PIWI and the miRNA Machinery in *Drosophila* Germline Determination. *Current Biology*, 16(19), 1884–1894. doi: 10.1016/j.cub.2006.08.051
- 108) Callan, M. A., Cabernard, C., Heck, J., Luo, S., Doe, C. Q., & Zarnescu, D. C. (2010). Fragile X protein controls neural stem cell proliferation in the *Drosophila*

brain. *Human molecular genetics*, 19(15), 3068–3079.
<https://doi.org/10.1093/hmg/ddq213>

- 109) Costa, A., Wang, Y., Dockendorff, T. C., Erdjument-Bromage, H., Tempst, P., Schedl, P., & Jongens, T. A. (2005). The *Drosophila* fragile X protein functions as a negative regulator in the orb autoregulatory pathway. *Developmental cell*, 8(3), 331–342. <https://doi.org/10.1016/j.devcel.2005.01.011>
- 110) Yang, L., Chen, D., Duan, R., Xia, L., Wang, J., Qurashi, A., Jin, P., & Chen, D. (2007). Argonaute 1 regulates the fate of germline stem cells in *Drosophila*. *Development (Cambridge, England)*, 134(23), 4265–4272. <https://doi.org/10.1242/dev.009159>
- 111) Wang, H., Dichtenberg, J. B., Ku, L., Li, W., Bassell, G. J., & Feng, Y. (2008). Dynamic association of the fragile X mental retardation protein as a messenger ribonucleoprotein between microtubules and polyribosomes. *Molecular biology of the cell*, 19(1), 105–114.
- 112) Luo, Y., Shan, G., Guo, W., Smrt, R. D., Johnson, E. B., Li, X., Pfeiffer, R. L., Szulwach, K. E., Duan, R., Barkho, B. Z., Li, W., Liu, C., Jin, P., & Zhao, X. (2010). Fragile x mental retardation protein regulates proliferation and differentiation of adult neural stem/progenitor cells. *PLoS genetics*, 6(4), e1000898. <https://doi.org/10.1371/journal.pgen.1000898>
- 113) Tervonen, K., Waissi, G., Petersen, E. J., Akkanen, J., & Kukkonen, J. V. (2010). Analysis of fullerene-C60 and kinetic measurements for its accumulation and depuration in *Daphnia magna*. *Environmental toxicology and chemistry*, 29(5), 1072–1078. <https://doi.org/10.1002/etc.124>
- 114) Barbee, S. A., Estes, P. S., Cziko, A. M., Hillebrand, J., Luedeman, R. A., Coller, J. M., Johnson, N., Howlett, I. C., Geng, C., Ueda, R., Brand, A. H., Newbury, S. F., Wilhelm, J. E., Levine, R. B., Nakamura, A., Parker, R., & Ramaswami, M. (2006).

Staufen- and FMRP-containing neuronal RNPs are structurally and functionally related to somatic P bodies. *Neuron*, 52(6), 997–1009. <https://doi.org/10.1016/j.neuron.2006.10.028>

- 115) Kugler, J. M., Chicoine, J., & Lasko, P. (2009). Bicaudal-C associates with a Trailer Hitch/Me31B complex and is required for efficient Gurken secretion. *Developmental biology*, 328(1), 160–172. <https://doi.org/10.1016/j.ydbio.2009.01.024>
- 116) Liu, L., Qi, H., Wang, J., & Lin, H. (2011). PAPI, a novel TUDOR-domain protein, complexes with AGO3, ME31B and TRAL in the nuage to silence transposition. *Development (Cambridge, England)*, 138(9), 1863–1873. <https://doi.org/10.1242/dev.059287>
- 117) Snee, M. J., & Macdonald, P. M. (2009). Bicaudal C and trailer hitch have similar roles in gurken mRNA localization and cytoskeletal organization. *Developmental biology*, 328(2), 434–444. <https://doi.org/10.1016/j.ydbio.2009.02.003>
- 118) Minakhina, S., Naryshkina, T., Changela, N., Tan, W., & Steward, R. (2016). Zfrp8/PDCD2 Interacts with RpS2 Connecting Ribosome Maturation and Gene-Specific Translation. *PloS one*, 11(1), e0147631. <https://doi.org/10.1371/journal.pone.0147631>
- 119) Stephanie E Mohr. 9/23/2016. “[Drosophila research resources at the DRSC and TRiP.](#)” Presentation to the Boston Area Drosophila Meeting (Sept. 2016).
- 120) Fish, M. P., Groth, A. C., Calos, M. P., & Nusse, R. (2007). Creating transgenic Drosophila by microinjecting the site-specific phiC31 integrase mRNA and a transgene-containing donor plasmid. *Nature protocols*, 2(10), 2325–2331. <https://doi.org/10.1038/nprot.2007.328>
- 121) Universal ProbeLibrary Assay Design Center (Roche ; Indianapolis, IN, USA; <http://www.lifescience.roche.com>. 2020

- 122) Integrated DNA Technologies, Inc. (IDT; Coralville, Iowa, USA: <http://www.idtdna.com>). 2020.
- 123) Inoue, H., Nojima, H., & Okayama, H. (1990). High efficiency transformation of *Escherichia coli* with plasmids. *Gene*, *96*(1), 23–28. [https://doi.org/10.1016/0378-1119\(90\)90336-p](https://doi.org/10.1016/0378-1119(90)90336-p)
- 124) Cell Signaling technology <http://www.cellsignal.com>. 2020
- 125) Jackson, A. L., & Linsley, P. S. (2010). Recognizing and avoiding siRNA off-target effects for target identification and therapeutic application. *Nature reviews. Drug discovery*, *9*(1), 57–67. <https://doi.org/10.1038/nrd3010>
- 126) Minakhina, S., Yang, J., & Steward, R. (2003). Tamo selectively modulates nuclear import in *Drosophila*. *Genes to Cells*, *8*(4), 299–310. doi: 10.1046/j.1365-2443.2002.00634.x
- 127) Huynh, N., Ou, Q., Cox, P., Lill, R., & King-Jones, K. (2019). Glycogen branching enzyme controls cellular iron homeostasis via Iron Regulatory Protein 1 and mitoNEET. *Nature communications*, *10*(1), 5463. <https://doi.org/10.1038/s41467-019-13237-8>
- 128) Friedreich, N. (1863). Ueber degenerative Atrophie der spinalen Hinterstränge. *Archiv Für Pathologische Anatomie Und Physiologie Und Für Klinische Medicin*, *27*(1-2), 1–26. doi: 10.1007/bf01938516
- 129) Dürr, A., Cossee, M., Agid, Y., Campuzano, V., Mignard, C., Penet, C., Mandel, J. L., Brice, A., & Koenig, M. (1996). Clinical and genetic abnormalities in patients with Friedreich's ataxia. *The New England journal of medicine*, *335*(16), 1169–1175. <https://doi.org/10.1056/NEJM199610173351601>

- 130) Bencze, K. Z., Kondapalli, K. C., Cook, J. D., McMahon, S., Millán-Pacheco, C., Pastor, N., & Stemmler, T. L. (2006). The structure and function of frataxin. *Critical reviews in biochemistry and molecular biology*, *41*(5), 269–291. <https://doi.org/10.1080/10409230600846058>
- 131) Plasterer, H. L., Deutsch, E. C., Belmonte, M., Egan, E., Lynch, D. R., & Rusche, J. R. (2013). Development of frataxin gene expression measures for the evaluation of experimental treatments in Friedreich's ataxia. *PloS one*, *8*(5), e63958. <https://doi.org/10.1371/journal.pone.0063958>
- 132) Cañizares, J., Blanca, J. M., Navarro, J. A., Monrós, E., Palau, F., & Moltó, M. D. (2000). dfh is a Drosophila homolog of the Friedreich's ataxia disease gene. *Gene*, *256*(1-2), 35–42. [https://doi.org/10.1016/s0378-1119\(00\)00343-7](https://doi.org/10.1016/s0378-1119(00)00343-7)
- 133) Calap-Quintana, P., Navarro, J. A., González-Fernández, J., Martínez-Sebastián, M. J., Moltó, M. D., & Llorens, J. V. (2018). *Drosophila melanogaster* Models of Friedreich's Ataxia. *BioMed research international*, *2018*, 5065190. <https://doi.org/10.1155/2018/5065190>
- 134) Kondapalli, K. C., Kok, N. M., Dancis, A., & Stemmler, T. L. (2008). Drosophila frataxin: an iron chaperone during cellular Fe-S cluster bioassembly. *Biochemistry*, *47*(26), 6917–6927. <https://doi.org/10.1021/bi800366d>
- 135) Boland, M. R., & Tatonetti, N. P. (2016). Investigation of 7-dehydrocholesterol reductase pathway to elucidate off-target prenatal effects of pharmaceuticals: a systematic review. *The pharmacogenomics journal*, *16*(5), 411–429. <https://doi.org/10.1038/tpj.2016.48>
- 136) Blassberg, R., Macrae, J. I., Briscoe, J., & Jacob, J. (2016). Reduced cholesterol levels impair Smoothed activation in Smith-Lemli-Opitz syndrome. *Human molecular genetics*, *25*(4), 693–705. <https://doi.org/10.1093/hmg/ddv507>

- 137) Rasband, W.S., ImageJ, U. S. National Institutes of Health, Bethesda, Maryland, USA, <https://imagej.nih.gov/ij/>, 1997-2018
- 138) Schneider, C.A., Rasband, W.S., Eliceiri, K.W. "NIH Image to ImageJ: 25 years of image analysis". *Nature Methods* 9, 671-675, 2012
- 139) Abramoff, M.D., Magalhaes, P.J., Ram, S.J. "Image Processing with ImageJ". *Biophotonics International*, volume 11, issue 7, pp. 36-42, 2004.
- 140) Uryu, O., Ou, Q., Komura-Kawa, T., Kamiyama, T., Iga, M., Syrzycka, M., Hirota, K., Kataoka, H., Honda, B. M., King-Jones, K., & Niwa, R. (2018). Cooperative Control of Ecdysone Biosynthesis in *Drosophila* by Transcription Factors Séance, Ouija Board, and Molting Defective. *Genetics*, 208(2), 605–622. <https://doi.org/10.1534/genetics.117.300268>
- 141) Yao, Q., Zhang, D., Tang, B., Chen, J., Chen, J., Lu, L., & Zhang, W. (2010). Identification of 20-hydroxyecdysone late-response genes in the chitin biosynthesis pathway. *PloS one*, 5(11), e14058. <https://doi.org/10.1371/journal.pone.0014058>
- 142) Knapp, E., & Sun, J. (2017). Steroid signaling in mature follicles is important for *Drosophila* ovulation. *Proceedings of the National Academy of Sciences of the United States of America*, 114(4), 699–704. <https://doi.org/10.1073/pnas.1614383114>
- 143) Payne, A. H., & Hales, D. B. (2004). Overview of steroidogenic enzymes in the pathway from cholesterol to active steroid hormones. *Endocrine reviews*, 25(6), 947–970. <https://doi.org/10.1210/er.2003-0030>
- 144) Niwa, R., & Niwa, Y. S. (2011). The Fruit Fly *Drosophila melanogaster* as a Model System to Study Cholesterol Metabolism and Homeostasis. *Cholesterol*, 2011, 1–6. doi: 10.1155/2011/176802

- 145) Porter, F. D., & Herman, G. E. (2011). Malformation syndromes caused by disorders of cholesterol synthesis. *Journal of lipid research*, 52(1), 6–34. <https://doi.org/10.1194/jlr.R009548>
- 146) Cardoso, G. A., Matioli, C. C., de Azeredo-Espin, A. M., & Torres, T. T. (2014). Selection and validation of reference genes for functional studies in the Calliphoridae family. *Journal of insect science (Online)*, 14, 2. <https://doi.org/10.1093/jis/14.1.2>
- 147) Tijet, N., Helvig, C., & Feyereisen, R. (2001). The cytochrome P450 gene superfamily in *Drosophila melanogaster*: annotation, intron-exon organization and phylogeny. *Gene*, 262(1-2), 189–198. [https://doi.org/10.1016/s0378-1119\(00\)00533-3](https://doi.org/10.1016/s0378-1119(00)00533-3)
- 148) Chávez, V. M., Marqués, G., Delbecque, J. P., Kobayashi, K., Hollingsworth, M., Burr, J., Natzle, J. E., & O'Connor, M. B. (2000). The *Drosophila* disembodied gene controls late embryonic morphogenesis and codes for a cytochrome P450 enzyme that regulates embryonic ecdysone levels. *Development (Cambridge, England)*, 127(19), 4115–4126.
- 149) Ejsmont, R. K., Sarov, M., Winkler, S., Lipinski, K. A., & Tomancak, P. (2009). A toolkit for high-throughput, cross-species gene engineering in *Drosophila*. *Nature methods*, 6(6), 435–437. <https://doi.org/10.1038/nmeth.1334>
- 150) Sigoillot, F. D., & King, R. W. (2011). Vigilance and validation: Keys to success in RNAi screening. *ACS chemical biology*, 6(1), 47–60. <https://doi.org/10.1021/cb100358f>
- 151) Qiu, S., Adema, C. M., & Lane, T. (2005). A computational study of off-target effects of RNA interference. *Nucleic acids research*, 33(6), 1834–1847. <https://doi.org/10.1093/nar/gki324>
- 152) Muckenthaler, M. U., Rivella, S., Hentze, M. W., & Galy, B. (2017). A Red Carpet for Iron Metabolism. *Cell*, 168(3), 344–361. <https://doi.org/10.1016/j.cell.2016.12.034>

- 153) Ganz, T., & Nemeth, E. (2012). Iron metabolism: interactions with normal and disordered erythropoiesis. *Cold Spring Harbor perspectives in medicine*, 2(5), a011668. <https://doi.org/10.1101/cshperspect.a011668>
- 154) Huang, X. (2005). A Drosophila model of the Niemann-Pick type C lysosome storage disease: *dnpcla* is required for molting and sterol homeostasis. *Development*, 132(22), 5115–5124. doi: 10.1242/dev.02079
- 155) Enya, S., Ameku, T., Igarashi, F., Iga, M., Kataoka, H., Shinoda, T., & Niwa, R. (2014). A Halloween gene *noppera-bo* encodes a glutathione S-transferase essential for ecdysteroid biosynthesis via regulating the behaviour of cholesterol in Drosophila. *Scientific reports*, 4, 6586. <https://doi.org/10.1038/srep06586>
- 156) Girvan, H. M., & Munro, A. W. (2013). Heme sensor proteins. *The Journal of biological chemistry*, 288(19), 13194–13203. <https://doi.org/10.1074/jbc.R112.422642>
- 157) Reinking, J., Lam, M. M., Pardee, K., Sampson, H. M., Liu, S., Yang, P., Williams, S., White, W., Lajoie, G., Edwards, A., & Krause, H. M. (2005). The Drosophila nuclear receptor *e75* contains heme and is gas responsive. *Cell*, 122(2), 195–207. <https://doi.org/10.1016/j.cell.2005.07.005>
- 158) Li, K., Tian, L., Guo, Z., Guo, S., Zhang, J., Gu, S. H., Palli, S. R., Cao, Y., & Li, S. (2016). 20-Hydroxyecdysone (20E) Primary Response Gene E75 Isoforms Mediate Steroidogenesis Autoregulation and Regulate Developmental Timing in Bombyx. *The Journal of biological chemistry*, 291(35), 18163–18175. <https://doi.org/10.1074/jbc.M116.737072>
- 159) Owens, G. P., Hahn, W. E., & Cohen, J. J. (1991). Identification of mRNAs associated with programmed cell death in immature thymocytes. *Molecular and Cellular Biology*, 11(8), 4177–4188. doi: 10.1128/mcb.11.8.4177

- 160) Vaux, D. L., & Häcker, G. (1995). Cloning of Mouse RP-8 cDNA and Its Expression During Apoptosis of Lymphoid and Myeloid Cells. *DNA and Cell Biology*, *14*(3), 189–193. doi: 10.1089/dna.1995.14.189
- 161) Thelander, E. F., Ichimura, K., Corcoran, M., Barbany, G., Nordgren, A., Heyman, M., ... Lagercrantz, S. (2008). Characterization of 6q deletions in mature B cell lymphomas and childhood acute lymphoblastic leukemia. *Leukemia & Lymphoma*, *49*(3), 477–487. doi: 10.1080/10428190701817282
- 162) Steinemann, D., Gesk, S., Zhang, Y., Harder, L., Pilarsky, C., Hinzmann, B., ... Schlegelberger, B. (2003). Identification of candidate tumor-suppressor genes in 6q27 by combined deletion mapping and electronic expression profiling in lymphoid neoplasms. *Genes, Chromosomes and Cancer*, *37*(4), 421–426. doi: 10.1002/gcc.10231
- 163) Kawakami, T., Furukawa, Y., Sudo, K., Saito, H., Takami, S., Takahashi, E., & Nakamura, Y. (1995). Isolation and mapping of a human gene (PDCD2) that is highly homologous to Rp8, a rat gene associated with programmed cell death. *Cytogenetic and Genome Research*, *71*(1), 41–43. doi: 10.1159/000134058
- 164) Mu, W., Munroe, R. J., Barker, A. K., & Schimenti, J. C. (2010). PDCD2 is essential for inner cell mass development and embryonic stem cell maintenance. *Developmental Biology*, *347*(2), 279–288. doi: 10.1016/j.ydbio.2010.08.026
- 165) Kramer, J., Granier, C. J., Davis, S., Piso, K., Hand, J., Rabson, A. B., & Sabaawy, H. E. (2013). PDCD2 controls hematopoietic stem cell differentiation during development. *Stem cells and development*, *22*(1), 58–72. <https://doi.org/10.1089/scd.2012.0074>
- 166) Ramalho-Santos M., Yoon S., Matsuzaki Y., Mulligan R. C., Melton D. A. (2002). “Stemness”:transcriptional profiling of embryonic and adult stem cells. *Science* **298**, 597–600. doi:10.1126/science.1072530

- 167) National Center for Biotechnology Information (US). Genes and Disease [Internet]. Bethesda (MD): National Center for Biotechnology Information (US); 1998-. The p53 tumor suppressor protein. Available from: <https://www.ncbi.nlm.nih.gov/books/NBK22268/>
- 168) Savatier P, Huang S, Szekely L, Wiman KG, Samarut J. (1994). Contrasting patterns of retinoblastoma protein expression in mouse embryonic stem cells and embryonic fibroblasts. *Oncogene*. Mar;9(3):809-818.
- 169) Savatier P., Afanassieff M. (2002). [Cell cycle control and self-renewal of embryonic stem cells]. *J. Soc. Biol.* **196**, 117–123.
- 170) Neganova, I., & Lako, M. (2008). G1 to S phase cell cycle transition in somatic and embryonic stem cells. *Journal of anatomy*, *213*(1), 30–44. <https://doi.org/10.1111/j.1469-7580.2008.00931.x>
- 171) Harris, S. L., & Levine, A. J. (2005). The p53 pathway: positive and negative feedback loops. *Oncogene*, *24*(17), 2899–2908. doi: 10.1038/sj.onc.1208615
- 172) Edgar, B. A., & Orr-Weaver, T. L. (2001). Endoreplication Cell Cycles. *Cell*, *105*(3), 297–306. doi: 10.1016/s0092-8674(01)00334-8
- 173) Szklarczyk, D., Franceschini, A., Wyder, S., Forslund, K., Heller, D., Huerta-Cepas, J., Simonovic, M., Roth, A., Santos, A., Tsafou, K. P., Kuhn, M., Bork, P., Jensen, L. J., & von Mering, C. (2015). STRING v10: protein-protein interaction networks, integrated over the tree of life. *Nucleic acids research*, *43*(Database issue), D447–D452. <https://doi.org/10.1093/nar/gku1003>
- 174) He, L., Liu, X., Yang, J., Li, W., Liu, S., Liu, X., Yang, Z., Ren, J., Wang, Y., Shan, L., Guan, C., Pei, F., Lei, L., Zhang, Y., Yi, X., Yang, X., Liang, J., Liu, R., Sun, L., & Shang, Y. (2018). Imbalance of the reciprocally inhibitory loop between the ubiquitin-

specific protease USP43 and EGFR/PI3K/AKT drives breast carcinogenesis. *Cell research*, 28(9), 934–951. <https://doi.org/10.1038/s41422-018-0079-6>

- 175) Chaugule, V. K., Burchell, L., Barber, K. R., Sidhu, A., Leslie, S. J., Shaw, G. S., & Walden, H. (2011). Autoregulation of Parkin activity through its ubiquitin-like domain. *The EMBO journal*, 30(14), 2853–2867. <https://doi.org/10.1038/emboj.2011.204>
- 176) Riley, B. E., Lougheed, J. C., Callaway, K., Velasquez, M., Brecht, E., Nguyen, L., Shaler, T., Walker, D., Yang, Y., Regnstrom, K., Diep, L., Zhang, Z., Chiou, S., Bova, M., Artis, D. R., Yao, N., Baker, J., Yednock, T., & Johnston, J. A. (2013). Structure and function of Parkin E3 ubiquitin ligase reveals aspects of RING and HECT ligases. *Nature communications*, 4, 1982. <https://doi.org/10.1038/ncomms2982>
- 177) Peng, J., Schwartz, D., Elias, J. E., Thoreen, C. C., Cheng, D., Marsischky, G., ... Gygi, S. P. (2003). A proteomics approach to understanding protein ubiquitination. *Nature Biotechnology*, 21(8), 921–926. doi: 10.1038/nbt849
- 178) Matsumoto, M., Hatakeyama, S., Oyamada, K., Oda, Y., Nishimura, T., & Nakayama, K. I. (2005). Large-scale analysis of the human ubiquitin-related proteome. *Proteomics*, 5(16), 4145–4151. doi: 10.1002/pmic.200401280
- 179) Xirodimas, D. P., Sundqvist, A., Nakamura, A., Shen, L., Botting, C., & Hay, R. T. (2008). Ribosomal proteins are targets for the NEDD8 pathway. *EMBO Reports*, 9(3), 280–286. doi: 10.1038/embor.2008.10
- 180) Matafora, V., Damato, A., Mori, S., Blasi, F., & Bachi, A. (2009). Proteomics Analysis of Nucleolar SUMO-1 Target Proteins upon Proteasome Inhibition. *Molecular & Cellular Proteomics*, 8(10), 2243–2255. doi: 10.1074/mcp.m900079-mcp200
- 181) Shcherbik, N., & Pestov, D. G. (n.d.). Ubiquitin and Ubiquitin-Like Proteins in the Nucleolus: Multitasking Tools for a Ribosome Factory - Natalia Shcherbik, Dimitri G.

Pestov, 2010. Retrieved from
<https://journals.sagepub.com/doi/full/10.1177/1947601910381382>

- 182) Volarevic, S. (2000). Proliferation, But Not Growth, Blocked by Conditional Deletion of 40S Ribosomal Protein S6. *Science*, 288(5473), 2045–2047. doi: 10.1126/science.288.5473.2045
- 183) Wilson, A., Lamarco, K., Peterson, M., & Herr, W. (1993). The VP16 accessory protein HCF is a family of polypeptides processed from a large precursor protein. *Trends in Genetics*, 9(10), 343. doi: 10.1016/0168-9525(93)90037-i
- 184) Kristie, T. M., & Sharp, P. A. (1993). Purification of the cellular C1 factor required for the stable recognition of the Oct-1 homeodomain by the herpes simplex virus alpha-trans-induction factor (VP16). *The Journal of biological chemistry*, 268(9), 6525–6534.
- 185) Kristie, T. M., Pomerantz, J. L., Twomey, T. C., Parent, S. A., & Sharp, P. A. (1995). The cellular C1 factor of the herpes simplex virus enhancer complex is a family of polypeptides. *The Journal of biological chemistry*, 270(9), 4387–4394. <https://doi.org/10.1074/jbc.270.9.4387>
- 186) Scarr, R. B., & Sharp, P. A. (2002). PDCD2 is a negative regulator of HCF-1 (C1). *Oncogene*, 21(34), 5245–5254. doi: 10.1038/sj.onc.1205647
- 187) Medvinsky, A., Rybtsov, S., & Taoudi, S. (2011). Embryonic origin of the adult hematopoietic system: advances and questions. *Development*, 138(6), 1017–1031. doi: 10.1242/dev.040998
- 188) Orkin, S. H., & Zon, L. I. (2008). Hematopoiesis: An Evolving Paradigm for Stem Cell Biology. *Cell*, 132(4), 631–644. doi: 10.1016/j.cell.2008.01.025

- 189) Lozzio, B. B., Lozzio, C. B., Bamberger, E. G., & Feliu, A. S. (1981). A Multipotential Leukemia Cell Line (K-562) of Human Origin. *Experimental Biology and Medicine*, 166(4), 546–550. doi: 10.3181/00379727-166-41106
- 190) Saito, K., Nishida, K. M., Mori, T., Kawamura, Y., Miyoshi, K., Nagami, T., Siomi, H., & Siomi, M. C. (2006). Specific association of Piwi with rasiRNAs derived from retrotransposon and heterochromatic regions in the *Drosophila* genome. *Genes & development*, 20(16), 2214–2222. <https://doi.org/10.1101/gad.1454806>
- 191) Vagin, V. V., Sigova, A., Li, C., Seitz, H., Gvozdev, V., & Zamore, P. D. (2006). A distinct small RNA pathway silences selfish genetic elements in the germline. *Science (New York, N.Y.)*, 313(5785), 320–324. <https://doi.org/10.1126/science.1129333>
- 192) Brennecke, J., Aravin, A. A., Stark, A., Dus, M., Kellis, M., Sachidanandam, R., & Hannon, G. J. (2007). Discrete small RNA-generating loci as master regulators of transposon activity in *Drosophila*. *Cell*, 128(6), 1089–1103. <https://doi.org/10.1016/j.cell.2007.01.043>
- 193) Vagin, V. V., Klenov, M. S., Kalmykova, A. I., Stolyarenko, A. D., Kotelnikov, R. N., & Gvozdev, V. A. (2004). The RNA interference proteins and vasa locus are involved in the silencing of retrotransposons in the female germline of *Drosophila melanogaster*. *RNA biology*, 1(1), 54–58.
- 194) Kalmykova, A. I., Klenov, M. S., & Gvozdev, V. A. (2005). Argonaute protein PIWI controls mobilization of retrotransposons in the *Drosophila* male germline. *Nucleic acids research*, 33(6), 2052–2059. <https://doi.org/10.1093/nar/gki323>
- 195) Savitsky, M., Kwon, D., Georgiev, P., Kalmykova, A., & Gvozdev, V. (2006). Telomere elongation is under the control of the RNAi-based mechanism in the *Drosophila* germline. *Genes & development*, 20(3), 345–354. <https://doi.org/10.1101/gad.370206>

- 196) Li, C., Vagin, V. V., Lee, S., Xu, J., Ma, S., Xi, H., Seitz, H., Horwich, M. D., Syrzycka, M., Honda, B. M., Kittler, E. L., Zapp, M. L., Klattenhoff, C., Schulz, N., Theurkauf, W. E., Weng, Z., & Zamore, P. D. (2009). Collapse of germline piRNAs in the absence of Argonaute3 reveals somatic piRNAs in flies. *Cell*, *137*(3), 509–521. <https://doi.org/10.1016/j.cell.2009.04.027>
- 197) Muerdter, F., Guzzardo, P. M., Gillis, J., Luo, Y., Yu, Y., Chen, C., Fekete, R., & Hannon, G. J. (2013). A genome-wide RNAi screen draws a genetic framework for transposon control and primary piRNA biogenesis in *Drosophila*. *Molecular cell*, *50*(5), 736–748. <https://doi.org/10.1016/j.molcel.2013.04.006>
- 198) Peng, J. C., & Lin, H. (2013). Beyond transposons: the epigenetic and somatic functions of the Piwi-piRNA mechanism. *Current opinion in cell biology*, *25*(2), 190–194. <https://doi.org/10.1016/j.ceb.2013.01.010>
- 199) Andress, A., Bei, Y., Fonslow, B. R., Giri, R., Wu, Y., Yates, J. R., 3rd, & Carthew, R. W. (2016). Spindle-E cycling between nuage and cytoplasm is controlled by Qin and PIWI proteins. *The Journal of cell biology*, *213*(2), 201–211. <https://doi.org/10.1083/jcb.201411076>
- 200) Chen, K. M., Campbell, E., Pandey, R. R., Yang, Z., McCarthy, A. A., & Pillai, R. S. (2015). Metazoan Maelstrom is an RNA-binding protein that has evolved from an ancient nuclease active in protists. *RNA (New York, N.Y.)*, *21*(5), 833–839. <https://doi.org/10.1261/rna.049437.114>
- 201) Matsumoto, N., Sato, K., Nishimasu, H., Namba, Y., Miyakubi, K., Dohmae, N., ... Nureki, O. (2015). Crystal Structure and Activity of the Endoribonuclease Domain of the piRNA Pathway Factor Maelstrom. *Cell Reports*, *11*(3), 366–375. doi: 10.1016/j.celrep.2015.03.030
- 202) Blake, A. J., Finger, D. S., Hardy, V. L., & Ables, E. T. (2017). RNAi-Based Techniques for the Analysis of Gene Function in *Drosophila* Germline Stem

Cells. *Methods in Molecular Biology RNAi and Small Regulatory RNAs in Stem Cells*, 161–184. doi: 10.1007/978-1-4939-7108-4_13

- 203) Duffy, J. B. (2002). GAL4 system in drosophila: A fly geneticists swiss army knife. *Genesis*, 34(1-2), 1–15. doi: 10.1002/gene.10150
- 204) Rørth, P. (1998). Gal4 in the Drosophila female germline. *Mechanisms of Development*, 78(1-2), 113–118. doi: 10.1016/s0925-4773(98)00157-9
- 205) George, S., Bhalerao, S. V., Lidstone, E. A., Ahmad, I. S., Abbasi, A., Cunningham, B. T., & Watkin, K. L. (2010). Cytotoxicity screening of Bangladeshi medicinal plant extracts on pancreatic cancer cells. *BMC complementary and alternative medicine*, 10, 52. <https://doi.org/10.1186/1472-6882-10-52>
- 206) *Drosophila* Genomic Resource Center, supported by NIH grant 2P40OD010949
- 207) Rieger, M. A., & Schroeder, T. (2012). Hematopoiesis. *Cold Spring Harbor perspectives in biology*, 4(12), a008250. <https://doi.org/10.1101/cshperspect.a008250>
- 208) Urban P. L. (2016). Quantitative mass spectrometry: an overview. *Philosophical transactions. Series A, Mathematical, physical, and engineering sciences*, 374(2079), 20150382. <https://doi.org/10.1098/rsta.2015.0382>
- 209) Salih E. (2005). Phosphoproteomics by mass spectrometry and classical protein chemistry approaches. *Mass spectrometry reviews*, 24(6), 828–846. <https://doi.org/10.1002/mas.20042>